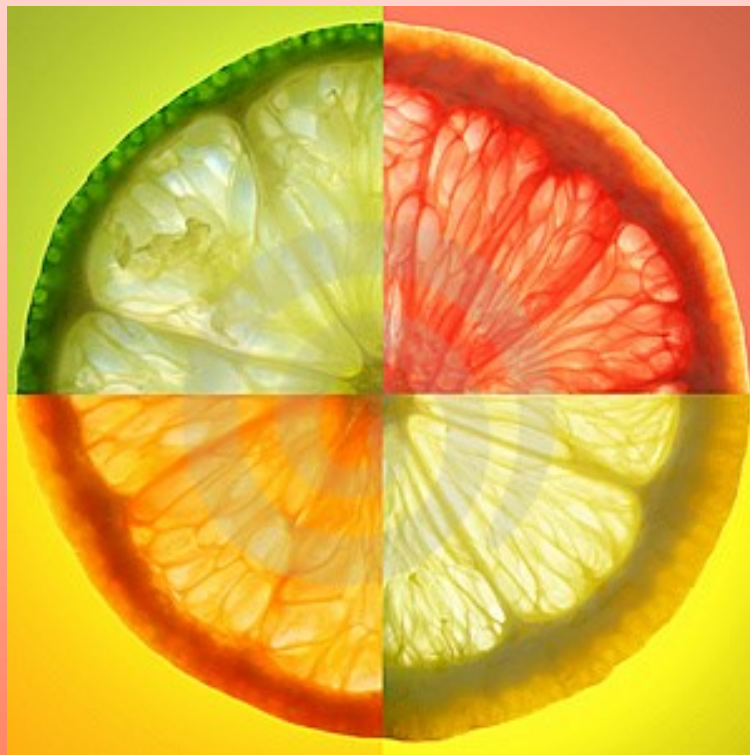




Recovery of molecules with healthy properties from orange press liquor by membrane fractionation

PhD Dissertation by
René Ruby-Figueroa



Supervisors

Prof. Bartolo Gabriele

Department of Pharmaceutical Sciences
Faculty of Pharmacy, Nutritional and Health Sciences
University of Calabria

Dr. Alfredo Cassano

National Research Council
Institute on Membrane Technology
(ITM-CNR)



UNIVERSITA' DELLA CALABRIA

Dipartimento di Chimica

Scuola di Dottorato

Scuola di Scienza e Tecnica Bernardino Telesio

Indirizzo

Organic Materials of Pharmaceutical Interest
(OMPI)


CICLO

XXVI

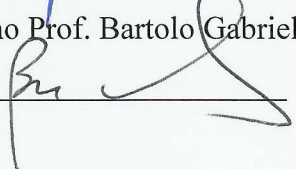
Recovery of molecules with healthy properties from orange press liquor by membrane fractionation

Settore Scientifico Disciplinare CHIM/06 – Chimica Organica

Direttore: Ch.mo Prof. Roberto Bartolino



Supervisor: Ch.mo Prof. Bartolo Gabriele



Dott. Alfredo Cassano



Dottorando: Dott. René Ruby Figueroa



Dedicated to my Family

SUMMARY

Fruits and vegetables are widely recognized as an important source of beneficial compounds for the human nutrition. Citrus and juices are widely consumed in the world. Their health benefits have been recognized for a long time now since first cultivated in Asia. The market of oranges is growing constantly, because consumers have become more convenience-oriented and health conscious. Consequently, efforts by researchers and industrial organizations have been made to develop processes more efficient, putting emphasis in food quality and safety. In addition, with the increasing emphasis on water pollution control, industries are establishing programs that will permit disposal of their wastewater without damaging the environment. The citrus fruit industry is no exception. Citrus wastes, such as wet peels and whole rejected fruit, which a great amount of organic matter that can be associated with environmental and health problems due to water runoff and uncontrolled fermentation. Therefore, the development of optimized systems for the treatment of citrus wastes is a crucial factor in the rationalization of the traditional industrial cycle.

Membrane operations in the last years have shown their potentialities in the rationalization of production systems. Their intrinsic characteristics of efficiency, operational simplicity and flexibility, relatively high selectivity and permeability for the transport of specific components, low energy requirements, good stability under a wide spectrum of operating conditions, environment compatibility, easy control and scale-up have been confirmed in a large variety of applications and operations in the food industry.

Recent R&D efforts aim to convert the potential of wastes into profitable products creating new segments of production and offsetting the disposal costs. Orange peels and pulp contain several bioactive compounds, such as flavonoids and phenolic acids, recognized for their beneficial implications in human health due to their antioxidant activity and free radical scavenging ability. These semi-solid wastes can be pressed to obtain a liquid rich in soluble sugars, named *press liquor*, that can be concentrated up to citrus molasses grade or alternatively exploited as a natural source for the extraction of

phenolic compounds which can be used as natural antioxidants mainly in pharmaceutical, cosmetic and foods industry.

This PhD dissertation is based on the opportunity to develop a technical alternative to solve some problems related to the disposal of citrus wastes from an economic and environmental point of view, specifically in terms of recovery of attractive compounds present in orange press liquor. The general aim of the work was devoted to the recovery of phenolic compounds by using an integrated membrane process, in which microfiltration (MF) or ultrafiltration (UF), nanofiltration (NF) and osmotic distillation (OD) processes were involved.

MF or UF processes were used for the clarification of the press liquor in order to separate macromolecules, such as pectins, and to obtain a clarified press liquor as permeate stream. In the second step the clarified press liquor obtained from the MF/UF process was treated by NF in order to obtain a retentate stream enriched in phenolic compounds with a low content of sugars. Finally, OD was used as final step to concentrate the NF retentate stream.

In the first Chapter, a general overview of membrane operations, including methodologies to evaluate their performance, is reported. The industrial transformation of citrus fruits and the associated production of citrus wastes is reported in Chapter 2. In this Chapter the chemico-physical characterization of citrus press liquor used for the experimental activities performed on membrane laboratory plants is also included. Chapter 3 is focused on the experimental activities concerning the clarification of citrus press liquor by using MF or UF processes. In Chapter 4 the fractionation of clarified press liquor by using NF membranes is analysed and discussed. Experimental activities related to the concentration of the NF retentate by using OD are described in Chapter 5

ACKNOWLEDGEMENT

I would like to express my deepest appreciation to my direct supervisor Dr. Alfredo Cassano for the useful comments, remarks and engagement through the learning process of this doctoral thesis. Furthermore, I would also like to thank my supervisor Prof. Bartolo Gabriele for the support on the way to obtaining my goals. Without their guidance and persistent help this dissertation would not have been possible.

I would also like to thank the *Ministero dell'Istruzione, dell'Università e della Ricerca* (MIUR) for their financial support granted through my doctoral fellowship. I would also like to thank the Institute on Membrane Technology (ITM-CNR) who gave me the space to develop my research.

A special thanks to Dr. Alessia Fazio, Dr. Monica Nardi and Dr. Pierluigi Plastina who helped me in some of the analytical measurements. I appreciated the camaraderie of the members of the ITM-CNR group; Carmela Conidi, Fitim Destani, Sabrina Prete, and Serena Russo and many more, who contributed immensely to my personal and professional growth during my time at University of Calabria.

I would like to thank my family, Monica Figueroa, Natalia Ruby, René Ruby, Ana Alvear, and Nicolas for their endless love and support, despite the long distance. I would also like to thank my partner, Maria Muro, for her love, kindness, and support she has shown during my PhD studies.

Lastly, my time at UNICAL was made enjoyable in large part due to the many friends that became a big part of my life. I would like to thank the friendship and support given to me by Luciano Marquez, Alejandra Noriega and Ana Lucia Acevedo.

René Ruby-Figueroa
University of Calabria
November 2013

INDEX

Summary	vii
Acknowledgement	ix
Chapter 1 Fundamentals of membrane separation processes	1
1.1 Membranes and Membrane Processes	1
1.2 Membrane materials	2
1.3 Membrane structure	4
1.4 Process design and operation	7
1.4.1 Membrane modules.....	7
1.4.2 Filtration methods.....	10
1.4.3 Process configuration.....	12
1.5 Membrane performance	13
1.5.1 Membrane rejection and volume reduction factor.....	14
1.5.2 Transport mechanisms.....	14
1.5.3 Concentration Polarization and membrane fouling.....	17
References	23
Chapter 2 Citrus fruit processing and orange press liquor characterization ...	27
2.1 Citrus fruits: properties and global market	27
2.2 Citrus processing	29
2.3 Press liquor characterization	33
2.3.1 Analysis of phenolic compounds.....	33
2.3.2 Analysis of Sugars.....	34
2.3.3 Determination of total phenols content.....	34
2.3.4 Determination of the total antioxidant activity (TAA).....	35
2.3.5 Analytical results.....	35
References	38
Chapter 3 Orange press liquor clarification	43
3.1 Clarification of orange press liquor: Evaluation of membrane characteristics	44
3.2 Clarification of orange press liquor: Evaluation of operating conditions	49
3.2.1 Optimization of multiple responses.....	70
3.3 Clarification of orange press liquor: UF with tubular PS membrane	71
References	75

Chapter 4 Fractionation of clarified press liquor	77
4.1 Introduction	77
4.2 Nanofiltration with flat-sheet membranes	78
4.3 Nanofiltration with a spiral-wound membrane module	86
References	90
Chapter 5 Concentration of NF retentate by osmotic distillation	93
5.1 Introduction	93
5.2 Experimental results	97
References	101
Conclusions	103
Annex	105

List of Tables

1.1	Materials used for the manufacture of membranes.....	3
1.2	Characteristics of different membrane modules.....	10
2.1	Physico-chemical characteristics of raw orange press liquor.....	36
3.1	Agents used in the conventional fruit juice clarification.....	44
3.2	Characteristics of selected membranes.....	46
3.3	Experimental range and levels of the independent variables for Box-Behnken design.....	51
3.4	Experimental design and results of Box-Behnken design.....	52
3.5	Plot of residuals against predicted response of TAA in the permeate stream.....	71
3.6	Results obtained during UF of orange press liquor by using tubular PS membrane.....	74
4.1	Characteristics of flat-sheet NF membranes.....	80
4.2	Analytical determination of hesperidin and sugars in samples coming from the treatment of clarified orange press liquor with flat-sheet membranes.....	84
4.3	Properties of 2.5 x 40 in. spiral-wound NF-PES-10 membrane.....	86
4.4	Results of hesperidin and sugars rejection obtained with the NF-PES-10 membrane. Operating conditions: TMP=17 bar, T=20.73±1.40°C.....	89
5.1	Characteristics of Liqui-Cell Extra-Flow membrane contactor.....	96

List of Figures

1.1	Cross section of: (a) cellulose acetate asymmetric flat sheet membrane; (b) polyamide hollow fibre asymmetric membrane.....	5
1.2	Filtration capability of pressure-driven membrane operations.....	6
1.3	Schematic representation of (a) plate and frame, (b) spiral-wound, (c) tubular, (d) hollow fiber membrane module.....	8
1.4	Schematic representation of (a) dead-end and (b) cross-flow filtration.....	11
1.5	Schematic diagram of (a) total recycle, (b) batch concentration, (c) feed-and-bleed and (d) diafiltration configuration.....	12
1.6	Schematic representation of concentration polarization (cw = gel concentration; cb = bulk concentration).....	18
1.7	Schematic representation of (a) complete blocking, (b) intermediate blocking, (c) cake filtration and (d) standard blocking in pressure-driven membrane processes.....	19
2.1	Flowchart of industrial orange juice processing.....	30
2.2	HPLC chromatogram of orange press liquor. black line at 280 nm (for hydroxybenzoic acids and flavones) and pink line at 360 nm (for hydroxycinnamic acids).....	36
3.1	Schematic diagram of the experimental set-up: (1) feed tank; (2) feed pump; (3,5) pressure gauges; (4) flat-sheet cell; (6) digital balance; (7) retentate valve; (8) permeate tank; (9) thermometer.....	45
3.2	Rejection of (a) sugar and (b) hesperidin obtained during MF-UF under TRC and BC configuration using flat-sheet membranes. Operating conditions: TMP= 1 bar, T= 25°C, feed flow rate= 185 L/h.....	47
3.3	Time course of permeate flux for MF and UF processes using flat-sheet membranes at TRC (a) and BCC (b). Operating conditions: TMP= 1 bar, T= 25°C, feed flow rate= 185 L/h.....	48
3.4	Scheme of UF experimental setup.....	50
3.5	Standardized pareto chart for the permeate flux.....	53
3.6	3D response surface with contour plot of permeate flux.....	55
3.7	Plot of residuals against predicted response of permeate flux in the UF process.....	56
3.8	Standardized Pareto chart for fouling index.....	57
3.9	3D response surface with contour plot of fouling index.....	58
3.10	Plot of residuals against predicted response of fouling index.....	59
3.11	Plot of residuals against predicted response of blocking index.....	60
3.12	Standardized Pareto chart for blocking index.....	61
3.13	3D response surface with contour plot of blocking index.....	62

3.14	Plot of residuals against predicted response of total polyphenols rejection.....	63
3.15	Standardized Pareto chart for total polyphenols rejection.....	64
3.16	3D response surface with contour plot for total polyphenols rejection.....	65
3.17	Standardized Pareto chart for TAA in the permeate stream.....	67
3.18	3D response surface with contour plot for TAA in the permeate stream.....	68
3.19	Plot of residuals against predicted response of TAA in the permeate stream.....	70
3.20	Experimental set-up used for the clarification of raw press liquor by UF.....	72
3.21	Time course of permeate flux for press liquor with PS ultrafiltration membrane of 100kDa, operating conditions: $T=21.31\pm 0.23^{\circ}\text{C}$; $\text{TMP} = 1.2$ bar).....	73
3.22	Samples coming from the UF treatment of orange press liquor.....	73
4.1	Experimental set-up used for the NF with flat-sheet membranes.....	78
4.2	Hydraulic permeability of NF membranes studied. Operating conditions: $\text{Temperature}=26.79\pm 1.72^{\circ}\text{C}$, $Q_f=500$ L/h.....	81
4.3	NF of clarified orange press liquor with flat-sheet membranes. Time course of permeate flux. Operating conditions: $\text{TMP}=17$ bar; $T=31.25\pm 0.56^{\circ}\text{C}$; $Q_f=500$ L/h.....	82
4.4	Time course for NF process using flat-sheet membranes. Operating conditions: 35 bar; $T=37.56\pm 0.78^{\circ}\text{C}$ and $Q_f=500$ L/h.....	83
4.5	Experimental set-up used for the NF of clarified orange press liquor with a spiral-wound membrane module.....	85
4.6	Time course of NF process with NF-PES-10 spiral wound membrane. Operating conditions: $\text{TMP}=17$ bar, $T=20.73\pm 1.40^{\circ}\text{C}$	87
4.7	Time course of NF process with NF-PES-10 spiral wound membrane. Operating conditions: $\text{TMP}=17$ bar, $T=20.73\pm 1.40^{\circ}\text{C}$	88
5.1	Schematic representation of water vapour flux through an OD membrane.....	94
5.2	Schematic diagram of OD experimental set-up.....	95
5.3	Treatment of NF retentate by OD. Time course of (a) evaporation flux and TSS content; (b) calcium chloride dehydrate concentration.....	98
5.4	Evolution in concentration of hesperidin during OD.....	99
5.5	Samples collected at different times during the concentration of the NF retentate by OD.....	100
5.6	Conceptual process design for the treatment of citrus press liquor based on an integrated membrane process.....	100

CHAPTER 1

Fundamentals of membrane separation processes

1.1 Membranes and Membrane Processes

The first commercial production of microporous membranes on small scale started in 1930 together with the first practical application of ion-exchange membranes and the development of the theory on ionic transport through charged membranes [1]. However, until the late 1960s membranes were used in a few laboratory and analytical applications, but not for industrial applications because they were too slow, too expensive and too unselective. The seminal discovery that transformed membrane separation from a laboratory to an industrial process was the development of defect-free ultrathin cellulose acetate membranes by Loeb-Sourirajan process in the 1960s [2,3].

Actually the situation is different because membranes are more robust, modules and equipment are better designed and costs have come down significantly, partly because of the maturing technology and partly because of competition from an increasing number of membrane suppliers and original equipment manufacturers [4]. Membrane technology is presently an established part of several industrial processes to produce drinking water from the sea, to clean industrial effluents and recover valuable constituents, to concentrate, purify, or fractionate macromolecular mixtures in the food and drug industries, and to separate gases and vapours [5]. Membrane separation technologies have attracted much attention in the food industries over recent decades as low energy processes providing a gentle treatment of the products at low-moderate temperatures and covering steps such as separation, fractionation, concentration, purification and clarification of various streams.

Membrane processes are guided by four major driving forces such as temperature, activity, electrical potential, and hydrostatic pressure gradients. Major applications of membrane processes in the food industry are related with pressure-driven processes, such as microfiltration (MF), ultrafiltration (UF), nanofiltration (NF) and reverse

osmosis (RO). These processes are based on the use of a permselective barrier through which fluids and solutes are selectively transported when a hydrostatic pressure is applied across it. As a result, the feed solution is converted in a *permeate* containing all the components which have permeated the membrane and a *retentate* containing all the compounds rejected by the membrane. In addition, a relatively new process, called osmotic distillation (OD), where the driving-force is a vapour pressure gradient between two sides of a hydrophobic membrane, has gained the attention for concentrating liquid foods because it works under normal pressure and temperature conditions, preserving the nutritious characteristics of the food [6].

The first section of this chapter will provide an overview on materials and structures of synthetic membranes. The last section is focused on membrane design and evaluation of membrane performance.

1.2 Membrane materials

A large variety of synthetic membranes has been reported in scientific and patent literature. The differences may be caused by material partitioning during membrane formation or by some selected surface postformation treatments. Membrane chemistry determines important properties as hydrophilicity or hydrophobicity, presence or absence of ionic charges, chemical and thermal resistance, binding affinity for solutes or particles, biocompatibility, etc. [4,5].

Membrane materials must be chemical resistant to both feed and cleaning solutions, mechanically and thermally stable, and characterised by high selectivity and permeability.

The materials used for the preparation of membranes can be synthetic polymers, cellulose derivatives, ceramics, inorganic and metals; they may be neutral or carry electrical charges. Although over 130 materials have been used to manufacture membranes, only a few have achieved commercial status, and fewer still have to obtain regulatory approval for use in food.

A summary of typical materials suitable for pressure-driven membrane processes is shown in Table 1.1.

Table 1.1. Materials used for the manufacture of membranes.

Material	Processes
Alumina	MF
Carbon-carbon composites	MF
Cellulose esters (mixed)	MF
Cellulose nitrate	MF
Polyamide, aliphatic (e.g., nylon)	MF
Polycarbonate (track-etch)	MF
Polyester (track-etch)	MF
Polypropylene	MF
Polytetrafluoroethylene (PTFE)	MF
Polyvinyl chloride (PCV)	MF
Polyvinylidene fluoride (PVDF)	MF
Sintered stainless steel	MF
Cellulose (regenerated)	MF, UF
Ceramic composites (zirconia on alumina)	MF, UF
Polyacrylonitrile (PAN)	MF, UF
Polyvinyl alcohol (PVA)	MF, UF
Polysulfone (PS)	MF, UF
Polyethersulfone (PES)	MF, UF, NF
Cellulose acetate (CA)	MF, UF, RO
Cellulose triacetate (CTA)	MF, UF, RO
Polyamide, aromatic (PA)	MF, UF, NF, RO
Polyamide (PI)	UF, RO
CA/CTA blends	RO
Composites (e.g., polyacrylic acid on zirconia or stainless steel)	RO
Composites, polymeric thin film (e.g., PA or polyetherurea on polysulfone)	RO
Polybenzimidazole (PBI)	RO
Polyetherimide (PEI)	RO

1.3 Membrane structure

Synthetic membranes can be classified on the basis of their structure as: porous membranes, homogeneous membranes, solid membranes carrying electrical charges and liquid or solid films containing selective carriers [5].

Porous membranes consist of a solid matrix with defined pores with diameters ranging from less than 1 nm to more than 10 μm . Porous membranes can be classified as: macroporous, with average pore diameters larger than 50 nm (i.e. MF and UF membranes); mesoporous, with average pore diameters in the range between 2 and 50 nm (i.e. NF membranes); microporous, if average pore diameters are between 0.1 and 2 nm. Dense membranes, such as those used in RO, have no individual permanent pores but the separation occurs through fluctuating free volumes.

Furthermore, the structure of membranes may be symmetric, if pore diameters do not vary over the membrane cross-section, or asymmetric, with pore diameters increasing from one side of the membrane to the other.

Symmetric porous membranes can be prepared by using different techniques such as sintering, track-etching and leaching [5]. Specific details related to these techniques are extensively reported in literature [7-15].

On the other hand, asymmetric membranes consist of a thin (0.1 to 1 μm) selective skin layer supported by a highly porous (100 to 200 μm) thick substructure. The skin layer represents the active layer of the membrane and the separation characteristics will depend on the nature of the material or the size of pores in the skin-layer. These membranes are generally used for UF, NF and RO applications. Asymmetric membranes can be prepared through two different techniques: (i) the phase inversion process, which leads to an integral structure with the skin and the support structure made from the same material in a single process (integral asymmetric membranes) [16]; (ii) the deposition of an extremely thin polymer film on a preformed porous substructure in a two-step process, leading to a so-called composite membrane [17]. Generally, the barrier and support are made from different materials.

Fig. 1.1 shows the cross section of asymmetric membranes in flat sheet and hollow fibre configurations.

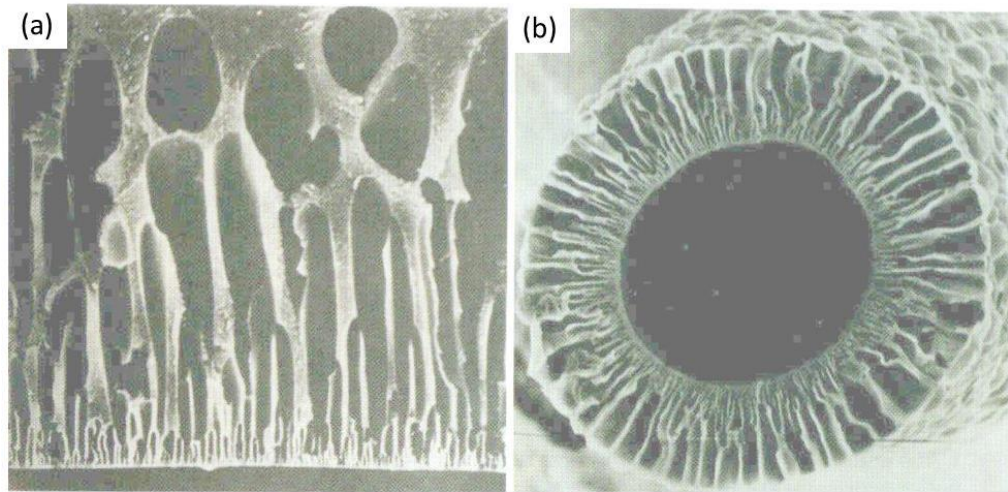


Fig. 1.1. Cross section of: (a) cellulose acetate asymmetric flat sheet membrane; (b) polyamide hollow fibre asymmetric membrane.

The filtration capability of pressure-driven membrane processes is shown in Fig. 1.2. MF is used to separate particles with diameters of 0.1-10 μm from a solvent or other low molecular weight compounds. These particles are generally larger than those separated by UF and RO. Consequently, the osmotic pressure for MF is negligible and hydrostatic pressure differences used in MF are relatively small (in the range of 0.5-4 bar). UF is based on the use of asymmetric membranes with pore sizes in the skin layer of 2-10 nm. Typically dissolved molecules or small particles not larger than 0.1 μm in diameter are retained. An UF membrane is typically characterized by its molecular weight cut-off (MWCO), defined as the equivalent molecular weight of the smallest species that exhibit 90% rejection. The MWCO of UF membranes is between 1 to 100 kDa. Hydrostatic pressures of 2-10 bar are typically used.

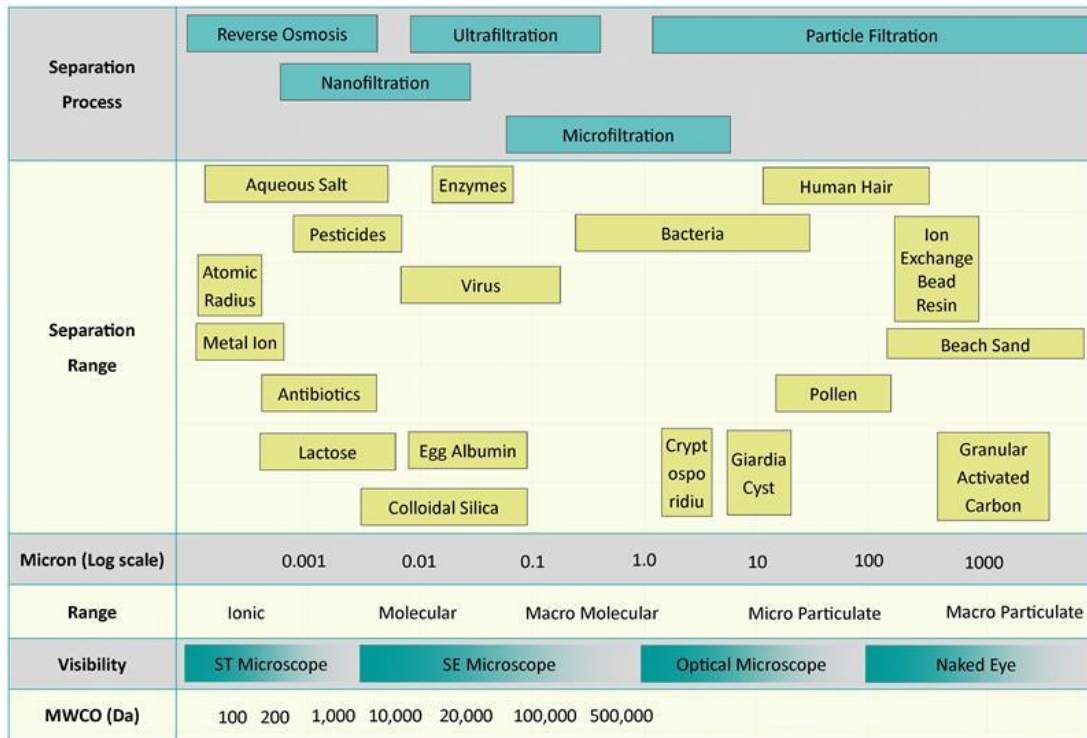


Fig.1.2. Filtration capability of pressure-driven membrane operations.

In the NF process, components of a fluid are fractionated mainly according to their size and charge. Multivalent ions and uncharged organic molecules with molecular weight between 100 and 1000 Da are typically separated. NF membranes are characterised by a charged surface with pore diameters in the range 1-3 nm. They operate at lower pressures (generally in the range 3-30 bar) than RO membranes.

RO membranes are typically used to separate low molecular weight compounds from a solvent, usually water. The particle size range for applications of RO is 0.1-1 nm and solutes with molecular weight greater than 300 Da are separated. The hydrostatic pressures applied as driving force in RO are of the order of 10-100 bar.

1.4 Process design and operation

The selection of the most effective membrane for a specific application plays an important role in determining the desired level of separation to be obtained. However, for an efficient utilization of membranes the process design is equally important.

The process design is defined by different aspects concerning the membrane configuration, filtration methods (dead-end and cross-flow configuration) and the process configuration. It is also of importance for the control of concentration polarization and fouling phenomena determining to a large extent the useful membrane for a specific separation.

1.4.1 Membrane modules

The membrane module concept denotes the device where the membrane must be installed to perform the separation process. On large industrial scale, membrane modules are available in six basic designs: cartridge, hollow fibre, spiral-wound, tubular, plate-and-frame and capillary. They are quite different in their design, mode of operation, production costs and energy requirement for pumping the feed solution through the module.

Pleated cartridge modules are used mainly in dead-end microfiltration; they consist of a pleated membrane cartridge installed in a pressurized housing. These systems are operated at relatively low pressures of 1 to 2 bar. The main applications are related with the sterile filtration of water and beverages such as wine, beer and fruit juices, as well as pharmaceutical solutions. At industrial scale they are used as pre-filters in RO water desalination plants [5].

The plate-and-frame configuration (Fig. 1.3-a) is mainly used for small-scale applications (production of pharmaceuticals, bioproducts or fine chemicals). Membranes, feed flow spacers and porous permeate support plates are layered together between two endplates and placed in a housing. The sheets are either in the form of

circular discs, elliptical sheets or rectangular plates. The feed mixture is pressurized in the housing and forced across the membrane surface. A portion passes through the membrane, enters the permeate channel, and makes its way to a central permeate collection manifold.

Plate-and-frame modules are quite expensive and the membrane replacement is labour intensive. They are used in a limited number of UF applications with highly fouling feeds. The feed channels are often less than 1 mm and although more sensitive to fouling are easier to clean as no mesh support is used.

The spiral-wound configuration, widely used in UF, NF and RO, is basically a variation of the plate-and-frame geometry. In this configuration the feed flow channel spacer, the membrane, and the porous membrane support form an envelope that is rolled around a perforated collection tube (Fig. 1.3-b). The module is placed inside a tubular pressure housing made from stainless steel or PVC. The feed solution passes axially through the feed channel across the membrane surface. The permeate stream is moved along the permeate channel and is collected in the collection tube.

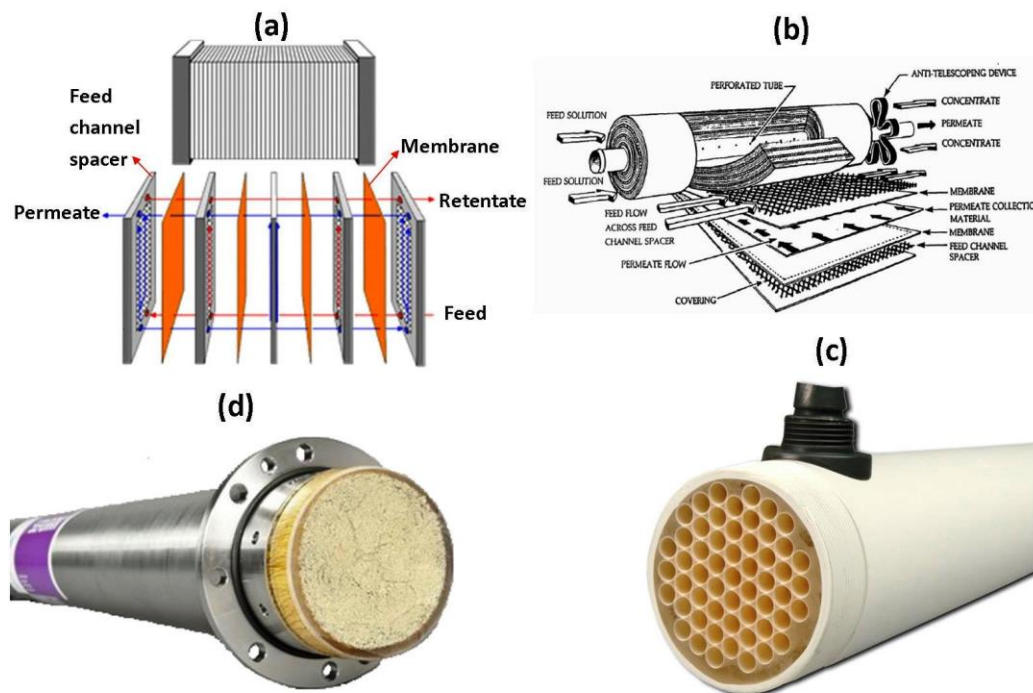


Fig. 1.3. Schematic representation of (a) plate and frame, (b) spiral-wound, (c) tubular, (d) hollow fiber membrane module.

The spiral wound configuration is compact providing a relatively large area per unit volume; so it is relatively inexpensive but prone to particulate fouling (thus pre-filtration is needed).

Tubular membrane modules (Fig. 1.3-c) consist of membrane tubes placed into porous stainless steel or fiberglass reinforced plastic pipes. The feed solution is pressurized internally along the tubes and the permeate is collected on the outer side of the porous support. Tube diameters are in the range of 1 to 2.5 cm and a number of tubes are placed in one pressure housing in order to increase the module productivity.

The main advantage of the tubular configuration is that concentration polarization effects and membrane fouling phenomena can be easily controlled; however, low surface areas can be installed in a given unit volume resulting in high production costs. Basically, tubular membrane modules are used to treat feed solutions characterised by high viscosity and high content of solids.

Capillary and hollow fibre membrane modules have the same basic spinning process for the preparation. The principal differences are related with the inner diameter and also with the position of the selective layer. Capillary membrane modules are constituted by a large number of capillaries with an inner diameter of 0.5-3 mm arranged in parallel as a bundle in a shell tube. The feed is pumped in the lumen of the membranes while the permeate is collected in the shell side. This configuration is characterised by a high membrane area per module volume and low production costs; another advantage is the possibility to control concentration polarization and membrane fouling through a physical process called back flushing in which the permeate flow is reversed allowing to dislodge the fouling material from the membrane surface. The required low operating pressure (4-6 bar as maximum values), due to the limited stability of the membranes, is the main drawback.

Hollow fibre membrane modules consist of a bundle of several membrane fibres with the free ends potted with an epoxy resin into a cylindrical housing. Typically the outer diameter of fibres is between 50 and 200 μm ; in this case the selective layer is on the outside of the fibres where the feed fluid is applied, while the permeate is removed down the fibre bore (Fig. 1.3-d).

Hollow fibre membrane modules consisting of fibres with diameter between 200 and 500 μm are also available. In these systems the solution is fed into the lumen of the fibres and the permeate is removed from the shell side. Hollow fibre membrane modules are characterised by the highest packing density if compared with other configurations and their production is very cost effective. Drawbacks are related to the difficult control of concentration polarization and membrane fouling. Consequently extensive pre-treatments of the solution are needed in order to remove particles, macromolecules or other materials which can precipitate at the membrane surface.

A brief summary of membrane module characteristics is shown in Table 1.2.

Table 1.2. Characteristics of different membrane modules.

Module Type	Area of standard module (m^2)	Characteristics
Hollow fine fiber	300-600	<ul style="list-style-type: none"> • Low cost per m^2 of membrane but modules easily fouled • Only suitable for clean fluids • Limited to low pressure applications <200psi; good fouling resistance, can be backflushed
Capillary fiber	50-150	<ul style="list-style-type: none"> • Important in ultrafiltration (UF) and microfiltration (MF) applications • The most common RO module
Spiral wound	20-40	<ul style="list-style-type: none"> • Increasingly used in UF and gas separation applications
Tubular	5-10	<ul style="list-style-type: none"> • High cost limits applications
Plate and Frame	5-10	<ul style="list-style-type: none"> • High cost limits applications

1.4.2 Filtration methods

Pressure-driven membrane operations can be operated either in dead-end or in cross-flow configurations. In the dead-end mode (Fig. 1.4-a) the feed flow is perpendicular to the membrane surface. It is forced through the membrane, which causes the retained

particles to accumulate and form a type of cake layer at the membrane surface. The thickness of the cake layer increases with the filtration time. Therefore, the permeation rate decreases by increasing the cake layer thickness. Dead-end filtration is often used as a method to estimate the specific cake resistance for cross-flow filtration and usually gives reasonable data for spherical and ellipsoidal-shaped cells [18].

In cross-flow filtration (Fig. 1.4-b), the fluid to be filtered flows according to a parallel direction to the membrane surface and permeates through the membrane due to the imposed transmembrane pressure difference. Unlike dead-end filtration, rejected particles form a cake layer on the membrane surface which does not build up indefinitely so the cake formed is of a limited thickness. Under the action of pressure drop and frictional drag on the cake particles, the compressible cake phenomena can be enumerated as follows: (i) successive particles rearrangement inside the cake under stress; (ii) matrix compression in gel-like cakes; (iii) complex cases where both the aforementioned phenomena interplay, such as in the case of a biofilm [19,20].

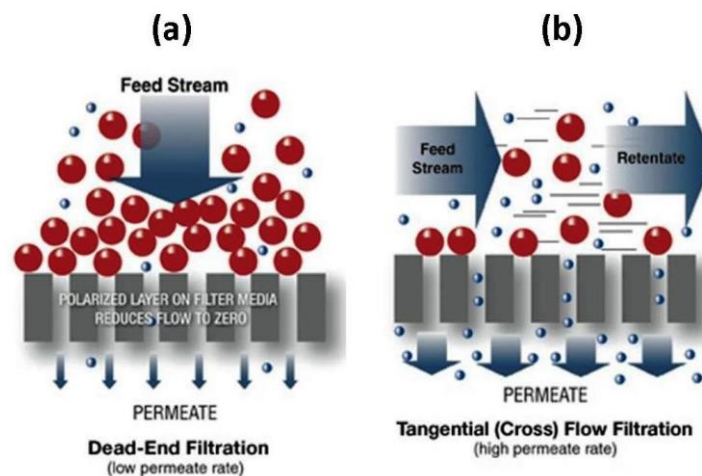


Fig. 1.4. Schematic representation of (a) dead-end and (b) cross-flow filtration.

The cake structure will be affected by different phenomena such as the collapse of the pore structure, pore compression and pore distortion. This set of phenomena will affect in different extent the porosity, the pore size and the pore tortuosity of the filtration cake [3].

1.4.3 Process configuration

The most common process configurations used in practical applications of pressure-driven membrane processes are illustrated in Fig. 1.5.

In the total recycle configuration (Fig. 1.5-a), permeate and retentate streams are recycled back to the feed reservoir so that a steady state is attained in fixed concentration of the feed. This configuration is mainly used in order to study the effect of different operating parameters (feed concentration, cross flow velocity, transmembrane pressure, temperature) on steady state permeate flux and permeate quality [21].

In the batch concentration configuration, the retentate is returned to the feed reservoir and the permeate is collected separately (Fig. 1.5-b). This approach requires the least membrane area to achieve a given separation/unit time. Batch operations are used when the permeate is the product of interest, such as in fruit juice clarification or treatment of effluents in which the retentate has to be discharged.

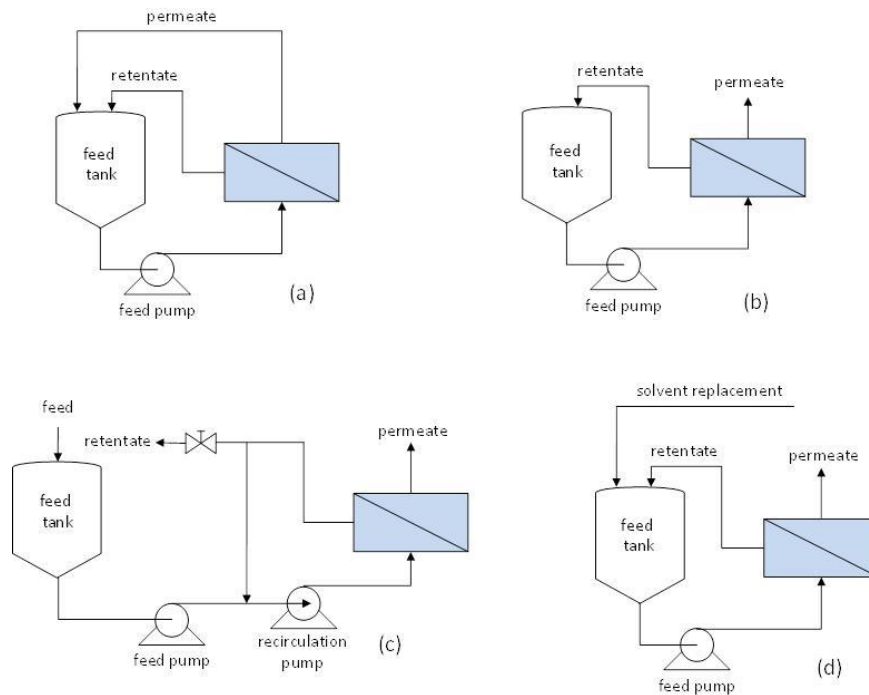


Fig. 1.5. Schematic diagram of (a) total recycle, (b) batch concentration, (c) feed-and-bleed and (d) diafiltration configuration.

The feed-and-bleed configuration is commonly used for continuous operation when a higher recovery rate must be obtained (for example in the food industries). In this case the permeate is removed from the system together with a small part of the retentate (Fig. 1.5-c). Most of the retentate is recycled and mixed with the feed solution to maintain a high tangential velocity in the membrane module. A feed pump and a recirculation pump are required to provide the transmembrane pressure and the cross-flow, respectively.

Diafiltration (Fig. 1.5-d) involves the addition of water to the retentate in order to overcome low permeate fluxes at high concentrations or to improve the separation of permeable compounds. It can be carried out in sequential form (by replacing the permeate with an equal volume of pure solvent) or continuously (by replacing the permeate with the same flow rate of added water). This configuration is often used when a more complete separation of micro- and macrosolutes is required.

1.5 Membrane performance

The membrane performance in pressure-driven membrane systems is determined by the filtration rate and membrane separation properties generally, evaluated in terms of membrane rejection.

Several mathematical models are available in literature that attempt to describe the mechanism of transport through membranes. Although the operating techniques of MF, UF, NF and RO are similar, some considerations should be taken into account. In MF and UF the convection of a bulk solution is the dominant form of transport, while diffusion is generally insignificant. In NF and RO, matter is transported through the membrane mainly by diffusion of individual molecules through a more or less homogenous membrane matrix, but convection can become significant with high flux membranes [5].

In this section a brief description of separation capabilities of membranes, transport mechanisms and concentration polarization and fouling phenomena in pressure-driven membrane systems is reported.

1.5.1 Membrane rejection and volume reduction factor

The separation capability of MF, UF, NF and RO membranes can be expressed in terms of membrane rejection according to the following equation:

$$R = \left(1 - \frac{C_p}{C_f}\right) \quad (1.1)$$

where R is the membrane rejection for a given component in defined conditions of hydrostatic pressure and feed solution concentration, while C_p and C_f are the concentrations of the component in the permeate stream and feed solution, respectively. However, the concentrations in the retentate and permeate streams depend not only on the membrane rejection but also on the recovery rate (Δ) which is given by:

$$\Delta = \frac{V_p}{V_0} \quad (1.2)$$

where $V_p=V_p(t)$ and V_0 are the permeate volume and the initial feed volume, respectively, and t is the time. The recovery rate ranges between 0 and 1. Sometimes data are also presented as volume reduction factor (VRF):

$$VRF = \frac{V_0}{V_r(t)} = \frac{V_0}{V_0 - V_p(t)} \quad (1.3)$$

where V_0 is the initial volume (mL) of the feed, $V_r(t)$ the final volume (mL) of the retentate at particular time (t) and $V_p(t)$ the volume collected on the permeate side at a particular time [22].

1.5.2 Transport mechanisms

The transport mechanisms in membrane operations are generally described by phenomenological equations such as Darcy's law, Fick's law, Hagen-Poiseuille's law and Ohm's law [5]. In MF and UF processes components that permeate through the

membrane are transported by a convective flow through the membrane pores under a pressure gradient as driving force and the separation occurs through a size exclusion mechanism. Darcy's law [4,23] describes this type of transport:

$$J_w = \frac{V_p}{A_m dt} = \frac{\Delta P}{\mu R_T} \quad (1.4)$$

where J_w is the volume flux (m/s), A_m is the membrane cross sectional area (m²), V_p is the filtrate volume (m³) collected on the permeate side at a particular time interval dt (s), ΔP is the applied transmembrane pressure (Pa), μ is the viscosity (Pa·s) of the permeate sample and R_T is the total membrane resistance (m⁻¹). R_T is given by:

$$R_T = R_C + R_F + R_M \quad (1.5)$$

where R_C is the cake layer resistance (m⁻¹) due to the concentration polarization and the deposition of solids on the membrane surface, R_F is the fouling layer resistance (m⁻¹) due to the internal fouling inside the pores and R_M the intrinsic membrane resistance.

Experimentally, the resistances defined in Eq. (1.5) can be determined from the values of the hydraulic permeability measured before and after the cleaning procedures. In particular, R_M can be calculated by measuring the hydraulic permeability of the new or clean membrane as:

$$R_M = \frac{\Delta P}{\mu_w L_p^0} \quad (1.6)$$

where μ_w is the viscosity of pure water [24,25] and $L_p^0 = J_w / \Delta P$ is the hydraulic permeability (m/s·Pa) of the new membrane. R_T can be calculated as:

$$R_T = \frac{1}{\mu_w L_p^1} \quad (1.7)$$

in which L_p^1 is the hydraulic permeability of the membrane after the treatment with a specific solution. R_C is removed by cleaning the membrane with water. The hydraulic permeability measured after such cleaning is L_p^2 , therefore:

$$R_M + R_F = \frac{1}{\mu_w L_p^2} \quad (1.8)$$

Finally, the resistance caused by the cake layer formation can be estimated as:

$$R_C = [R_T - (R_M + R_F)] \quad (1.9)$$

In an ideal situation (pores uniformly distributed, no fouling and negligible concentration polarization) the fluid flow through a porous membrane can be described by the Hagen-Poiseuille law:

$$J_w = \frac{\varepsilon d_p^2 P_T}{32 \Delta x \mu} \quad (1.10)$$

where ε is the surface porosity of the membrane, d_p the mean pore diameter, P_T the applied transmembrane pressure, Δx the length of the channel and μ the viscosity of the fluid permeating the membrane.

The net driving force ΔP for an ideal membrane process should be $(P_T - \Delta \pi)$ where:

$$P_T = P_F - P_P \quad (1.11)$$

$$\Delta \pi = \pi_F - \pi_P \quad (1.12)$$

in which P_F and P_P are the pressures on the feed and permeate side of the membrane, respectively; similarly, π_F and π_P are the osmotic pressures on the feed and permeate side.

The cross flow mode gives rise to a pressure drop from the inlet to the outlet of the membrane module, so that the feed side pressure is expressed as:

$$P_F = \frac{P_i + P_o}{2} \quad (1.13)$$

where P_i is the inlet pressure of the membrane module and P_o the outlet pressure.

The Hagen-Poiseuille law assumes that the flow through the pores is laminar and independent of time, the density is constant, the fluid is Newtonian and end-effects are negligible.

According to the Equation (1.10), the flux is directly proportional to the applied pressure and inversely proportional to the viscosity. Basically, viscosity is controlled by solids concentration and temperature; for non-Newtonian liquids, it is also affected by shear rate and velocity.

The model is largely true under certain conditions such as low pressure, low feed concentration and high feed velocity; when the process deviates from any of these conditions, flux becomes independent of pressure. In these conditions mass transfer limited models, such as the film theory, can effectively describe the process.

1.5.3 Concentration Polarization and membrane fouling

Concentration polarization is a natural consequence of the selectivity of a membrane. When a feed solution containing a solvent and a solute or suspended solids is filtered through a porous membrane, some components permeate the membrane under a given driving force while others are retained. This leads to an accumulation of particles or solutes in a mass transfer boundary layer adjacent to the membrane surface that can affect the flux. A concentration gradient between the solution at the membrane surface and the bulk is established which leads to a back transport of the material accumulated at the membrane surface by diffusion and eventually other means. This phenomenon, schematically represented in Fig. 1.6, is referred to as *concentration polarization* [26,27]. It is not to be confused with the membrane fouling phenomenon that is essentially due to a deposition of retained particles onto the membrane surface or in the membrane pores.

In NF and RO, mainly low molecular weight materials are separated from a solvent such as water producing an increase in the osmotic pressure which is directly proportional to the solute concentration at the membrane surface and thus a decrease in the membrane flux at constant applied hydrostatic pressures [28]. On the other hand in MF and UF the mechanism is different due to the fact that macromolecules and particles are retained by the membrane, thus osmotic pressure is generally quite low. The retained components often are precipitated and form a solid layer at the membrane surface. This layer, which often exhibits membrane properties itself, can affect the membrane separation characteristics significantly by reducing the membrane flux and by changing the rejection of lower molecular weight compounds [5].

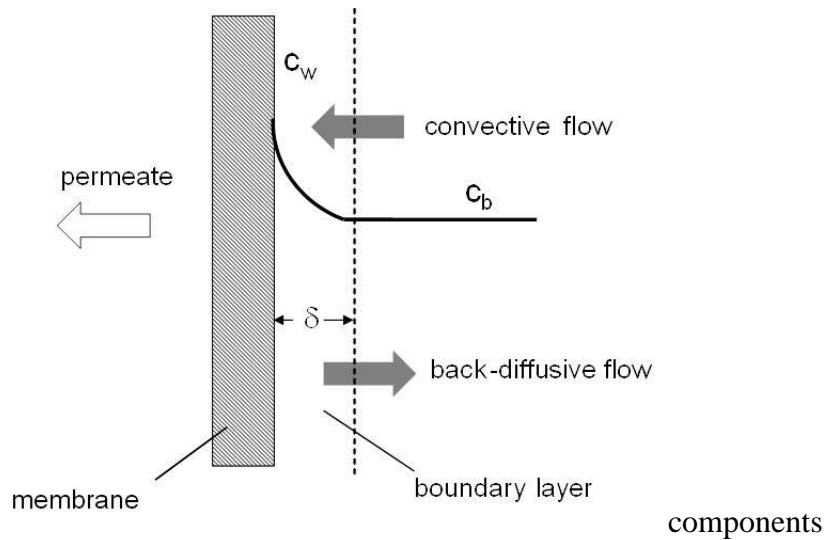


Fig. 1.6. Schematic representation of concentration polarization (c_w = gel concentration; c_b = bulk concentration).

The term *fouling* is referred to a long term flux decline caused by the deposition of retained particles (colloids, suspended particles, macromolecules, etc.) onto the membrane surface and/or within the pores of the membrane. The fouling behavior is strongly affected by the physico-chemical nature of the membrane, the solutes and the fluid dynamic system design.

According to Bacchin et al. [29] the build-up of material may take different forms such as: i) adsorption, when attractive interactions between the membrane and particles exist; ii) pore blockage, with a reduction in flux due to the closure (or partial closure) of pores (this phenomenon is predominant in porous membranes such as MF and UF membranes); iii) a deposit of particles which can grow layer by layer at membrane surface leading to an additional hydraulic resistance; iv) a gel formation due to concentration polarization of macromolecules like pectins.

The type of fouling, described above, can be determined experimentally by using the empirical model developed by Hermia [30-34]. The type of fouling is obtained from the i value obtained in the equation 1.14.

$$\frac{\partial^2 t}{\partial v^2} = k \left(\frac{\partial t}{\partial v} \right)^i \quad (1.14)$$

where the blocking index i and the resistance coefficient k are functions of the blocking models. The model expressed by eq. 1.14 permits, on the basis of experimental data, to point out the fouling mechanism involved in the filtration process, according to the estimated value for i ; for example, $i=2$ is complete blocking, $i=1.5$ is standard blocking, $i=1$ is intermediate blocking, and $i=0$ is cake filtration (Fig. 1.7). The blocking index and the resistance coefficient can be calculated by plotting d^2t/dv^2 versus dt/dv or solving eq.1.14 [35].

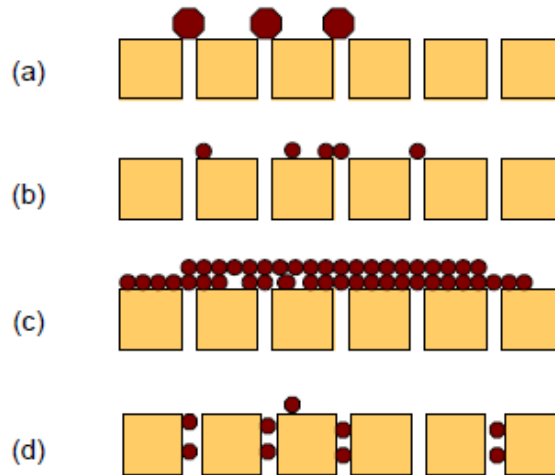


Fig. 1.7. Schematic representation of (a) complete blocking, (b) intermediate blocking, (c) cake filtration and (d) standard blocking in pressure-driven membrane processes.

In addition, fouling can be evaluated by comparing the hydraulic permeability before and after the treatment according to the following equation:

$$Fouling\ Index = \left(1 - \frac{L_p^1}{L_p^0} \right) * 100 \quad (1.15)$$

where L_p^1 and L_p^0 are the hydraulic permeabilities measured after and before the treatment of the feed solution, respectively.

Although polarization concentration and fouling phenomena determine a reduction of the permeate flux they can have an opposite effect on the observed rejection.

The concentration polarization determines a reduction of the rejection; in case of fouling, if the build-up of solids on the membrane is significant enough, it may act as a secondary membrane and change the effective sieving and transport properties of the system: consequently, the rejection can be increased or maintained constant. In addition, while the concentration polarization is a reversible process based on diffusion taking place over a few seconds, fouling is generally irreversible and the flux decline is a long term process. Finally, the concentration polarization can be minimized by hydrodynamic means, such as the feed flow velocity and the membrane module design; on the contrary, the control of membrane fouling is more difficult.

Methods generally accepted to control and minimize fouling phenomena include feed pre-treatment, modification of membrane properties, modification of operating conditions, flow manipulation and membrane cleaning with proper chemical agents. A mathematical model generally accepted to describe concentration polarization phenomena is the well-known *film theory*. As previously reported, this model is more useful in describing transport phenomena through membranes when a polarized layer is reached and the flux becomes independent of pressure.

The film model assumes that the solute is brought to the membrane surface by convective transport at a rate J_s defined as:

$$J_s = J C_B \quad (1.16)$$

where J is the permeate flux and C_B is the bulk concentration of rejected solute. The resulting gradient causes a back-transport of solute into the bulk of the solution due to diffusional effect, which can be described as:

$$J_s = D \frac{dc}{dx} \quad (1.17)$$

where D is the diffusion coefficient and dC/dx is the concentration gradient over a differential element in the boundary layer. Once the steady state is reached, the two mechanisms will balance each other, and Equations (1.16) and (1.17) can be equated and integrated over the boundary layer leading to the following equation:

$$J = \frac{D}{\delta} \ln \frac{C_G}{C_B} = k \ln \frac{C_G}{C_B} \quad (1.18)$$

where C_G is the gel concentration (solute concentration at the membrane surface), and k is the mass transfer coefficient given by:

$$k = \frac{D}{\delta} \quad (1.19)$$

where δ is the thickness of the boundary layer over which the concentration gradient exists.

Several relationships to correlate the mass-transfer coefficients with physical properties, flow channel dimensions, and operating parameters have been reported in literature [36-38]. These relationships generally adapted to specific applications are not universally applicable.

An estimation of the mass transfer coefficient can be approached through a dimensional analysis. By using the π theorem the following equation can be derived:

$$Sh = A (Re)^\alpha (Sc)^\beta \quad (1.20)$$

where Sh , Re and Sc are Sherwood, Reynolds and Schmidt numbers, respectively. The dimensionless numbers can be obtained through Equations (1.21), (1.23) and (1.24).

$$Sh = \frac{k d_h}{D} \quad (1.21)$$

here d_h is the hydraulic diameter that can be calculated as:

$$d_h = 4 \frac{\text{cross section available for flow}}{\text{wetted perimeter of the channel}} \quad (1.22)$$

The Sherwood number is a measure of the ratio of convective mass transfer to molecular mass transfer; the Reynolds number is a measure of the ratio of inertia effect to viscous effect and the state of turbulence in a system can be obtained as:

$$Re = \frac{d_h V \rho}{\mu} \quad (1.23)$$

In general, Re values less than 1800 are considered to be laminar flow, and Re greater than 4000 turbulent flow [4].

The Schmidt number represents the ratio of momentum diffusivity (viscosity) and mass transfer; it is given by:

$$Sc = \frac{\mu}{\rho D} \quad (1.24)$$

The exponents α and β in equation (1.20) are constants determined by the state of development of the velocity and concentration profiles along the channel.

On the other hand, in processes such as NF and RO where membranes are non-porous, the separation occurs by means of a different solubility and diffusivity of components across the membrane due to a concentration or chemical potential gradient. The molecules diffusion through homogeneous dense membranes occurs through the free volume elements, or empty spaces between polymer chains caused by thermal motion of the polymer molecules, which fluctuate in position and volume on the same time scale as the molecule permeates. This type of transport is described by the Fick's law:

$$J_i = -D_i \frac{dC_i}{dz} \quad (1.25)$$

where C_i is the concentration and D_i the diffusion coefficient of a component i .

References

- [1] S.P. Nunes, K.V. Peinemann. 2001. Membrane Technology in the Chemical Industry. Weinheim: Wiley-VCH Verlag GmbH.
- [2] S. Loeb, S. Sourirajan. 1962. Seawater demineralization by means of a semipermeable membrane. In *Advances in Chemistry*, ed. R. Gould, 117-132. Washington: American Chemical Society.
- [3] M. Mota, J.A. Teixeira, A. Yelshin. Influence of cell-shape on the cake resistance in dead-end and cross-flow filtrations. *Separation and Purification Technology*, 27 (2002) 137-44.
- [4] M. Cheryan, 1998. *Ultrafiltration and Microfiltration handbook*. Lancaster: Technomic Publishing Company.
- [5] H. Strathmann, L. Giorno, E. Drioli. 2006. *An introduction to membrane science and technology*. Roma: Consiglio Nazionale delle Ricerche.
- [6] P. Hogan, R. Canning, P. Peterson, R. Johnson, A. Michaels, A new option: osmotic distillation. *Chemical Engineering Progress*, 94 (1998) 49–61.
- [7] R.R. Bhave. 1991. *Inorganic Membranes: Synthesis, Characterization and Application*. New York: Van Nostrand Reinhold.
- [8] J.E. Cadotte. 1985. Evolution of composite reverse osmosis membranes. In *Material Science of Synthetic Membranes*, ed. D.R. Lloyd, ACS Symposium Series 269, 273-294. Washington: American Chemical Society.
- [9] M.A. Frommer, I. Feiner O. Kedem, R. Bloch. Mechanism for formation of skinned membranes: II. Equilibrium properties and osmotic flows determining membrane structure. *Desalination*, 7 (1970) 393-402.
- [10] W.C. Hiatt, G.H. Vitzthum, K.B. Wagner, K. Gerlach, C. Josefiak. 1985. Microporous membranes via upper critical temperature phase separation. In *Material Science of Synthetic Membranes*, ed. D.R. Lloyd, ACS Symposium Series 269, 229-244. Washington: American Chemical Society.
- [11] K. Kamide, S. Manabe. 1985. Role of microphase separation phenomena in the formation of porous polymeric membranes. In *Material Science of Synthetic Membranes*, ed. D.R. Lloyd, ACS Symposium Series 269, 197-228. Washington: American Chemical Society.

- [12] R.E. Kesting. 1985. Phase inversion membranes. In *Material Science of Synthetic Membranes*, ed. D.R. Lloyd, ACS Symposium Series 269, 131-164. Washington: American Chemical Society.
- [13] J. Smid, C. Avci, V. Guenay, R.A. Terpstra, J.P.G.M. Van Eijk.. Preparation and characterization of microporous ceramic hollow fiber membranes. *Journal of Membrane Science*, 112 (1996) 85-90.
- [14] S. Sourirajan, B. Kunst. 1977. Cellulose acetate and other cellulose ester membranes. In *Reverse osmosis and synthetic membranes*, ed. S. Sourirajan, 129-152. Ottawa: National Research Council Canada.
- [15] H. Strathmann. 1985. Production of microporous media by phase inversion processes. In *Material Science of Synthetic Membranes*, ed. D.R. Lloyd, ACS Symposium Series 269, 165-195. Washington: American Chemical Society.
- [16] R.E. Kesting. 1971. *Synthetic polymeric membranes*. New York: McGraw-Hill.
- [17] J.E. Cadotte, R.I. Petersen. 1981. Thin film reverse osmosis membranes: Origin, development, and recent advances. In: *Synthetic membranes*, ed. A.F. Turbak, ACS Symposium series 153, 305-325. Washington: American Chemical Society.
- [18] T. Tanaka, K.I. Abe, H. Asakawa, H. Yoshida, K. Nakanishi. Filtration characteristics and structure of cake in cross-flow filtration of bacterial suspension. *Journal of Fermentation and Bioengineering*, 78 (1994) 455-61.
- [19] F.M. Tiller, H.R. Cooper. The role of porosity in filtration. Part V, Porosity variation in filter cakes. *American Institute of Chemical Engineers* 8 (1962)445-9.
- [20] F.M. Tiller, C.S. Yeh. The role of porosity in filtration. Part X. Deposition of compressible cakes on external radial surface. *American Institute of Chemical Engineers*, 31 (1985) 1241-8.
- [21] P. Rai, G.C. Majumdar, G. Sharma, S. DasGupta, S. De. Effect of various cutoff membranes on permeate flux and quality during filtration of mosambi (*Citrus sinensis* L.) Osbeck juice. *Food and Bioproducts Processing*, 84 (2006) 213-9.
- [22] V. Singh, P.K. Jain, C. Das. Performance of spiral wound ultrafiltration membrane module for with and without permeate recycle: Experimental and theoretical consideration. *Desalination*, 322 (2013) 94-103.
- [23] S.F. Mexis, M.G. Kontominas. Effect of oxygen absorber, nitrogenflushing, packaging material oxygen transmission rate and storage conditions on quality retention of raw whole unpeeled almond kernels (*Prunus dulcis*). *LWT-Food Science and Technology*, 43 (2010) 1-11.

- [24] C. Das, P. Patel, S. De, S. Das Gupta. Treatment of tanning effluent using nanofiltration followed by reverse osmosis. *Separation and Purification Technology*, 50 (2006) 291-9.
- [25] K.S. Youn, J.H. Hong, D.H. Bae, S.J. Kim, S.D. Kim. Effective clarifying process of reconstituted apple juice using membrane filtration with filter-aid pretreatment. *Journal of Membrane Science*, 228 (2004) 179-86.
- [26] P. Aimar, J.A. Howell, M. Turner. Effects of concentration boundary layer development on the flux limitations of ultrafiltration. *Chemical Engineering Research and Design*, 67 (1989) 255-61.
- [27] M. Mulder. 1991. *Basic Principles of Membrane Technology*. Dordrecht: Kluwer Academic Publishers.
- [28] G. Belfort. Fluid mechanics in membrane filtration. *Journal of Membrane Science*, 40 (1989) 123-147.
- [29] P. Bacchin, P. Aimar, R.W. Field. Critical and sustainable fluxes: Theory, experiments and applications. *Journal of Membrane Science*, 281 (2006) 42–69.
- [30] M.C. Vincent Vela, S. Alvarez Blanco, J. Lora García, E. Bergantiños Rodríguez, Analysis of membrane pore blocking models adapted to crossflow ultrafiltration in the ultrafiltration of PEG. *Chemical Engineering Journal*, 149 (2009) 232–241.
- [31] R.W. Field, D. Wu, J.A. Howell, B.B. Gupta, Critical flux concept for microfiltration fouling. *Journal of Membrane Science*, 100 (1995) 259–272.
- [32] J. Hermia, Constant pressure blocking filtration law: application to power law non-Newtonian fluids. *Transaction of the Institution of Chemical Engineers*, 60 (1982) 183–187.
- [33] C. Duclos-Orsello, W. Li, C.C. Ho, A three mechanism model to describe fouling of microfiltration membranes. *Journal of Membrane Science*, 280 (2006) 856–866.
- [34] M.C. Vincent Vela, S. Alvarez Blanco, J. Lora García, E. Bergantiños Rodríguez, Analysis of membrane pore blocking models applied to the ultrafiltration of PEG. *Separation and Purification Technology*, 62 (2008) 489–498.
- [35] K.J. Hwang, C.Y. Liao, K.L. Tung, Analysis of particle fouling during microfiltration by use of blocking models. *Journal of Membrane Science*, 287 (2007) 287–293.

- [36] V. Gekas, B. Hallstrom. Mass transfer in the membrane concentration polarization layer under turbulent cross flow: I. Critical literature review and adaptation of existing Sherwood correlation to membrane operations. *Journal of Membrane Science*, 30 (1987) 153-70.
- [37] R.K. Sherwood, R.L. Pigford, C.R. Wilke. 1975. *Mass transfer*. New York: McGraw-Hill.
- [38] R.E. Treybal. 1981. *Mass transfer operations*. New York: McGraw-Hill.

CHAPTER 2

Citrus fruit processing and orange press liquor characterization

2.1 Citrus fruits: properties and global market

Citrus fruits are probably the most known and extensive fruits around the world. Citrus is the general terms referred to products such as oranges, lemons, grapefruits and limes. Several authors have mentioned that the origin of citrus was in the southeast China and Southeast Asia [1]. Today citrus is cultivated principally in subtropical areas, where the environmental conditions are optimal for its productions. World citrus production and consumption have grown strongly since the mid-1980s. Production of oranges, tangerines, lemons and limes has expanded rapidly, and even faster growth has been realized for processed citrus products as improvements in transportation and packaging have lowered costs and improved quality. The projected orange production in 2010 was 66.4 million tonnes, approximately 14 percent greater than that realized over the 1997-99 period. The projected production was expected to be utilized as 36.3 million tonnes fresh and 30.1 million tonnes processed. Italy is an important orange producer in the EU with a production equal to 2,393,660 tonnes/year that represents the 3.45% of the world production according with the data published by the Food and Agriculture Organization of the United Nations (FAOSTAT) [2].

Citrus is a product with many desirable characteristics for consumers who are health-conscious, demand convenience and place a premium on food safety. Phenolic compounds present in citrus fruits have gained a lot of importance due to their potential as prophylactic and therapeutic agents in many diseases [3-9]. In human body reactive oxygen species (ROS) and reactive nitrogen species (RNS) are constantly generated for physiological purposes and often over-produced in pathological conditions, resulting in oxidative stress which is defined as “an imbalance” between oxidants and antioxidants in favour of the oxidants, potentially leading to damage [10-12]. Oxidative stress can damage lipids, proteins, enzymes, carbohydrates and DNA in cells and tissues, resulting

in membrane damage, fragmentation or random cross linking of molecules like DNA, enzymes and structural proteins and even lead to cell death induced by DNA fragmentation and lipid peroxidation [13]. These consequences of oxidative stress construct the molecular basis in the development of cancer, neurodegenerative disorders, cardiovascular diseases, diabetes and autoimmune disorders [3].

The antioxidant defence system in the human body consist of in several systems such as enzymatic scavengers, hydrophilic scavengers and lipophilic radical scavengers [10,11]. Some of these agents are synthesized by cell itself; however the majority, including ascorbic acid, polyphenols and carotenoids, are derived from dietary sources. For this reason antioxidants have gained a great interest in recent year because of their potential as prophylactic and therapeutic agents in many diseases. The discovery of the role of free radicals in cancer, diabetes, cardiovascular diseases, autoimmune diseases, neurodegenerative disorders, aging and other diseases has led to a medical revolution that is promising a new paradigm of healthcare [3-9].

The global market of antioxidants is increasing rapidly, because of the increased health risk in a constantly polluting environment. These agents also have cosmetic applications, leading to the development of researchers at industrial and academic level to explore these molecules and their analogues [3]. In this way there is a great biomedical interest in the separation, purification and recovery of antioxidant compounds from natural sources. In particular, the consumption of citrus fruits appears to be associated with lower risk of colorectal, esophageal [14,15], gastric [16,17], and stomach [18] cancers, and stroke [17,19-21]. Citrus fruits also appear to be associated with improved blood lipid profiles [22], and improved survival in the elderly [23]. The components responsible for these beneficial effects are unknown, but the citrus flavonoids are one group of compounds that may be involved [24-38]. Some flavonoids have been reported to possess a variety of biological activities and pharmacological properties, including antiallergic, antidiabetic, antiinflammatory, antiviral, antiproliferative, and anticarcinogenic activities, in addition to having effects on mammalian metabolism [17,39].

Flavonoids are widely distributed in fruits, vegetables, fruit juices, cocoa, teas and wines [40] where their distribution depends on several factors, including variation and

degree of light exposure [41]. Most Citrus species accumulate substantial quantities of flavonoids during the development of their different organs [40].

More than 5000 different plant-derived flavonoids have been isolated from various plants [42]. They are classified into at least 10 chemical groups. Flavanones, flavones, isoflavonoids, flavans (flavanols), anthocyanins, and flavonols are particularly common in the diet [42-44]. Flavanones are mainly found in citrus fruits [45]. The dominant flavanone glycosides in sweet oranges (*Citrus sinensis*) are hesperidin and narirutin [46].

Plant material wastes from industries contain high levels of phenolic compounds. Importantly, most of this phytonutrients are found in the orange peel, in the inner white pulp, rather than in the juice, so these beneficial compounds are too often removed by the processing of orange into juice [4,47,48]. Membrane processes such as microfiltration (MF) and ultrafiltration (UF) can be considered a valid approach for separating and recovering valuable compounds from finely divided solid materials present in orange wastes [49].

2.2 Citrus processing

The popularity of orange juice dramatically increased again with the development of the commercial orange juice industry in the late 1920s. In its early days, the juice industry primarily relied on salvaged fruit, which was unsuitable for regular consumption because it was misshapen, badly coloured or blemished. In the 1930s, development of porcelain-lined cans and advances in pasteurization techniques led to improved juice quality and the industry expanded significantly. Then, in 1944, scientists found a way to concentrate the juice by thermal and freezing system without destroying the flavour or vitamin content. After the second world war, concentrated juices became the predominant form.

An overview of the classical production process of orange juice is shown in Fig. 2.1. The major unit operations will be described in the following.

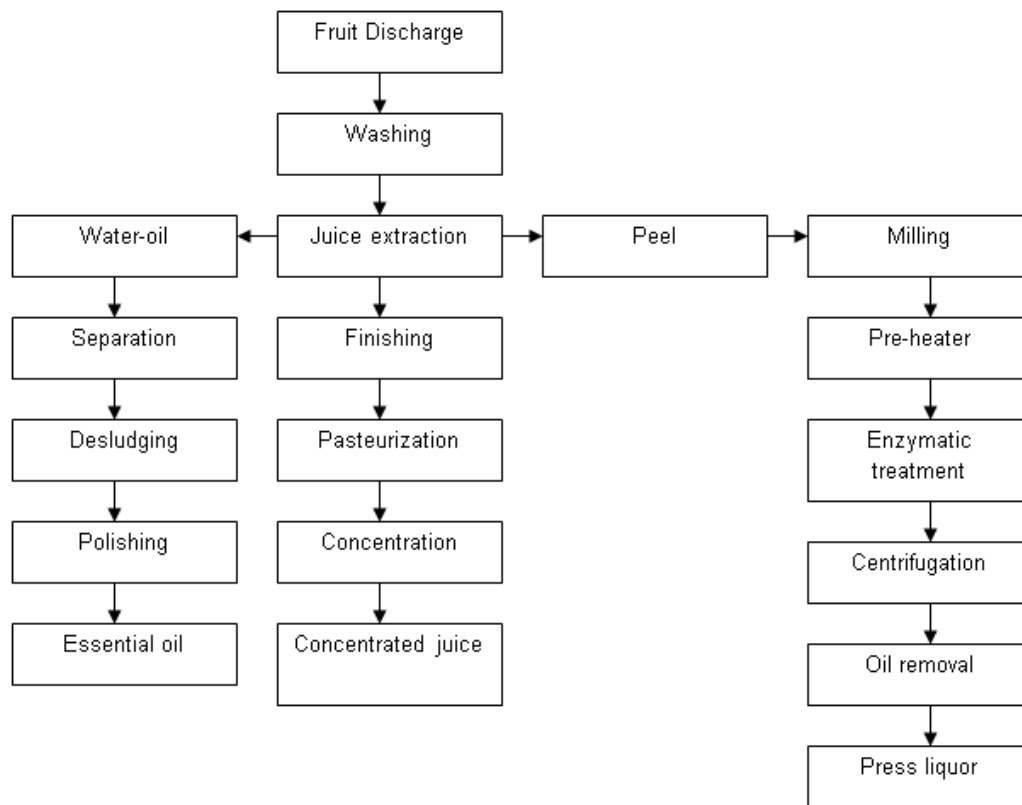


Fig. 2.1. Flowchart of industrial orange juice processing.

Cleaning/Grading: The fruit is transported along a conveyor belt where it is washed with a detergent as it passes over roller brushes. This process removes debris and dirt and reduces the number of microbes. The fruit is rinsed and dried. Graders remove bad fruit as it passes over the rollers and the remaining quality pieces are automatically segregated by size prior to extraction. Proper size is critical for the extraction process.

Extraction: Proper juice extraction is important to optimize the efficiency of the juice production process as well as the quality of the finished drink. The latter is true because oranges have thick peels, which contain bitter resins that must be carefully separated to avoid tainting the sweeter juice. There are two automated extraction methods commonly used by the industry. The first places the fruit between two metal cups with sharpened metal tubes at their base. The upper cup descends and the fingers on each cup mesh to express the juice as the tubes cut holes in the top and bottom of the fruit. The fruit solids are compressed into the bottom tube between the two plugs of peel while the juice is

forced out through perforations in the tube wall. At the same time, a water spray washes away the oil from the peel. This oil is reclaimed for later use.

The second type of extraction has the oranges cut in half before the juice is removed. The fruits are sliced as they pass by a stationary knife and the halves are then picked up by rubber suction cups and moved against plastic serrated reamers. The rotating reamers express the juice as the orange halves travel around the conveyor line.

Some of the peel oil may be removed prior to extraction by needles which prick the skin, thereby releasing the oil which is washed away. Modern extraction equipment of this type can slice, ream, and eject a peel in about 3 seconds.

The extracted juice is filtered through a stainless steel screen before it is ready for the next stage. At this point, the juice can be chilled or concentrated.

Pasteurization: Thanks to its low pH (about 4), orange juice has some natural protection from bacteria, yeast, and mold growth. However, pasteurization is still required to further retard spoilage. Pasteurization also inactivates certain enzymes which cause the pulp to separate from the juice, resulting in an aesthetically undesirable beverage. This enzyme related clarification is one of the reasons why fresh squeezed juice has a shelf life of only a few hours. Flash pasteurization minimizes flavour changes from heat treatment and is recommended for premium quality products. Several pasteurization methods are commercially used. One common method passes juice through a tube next to a plate heat exchanger, so the juice is heated without direct contact with the heating surface. Another method uses hot, pasteurized juice to preheat incoming unpasteurized juice. The preheated juice is further heated with steam or hot water to the pasteurization temperature. Typically, reaching a temperature of 85-94°C for about 30 seconds is adequate to reduce the microbe count.

Concentration: Concentrated juice is approximately five times more concentrated than squeezed juice. Concentration is useful because it extends the shelf life of the juice and makes storage and shipping more economical. Juice is commonly concentrated with a piece of equipment known as a Thermally Accelerated Short-Time Evaporator

(TASTE). Concentrated juice is discharged to a vacuum flash cooler, which reduces the product temperature to about 13°C.

Packaging/filling: To ensure sterility, the pasteurized juice should be filled while still hot. Where possible, metal or glass bottles and cans can be preheated. Packaging which cannot withstand high temperatures (e.g., aseptic, multilayer plastic juice boxes which do not require refrigeration) must be filled in a sterile environment. Instead of heat, hydrogen peroxide or another approved sterilizing agent may be used prior to filling. In any case, the empty packages are fed down a conveyor belt to liquid filling machinery, which is fed juice from bulk storage tanks. The filling head meters the precise amount of product into the container, and depending on the design of the package, it may immediately invert to sterilize the lid. After filling, the containers are cooled as fast as possible. Orange juice packaged in this manner has a shelf life of 6-8 months at room temperature.

During the juice production two-thirds of the mass becomes juice. The wastes generated consist basically in wet peels and whole rejected fruits that contain 82% of water [50]. These residues have a great amount of organic matter that can be associated with environmental and health problems due to water runoff and uncontrolled fermentation; consequently, their treatment is necessary. Recent R&D efforts aim to convert the potential of wastes into profitable products creating new segments of production and offsetting the disposal costs. Orange peels and pulp contain several bioactive compounds, such as flavonoids and phenolic acids, recognized for their beneficial implications in human health due to their antioxidant activity and free radical scavenging ability [51]. These semi-solid wastes can be pressed to obtain a liquid rich in soluble sugars, named *press liquor*, that can be concentrated up to citrus molasses grade or alternatively exploited as a natural source for the extraction of phenolic compounds which can be used as natural antioxidants mainly in foods to prevent the rancidity and oxidation of lipids.

2.3 Press liquor characterization

The orange press liquor contains different components that could be summarised in three principal groups: i) macromolecules (i.e. pectins); ii) high levels of phenolic compounds, including flavonoids [4] and phenolic acids; iii) sugars such as fructose, glucose and sucrose [52].

In this work experimental activities were performed starting from a raw orange press liquor supplied by Gioia Succhi Srl (Rosarno, Reggio Calabria, Italy).

Several analysis, as described in the following, were performed to characterise the raw press liquor as well as fractions (permeates and retentates) produced in experimental activities performed by using membrane operations. Analysis were mainly focused in the evaluation of phenolic compounds and sugars.

2.3.1 Analysis of phenolic compounds

The determination and quantification of flavonoids was carried out by using a HPLC system (Shimadzu LC-20AB, Kyoto, Japan) equipped with a UV/vis detector (SPD-20A), monitored at 284 nm and 360 nm. The system consisted of a binary pump and auto sampler. The column used was a Discovery C18: 25cm x 4.6mm, 5 μ m. The mobile phase consisted of two solvents: Solvent A, water/ phosphoric acid (0.1% v/v) and Solvent B, acetonitrile. Phenolic compounds were eluted under the following conditions: 1 mL/min flow rate and ambient temperature; gradient conditions from 0% to 5% B in 0.01 min, from 5% to 10% B in 19.9 min, from 10% to 20% B in 20 min, from 20% to 25% B in 20 min, from 25% to 35% B in 20 min, from 35% to 60% B in 15 min, from 60% to 5% B in 3 min, followed by washing and reconditioning the column. The identification of phenolic compounds was obtained comparing the retention times using authentic standards, while quantification of hesperidin was performed by external calibration with standards.

2.3.2 Analysis of sugars

The quantification of sugars was carried out by using a HPLC approach as well as a refractometric method. HPLC analysis were carried out at 40°C on an Agilent 1100 HPLC system (Agilent Technologies, Palo Alto, CA-USA) equipped with a Luna reverse phase C18 column (5 μ , 100 Å, 250×4.6 mm i.d. from Phenomenex), an isocratic pump (model series 1100) and a refractive index detector (Series 200a). Isocratic elution was used at a flow rate of 1 mL/min with two solvents: Solvent A, water/acetic acid (0.1% v/v), 80%, and Solvent B, methanol, 20%. For each reference sugar, a set of calibration standards using stock and working reference standard solutions were prepared. Sugars (glucose, fructose and sucrose) were purchased from Sigma-Aldrich (Milan, Italy). Sugar standards were dried at 60 °C in a vacuum oven overnight and dissolved in 50% methanol (injection solvent). The resulting solutions were filtered using a syringe filter and injected into HPLC. The injection volume was 20 μ l. Sugar concentration of glucose, fructose and sucrose for each sample was calculated based on peak area measurements and expressed in mg/L.

Total soluble solids (TSS) were determined by using ATAGO (Tokyo, Japan) refractometer at 20°C. Results were expressed as °Brix (1°Brix is equivalent to 1g of TSS per 100g of press liquor).

2.3.3 Determination of total phenols content

Total phenols were estimated colorimetrically by using the Folin–Ciocalteu method [53,54]. The method is based on the reduction of tungstate and/or molybdate in the Folin–Ciocalteu reagent by phenols in alkaline medium resulting in a blue coloured product. Gallic acid was used as a calibration standard and results were expressed as gallic acid equivalent (GAE) (mg GAE/L). The absorbance was measured by using a UV–visible spectrophotometer (Shimadzu UV-160A, Japan) at 765 nm.

2.3.4 Determination of the total antioxidant activity (TAA)

Total Antioxidant Activity (TAA) was determined by an improved version of the ABTS radical cation decolourisation assay in which the chromogenic ABTS (2,2-azino-bis-(3-ethylbenzothiazoline-6-sulfonic acid) radical cation is generated by oxidation of ABTS with potassium persulphate before the addition of the antioxidant [55,56]. The ABTS decolourisation was measured as inhibition percentage of the absorbance at 734 nm. The concentration of antioxidant giving the same inhibition percentage of absorbance of the radical cation as 1 mM 6-hydroxy-2,5,7,8-tetramethylchroman-2-carboxylic acid (Trolox) was calculated in terms of the Trolox Equivalent Antioxidant Capacity (TEAC) at 5 min contact.

2.3.5 Analytical results

Fig. 2.2 shows the chromatographic profile of phenolic compounds obtained for the raw press liquor. Phenolic compounds were better appreciated at 280 nm. The highest peak was found to be hesperidin with an intensity value of 105763 μ V and a retention time of 46.958 min. To quantify the hesperidin a calibration curve was developed using four levels of concentration (20, 50, 100 and 200 mg/L). The calibration curve had coefficient of linear correlation equal to 0.992 with y-intercept close to zero.

These results are in agreement with similar works, where hesperidin has been found as the principal flavonoid present in the orange peel [46]. Although there are at least ten phenolic compounds in the press liquor, hesperidin was selected to evaluate the membrane performance in terms of selectivity towards flavonoids.

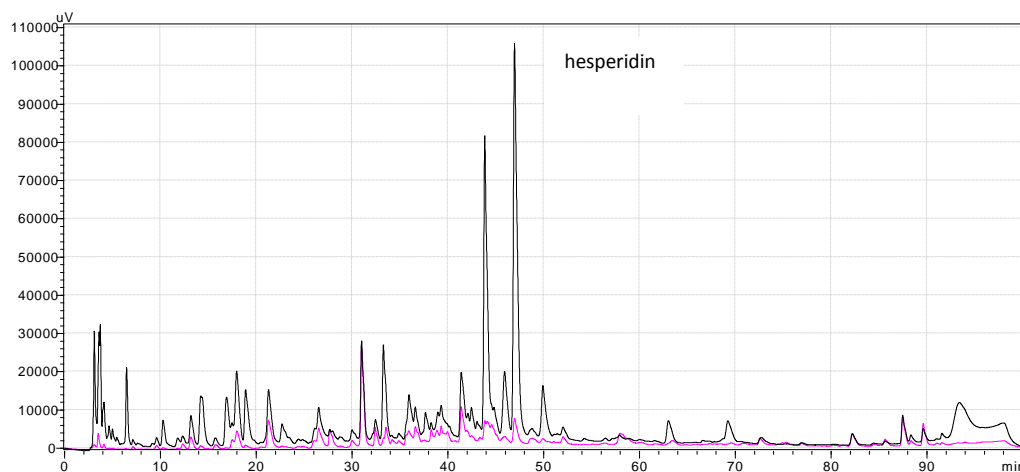


Fig. 2.2. HPLC chromatogram of orange press liquor. black line at 280 nm (for hydroxybenzoic acids and flavones) and pink line at 360 nm (for hydroxycinnamic acids).

Results related to the physico-chemical characterization of raw press liquor is shown in Table 2.1.

Table 2.1. Physico-chemical characteristics of raw orange press liquor.

	Value	
Hesperidin (mg/L)	159.60 ± 14.42	
Glucose (mg/L)	132.30	
Fructose (mg/L)	169.32	
Sucrose (mg/L)	21.07	
Total soluble solid (°brix)	8.6 ± 0.1	
Solid content, after lyophilisation (g/100mL)	4.94 ± 0.04	
Density (kg/L)	1.02835 ± 0.0005	
pH	3.58 ± 0.03	
Total antioxidant activity (TAA) (mM trolox)	63.66 ± 0.87	
	15°C	1.60 ± 0.02
Viscosity (cp)	25°C	1.45 ± 0.01
	35°C	1.31 ± 0.03

The press liquor is a colloidal suspension similar to a cloudy orange juice. Components such as pectin, sugars, and the dispersed (colloidal) matter are mainly formed by cellular tissue crushed during processing. Therefore, the first step, included in the following Chapter, was devoted to clarify the press liquor in order to remove suspended solids, fibres and macromolecular compounds responsible of its turbidity.

References

- [1] F. Gmitter, X. Hu. The possible role of Yunnan, China, in the origin of contemporary citrus species (rutaceae). *Economic Botany*, 44 (1990) 267-277.
- [2] FAOSTAT, 2010, Available at: <http://faostat.fao.org/site/479/default.aspx> (accessed May 2012).
- [3] D.V. Ratnam, D.D Ankola, V. Bharswaj, D.K Sahana, M.N.V Ravi Kumar, Role of antioxidants in prophylaxis and therapy: A pharmaceutical perspective. *Journal of Controlled Release*, 113 (2006) 189-207
- [4] S.M.S. Sawalha, D. Arráez-Román, A. Segura-Carretero, A. Fernández-Gutiérrez, Quantification of main phenolic compound in sweet and bitter orange Peel using CE-MS/MS. *Food Chemistry*, 116 (2009) 567-574
- [5] P.M. Kris-Etherton, K.D. Hecker, A. Bonanome, S.M. Coval, A.E. Binkoski, K.F. Hilpert. Bioactive compounds in foods: their role in the prevention of cardiovascular disease and cancer. *The American Journal of Medicine*, 113(9) (2002) 71–88.
- [6] S. Liu, J.E. Manson, I.M. Lee, R.C. Stephen, C.H. Hennekens, W.C. Willett. Fruit and vegetable intake and risk of cardiovascular disease: the women’s health study. *American Journal of Clinical Nutrition*, 72 (2000) 922–928.
- [7] N. Salah, N.J. Miller, G. Paganga, L. Tijburg, G.P. Bolwell, C. Riceevans. Polyphenolic flavanols as scavengers of aqueous phase radicals and as chain-breaking antioxidants. *Archives of Biochemistry and Biophysics*, 322(2) (1995) 339–346.
- [8] J.W. Lampe. Health effects of vegetables and fruits: assessing mechanisms of action in human experimental studies. *American Journal of Clinical Nutrition*, 70 (1999) 475s–490s.
- [9] C.J. Guo, J.J. Yang. Progress in the study of antioxidant capacity of fruits and vegetables. *China Public Health*, 17 (2001) 87–88.
- [10] Y.Z.S. Fang, S. Yang, G.Y. Wu. Free radicals, antioxidants and nutrition, *Nutrition*, 18 (2002) 872–879.
- [11] R.A. Jacob. The integrated antioxidant system. *Nutrition Research*, 15 (1995) 755–766.

- [12] H. Sies. Oxidative stress: oxidants and antioxidants. *Experimental Physiology*, 82 (1997) 291–295.
- [13] K.B. Beckman, B.N. Ames. The free radical theory of aging matures. *Physiological Reviews*, 78 (1998) 547–581.
- [14] H. Chen, M. Ward, B. Graubard, E. Heineman, R. Markin, N. Potischman, R. Russell, D. Weisenburger, L. Tucker. Dietary patterns and adenocarcinoma of the esophagus and distal stomach. *The American Journal of Clinical Nutrition*, 75, (2002) 137–144.
- [15] F. Levi, C. Pasche, F. Lucchini, C. Bosetti, S. Franceschi, P. Monnier, C. La Vecchia. Food groups and oesophageal cancer risk in Vaud, Switzerland. *European Journal of Cancer Prevention*, 9 (2000) 257–263.
- [16] D. Palli, A. Russo, L. Ottini, G. Masala, C. Saieva, A. Amorosi, A. Cama, C. D'Amico, M. Falchetti, R. Palmirota, A. Decarli, R.M. Costantini, J.F. Fraumeni Jr. Red meat, family history, and increased risk of gastric cancer with microsatellite instability. *Cancer Research*, 61 (2001) 5415–5419.
- [17] R.S.R. Zand, D.J.A. Jenkins, E.P. Diamandis. Flavonoids and steroid hormone-dependent cancers. *Journal of Chromatography B*, 777 (2002) 219–232.
- [18] M. McCullough, A. Robertson, E. Jacobs, A. Chao, E. Calle, M. Thun. A prospective study of diet and stomach cancer mortality in United States men and women. *Cancer Epidemiology, Biomarkers and Prevention*, 10 (2001) 1201–1205.
- [19] E. Feldman. Fruits and vegetables and the risk of stroke. *Nutrition Reviews*, 59 (2001) 24–27.
- [20] K. Joshipura, A. Ascherio, J. Manson, M. Stampfer, E. Rimm, F. Speizer, C. Hennekens, D. Spiegelman, W. Willett. Fruit and vegetable intake in relation to risk of ischemic stroke. *JAMA*, 282 (1999) 1233–1239.
- [21] A.M. Hackett, (1986). The metabolism of flavonoid compounds in mammals. In *Plant Flavonoids in Biology and Medicine: Biochemical Pharmacological, and Structural-Activity Relationships*, p. 177-194, Alan R. Liss, New York, NY USA
- [22] E. Kurowska, J. Spence, J. Jordan, S. Wetmore, D. Freeman, L. Piche, P. Serratore. HDL-cholesterol-raising effect of orange juice in subjects with hypercholesterolemia. *The American Journal of Clinical Nutrition*, 72 (2000) 1095–1100.

- [23] C. Fortes, F. Forastiere, S. Farchi, E. Rapiti, G. Pastori, C. Perucci. Diet and overall survival in a cohort of very elderly people. *Epidemiology*, 11 (2000) 440–445.
- [24] F. Areias, A. Rego, C. Oliveira, R. Seabra. Antioxidant effect of flavonoids after ascorbate/Fe(2+)-induced oxidative stress in cultured retinal cells. *Biochemical Pharmacology*, 62 (2001) 111–118.
- [25] E. Bae, M. Han, D. Kin. In vitro anti-helicobacter pylori activity of some flavonoids and their metabolites. *Planta Medica*, 65 (1999) 442–443.
- [26] W. Bear, R. Teel. Effects of citrus phytochemicals on liver and drug cytochrome P450 activity and on the in vitro metabolism of the tobacco-specific nitrosamine NNK. *Anticancer Research*, 20 (2000) 3323–3329.
- [27] W. Bear, R. Teel. Effects of citrus flavonoids on the mutagenicity of heterocyclic amines and on cytochrome P450 1A2 activity. *Anticancer Research*, 20 (2000) 3609–3614.
- [28] N. Borradaile, K. Carroll, E. Kurowska. Regulation of HepG2 cell apolipoprotein B metabolism by the citrus flavanones hesperetin and naringenin. *Lipids*, 34 (1999) 591–598.
- [29] C. de Gregorio Alapont, R. Garcia-Domenech, J. Galvez, M. Ros, S. Wolski, M. Garcia. Molecular topology, a useful tool for the search of new antibacterials. *Bioorganic and Medicinal Chemistry Letters*, 10 (2000) 2033–2036.
- [30] S. Jeon, S. Bok, M. Jang, M. Lee, K. Nam, Y. Park, S. Rhee, M. Choi. Antioxidative activity of naringin and lovastatin in high cholesterol-fed rabbits. *Life Sciences*, 69 (2001) 2855–2866.
- [31] Y. Kato, Y. Miyake, K. Yamamoto, Y. Shimomura, H. Ochi, Y. Mori, T. Osawa. Preparation of a monoclonal antibody to N(epsilon)-(hexanonyl)lysine, application to the evaluation of protective effects of flavonoid supplementation against exercise-induced oxidative stress in rat skeletal muscle. *Biochemical and Biophysical Research Communications*, 274 (2000) 389–393.
- [32] D. Kim, M. Song, E. Bae, M. Han. Inhibitory effect of herbal medicines on rotavirus infectivity. *Biological and Pharmaceutical Bulletin*, 23 (2000) 356–358.
- [33] H. Kohno, M. Taima, T. Sumida, Y. Azuma, H. Ogawa, T. Tanaka. Inhibitory effect of mandarin juice rich in beta-cryptoxanthin and hesperidin on 4-(methylnitrosamino)-1-(3-pyridyl)-1-butanone-induced pulmonary tumorigenesis in mice. *Cancer Letters*, 174 (2001) 141–150.

- [34] J. Manthey, K. Grohmann, N. Guthrie. Biological properties of citrus flavonoids pertaining to cancer and inflammation. *Current Medicinal Chemistry*, 8 (2001) 135–153.
- [35] Y. Miyagi, A. Om, K. Chee, M. Bennink. Inhibition of azoxymethane-induced colon cancer by orange juice. *Nutrition and Cancer*, 36 (2000) 224–229.
- [36] Y. Miyake, K. Shimoi, S. Kumazawa, K. Yamamoto, N. Kinae, T. Osawa. Identification and antioxidant activity of flavonoid metabolites in plasma and urine of eriocitrin-treated rats. *Journal of Agricultural and Food Chemistry*, 48 (2000) 3217–3224.
- [37] L. Wilcox, N. Borradaile, L. de Dreu, M. Huff. Secretion of hepatocyte apoB is inhibited by the flavonoids, naringenin and hesperetin, via reduced activity and expression of ACAT2 and MTP. *Journal of Lipid Research*, 45 (2001) 725–734.
- [38] M. Zhang, J. Zhang, H. Ji, J. Wang, D. Qian. Effect of six flavonoids on proliferation of hepatic stellate cells in vitro. *Acta Pharmacologica Sinica*, 21 (2000) 253–256.
- [39] W. Ren, Z. Qian, H. Wang, L. Zhu, L. Zhang. Flavonoids: Promising anticancer agents. *Medicinal Research Reviews*, 23(4) (2003) 519–534.
- [40] O. Benavente-Garcia, J. Castillo, J.A. Del Rio. Changes in neodiosmin levels during the development of *Citrus aurantium* leaves and fruits postulation of a neodiosmin biosynthetic pathway. *Journal of Agricultural and Food Chemistry*, 41 (1993) 1916–1919.
- [41] M.T. Huang, T. Osawa, C.T. Ho, R.T. Rosen. (1994) *Food Phytochemicals for Cancer Prevention. I. Fruits and Vegetables*. Austin, TX: American Chemical Society.
- [42] N.C. Cook, S. Samman. Review: Flavonoids—chemistry, metabolism, cardioprotective effects, and dietary sources. *Journal of Nutritional Biochemistry*, 7 (1996) 66–76.
- [43] L. Bravo. Polyphenols: Chemistry, dietary sources, metabolism, and nutritional significance. *Nutrition Reviews*, 56 (1988) 317–333.
- [44] A.S. Aherne, N.M. O'Brien. Dietary flavonols: Chemistry, food content and metabolism. *Nutrition*, 18 (2002) 75–81.
- [45] L.H. Yao, Y.M. Jiang, J. Shi, F.A. Tomás, S. Barbera, N. Datta, R. Singanusong, S.S. Chen. Flavonoids in Food and Their Health Benefits. *Plant Foods for Human Nutrition*, 59 (2004) 113–122

- [46] J.J. Petersona, J.T. Dwyera, G.R. Beecherb, S.A. Bhagwatc, S.E. Gebhardtc, D.B. Haytowitzc, J.M. Holdenc. Flavanones in oranges, tangerines (mandarins), tangors, and tangelos: a compilation and review of the data from the analytical literature. *Journal of Food Composition and Analysis*, 19 (2006) S66–S73
- [47] D. Bagchi, M. Bagchi, S.J. Stohs, S.D. Ray, C.K. Sen, H.G. Preuss. Free radicals and grape seed proanthocyanidin extract: importance in human health and disease prevention. *Toxicology*, 148 (2) (2000) 187–189.
- [48] R.P. Singh, K.N.C. Murthy, G.K. Jayaprakasha. Studies on the antioxidant activity of pomegranate peel and seed extracts using in vitro models. *Journal of Agricultural and Food Chemistry*, 50 (2002) 81–86.
- [49] R.A. Ruby-Figueroa, A. Cassano, E. Drioli, Ultrafiltration of orange press liquor: Optimization for permeate flux and fouling index by response surface methodology. *Separation and purification technology*, 80 (2011) 1-10.
- [50] R.M. Goodrich, R.J. Braddock. 2004. Major By-products of the Florida Citrus Processing Industry, Series of the Food Science and Human Nutrition Department, University of Florida, FSHN05-22.
- [51] U. Imeh, S. Khokhar. Distribution of conjugated and free phenols in fruits: antioxidant activity and cultivar variations. *Journal of Agricultural and Food Chemistry*, 50 (2002) 6301-6306.
- [52] E.M. Garcia-Castello, J. R. McCutcheon. Dewatering press liquor derived from orange production by forward osmosis. *Journal of Membrane Science*, 372 (2011) 97–101.
- [53] E. Roura, C. Andrés-Lacueva, R. Estruch, M.R. Lamuela-Raventós. Total polyphenol intake estimated by modified Folin–Ciocalteu assay of urine. *Clinical Chemistry*, 52 (2006) 749–752.
- [54] V.L. Singleton, R. Orthofer, R.M. Lamuela-Raventos, Analysis of total phenols and other oxidation substrates and antioxidants by means of Folin–Ciocalteu reagent. *Method in Enzymology*, 299 (1999) 152.
- [55] C.A. Rice-Evans, N.J. Miller. Total antioxidant status in plasma and body fluids. *Method in Enzymology*, 243 (1994) 279–298.
- [56] R. Re, N. Pellegrini, A. Proteggente, A. Pannala, M. Yang, C.A. Rice-Evans, Antioxidant activity applying and improved ABTS radical cation decolorization assay. *Free Radical Biology and Medicine*, 26 (1999) 1231–1237.

CHAPTER 3

Orange press liquor clarification

Orange press liquor is a colloidal suspension with physico-chemical properties similar to that of cloudy orange juice. Components such as pectin, sugars, and the dispersed (colloidal) matter are mainly formed by cellular tissue crushed during processing. Particles in this cloudy press liquor adhere together and form aggregates of increasing size (flocculation) which may settle due to gravity. An irreversible process, named coagulation, may be reached when the aggregates change to a much denser form. To obtain a clear liquor the suspended particles have to be removed in a process called clarification [1]. Clarification is an important step in the processing of fruit juices [1,2]. Traditional processes are carried out by using enzymatic treatments, clarifying agents or centrifugation [3]. The enzyme depectinization has two effects: it degrades the viscous soluble pectin and, at the same time, causes the aggregation of cloud particles. In acidic conditions (press liquor has a pH of 3.58 ± 0.03) pectin molecules carry a negative charge allowing them to repel one another. Pectinases, enzymes typically used for this process, degrade the pectin and expose part of the positively charged protein reducing the electrostatic repulsion between cloud particles clumping together. These larger particles will eventually settle out, but to improve the process, flocculating or fining agents, as shown in Table 3.1, must be added [1]. Fining agents work either by sticking to particles, making them heavy enough to sink, or by using charged ions to cause particles to stick to each other, making them settle to the bottom. Posteriorly, a centrifugation and subsequent filtration (fining) are needed to give the clear juice [1].

The conventional process has several disadvantages. It is labour-intensive, time-consuming and requires a discontinuous operation. In addition, the use of additives (fining agents and filter aids) can leave a slight after taste in the juice [4]. In this sense membrane processes such as MF and UF have been proposed as a successful alternative, because compared with traditional juice processing methods, they are low-cost and non-thermal separation techniques which involve no phase change or chemical agents [5,6].

Table 3.1. Agents used in the conventional fruit juice clarification (adapted from [1]).

Name	Description
Sparkolloid	A natural albuminous protein extracted from kelp and very finely powdered
Gelatin	Mixture of gelatins and silicon dioxide, with the active ingredient being animal collagen
Kieselsool	Suspension of small silica particles usually used in combination with gelatins. This fining aids in pulling proteins out of suspension
Bentonite	Refined clay (montmorillonite) presented as powder or coarse granules. Bentonite must be added to hot water: stir well and let it stand for 36–48h before use, so that it swells and becomes almost gelatin-like
Isinglass	Protein produced from sturgeon swim bladders. It is presented either as a fine powder or as dry hard fragments

Considering the advantages of membrane processes MF and UF membranes were used and tested for the clarification of orange press liquor. The effectiveness of the membrane treatment was analysed experimentally evaluating the membrane performance in terms of productivity and selectivity towards specific components. In membrane process several factors, such as membrane characteristics and operating conditions, affect the membrane performance. Therefore, MF and UF membranes were evaluated for their characteristics and at different operating conditions in order to determine a suitable membrane and the optimal conditions to reach a maximum permeate flux and a minimum rejection towards components of interest (i.e. hesperidin).

3.1 Clarification of orange press liquor: Evaluation of membrane characteristics

MF and UF membranes were tested to evaluate their performance in terms of permeate flux and rejection of polyphenols. The results obtained in this step allow to select the suitable membrane for the clarification of the raw press liquor. Experiments were performed by using a laboratory bench plant (Fig. 3.1) equipped with a stainless steel

cell suitable for containing a flat-sheet membrane with a membrane surface of 17.49 cm². Experimental runs were performed by using three flat-sheet membranes, made in PVDF and supplied by Microdyn-Nadir GmbH (Wiesbaden, Germany) the properties of which are shown in Table 3.2.

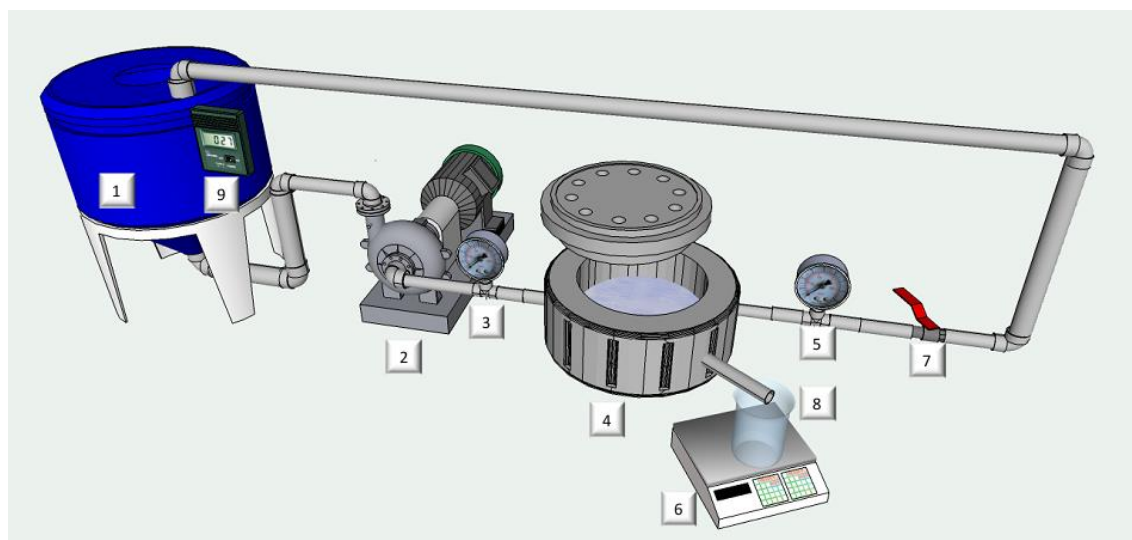


Fig. 3.1. Schematic diagram of the experimental set-up: (1) feed tank; (2) feed pump; (3,5) pressure gauges; (4) flat-sheet cell; (6) digital balance; (7) retentate valve; (8) permeate tank; (9) thermometer.

Experimental runs were performed according to the total recycle configuration (TRC) in which both permeate and retentate streams were continuously recycled back to the feed tank. This configuration ensured a steady state in the volume and composition of the feed. In order to evaluate the effect of feed concentration on the membrane performance, experiments were also performed according to the batch concentration configuration (BCC) in which the permeate stream was continuously removed. In both configurations operating conditions such as transmembrane pressure (TMP), temperature and feed flow rate were fixed at 1 bar, $25.26 \pm 0.3^\circ\text{C}$ and 185 L/h, respectively. Each run was stopped after 180 min of continuous operation. The analysis of responses variables such as hesperidin, sugars were obtained according with the procedure described in section 2.3.

Table 3.2. Characteristics of selected membranes.

	Membrane type		
	MV020T	UV150T	FMU6R2
Membrane process	MF	UF	UF
Thickness (mm)	0.188±0.005**	0.212±0.004**	0.190±0.003**
Molecular weight cut-off (kDa)	-	150*	200*
Pore size (µm)	0.2*	-	-
Maximum pore size distribution (frequency %)	93.21**	79.77**	40.47**
Diameter at maximum pore size distribution (µm)	0.488±0.1970**	0.195±0.0030**	0.212±0.0004**
Contact angle (°)	79.78±0.133**	74.60±0.356**	68.83±0.405**

* Values obtained from the manufacturer

** Values obtained experimentally

Results obtained under TRC showed that the FMU6R2 membrane, with a molecular weight cut-off of 200 kDa, presented the lowest rejection for hesperidin and sugars corresponding to 39.1% and 30.8%, respectively (Fig. 3.2-a and 3.2-b). The MV020 and UV150 membranes having higher and lower pore size in comparison with the FMU6R2 membrane, respectively, showed higher values of rejection. This behaviour can be attributed to different types of fouling characterising each membrane. For the MV020 membrane a complete or intermediate pore blocking is the dominant type of fouling, producing a reduction in pore size that results in a higher rejection. On the other hand, for the UV150 membrane, a cake layer formation due to the build-up of macromolecules on the membrane surface, acts as an additional barrier which produces an increase in the rejection of hesperidin and sugar.

Permeate fluxes are also strictly related with membrane characteristics as well as with fouling phenomena. Fig. 3.3-a shows the time course of permeate flux observed for the investigated membranes in selected operating conditions according with the total recycle configuration (TRC). Results showed that differences between the investigated

membranes are not statistically significant ($p=0.1096$; $F\text{-ratio}=2.30$). Different initial permeate flux values were observed for different membranes. In particular, the MV020 membrane showed the highest initial permeate flux (Fig. 3.3-a), due to its highest pore size. These effects can be appreciated until a steady-state permeate flux is reached; after this point (around 50 min of process) the differences in permeate flux between different membranes are not evident. Even though the MV020 membrane presented the highest initial permeate flux, this membrane showed also a greater value of flux drop (about 51.4%) in comparison with UV150 and FMU6R2 membranes (36.1% and 38.4%, respectively).

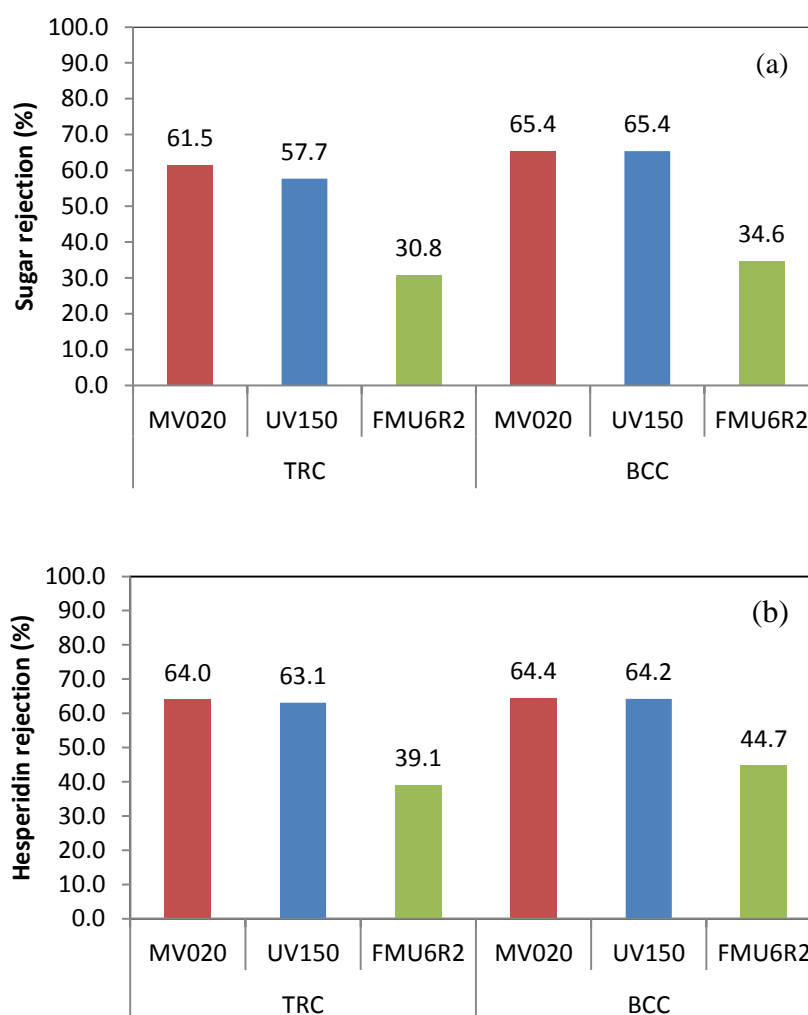


Fig. 3.2. Rejection of (a) sugar and (b) hesperidin obtained during MF-UF under TRC and BC configuration using flat-sheet membranes. Operating conditions: TMP= 1 bar, T= 25°C, feed flow rate= 185 L/h.

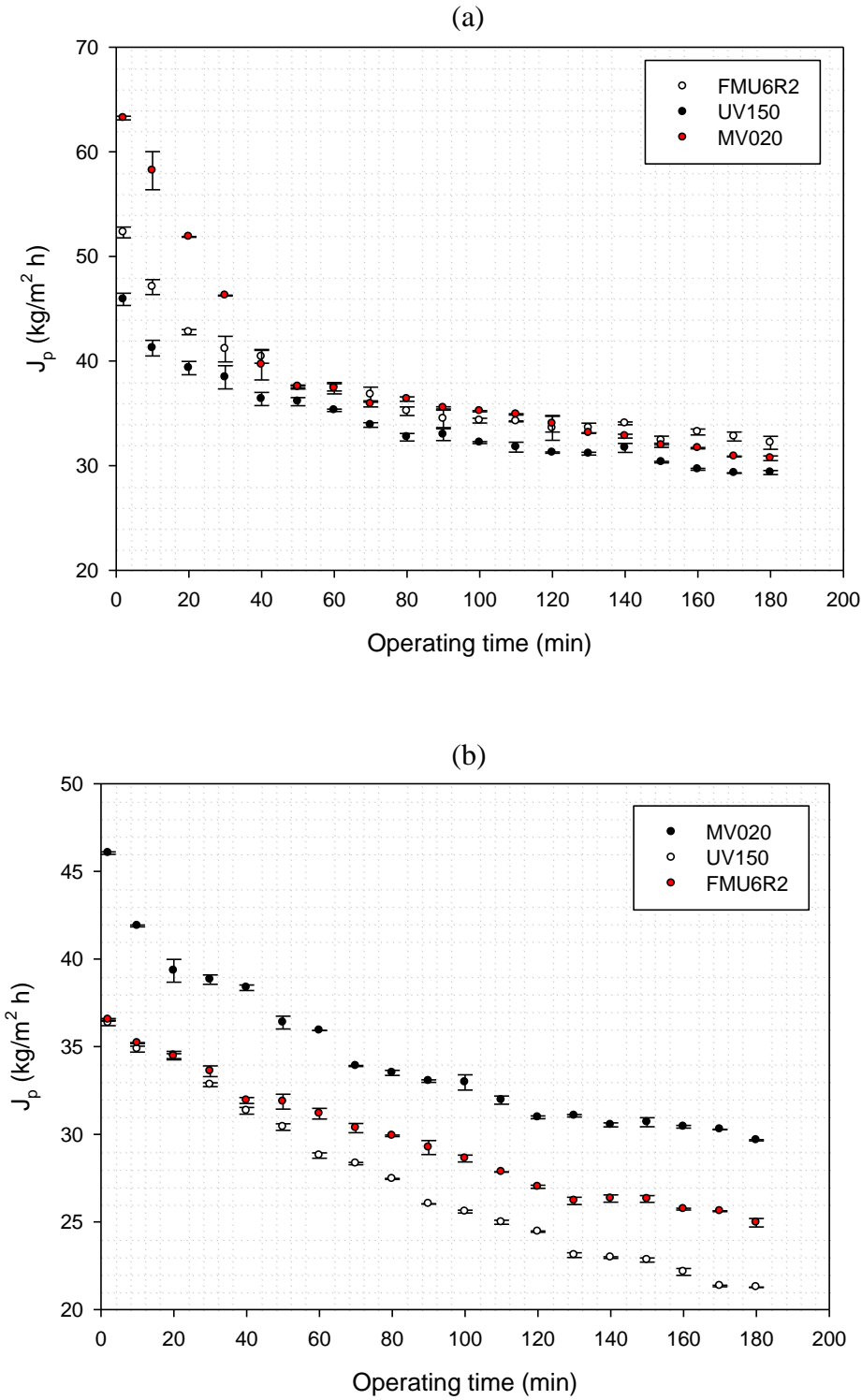


Fig. 3.3. Time course of permeate flux for MF and UF processes using flat-sheet membranes at TRC (a) and BCC (b). Operating conditions: TMP= 1 bar, T= 25°C, feed flow rate= 185 L/h.

Similar results were obtained during BCC experiments, where MV020 showed the highest values of hesperidin and sugar rejection (Fig. 3.2-a and 3.2-b). Under BCC all the investigated membranes showed higher values in hesperidin and sugar rejection in comparison with TRC. This effect is associated with the increase of feed concentration which produces an increasing of fouling phenomena. The increase in fouling can be also appreciated through a permeate flux decay, where statistically significant differences ($p=0.000$; $F\text{-ratio}=13.38$) were observed between the investigated membranes. These differences were not appreciated between UV150 and FMU6R2 membranes ($p=0.1075$; $F\text{-ratio}=2.73$). The permeate flux decay under BCC was higher when compared with TRC, as shown in Fig. 3.3-b.

The results obtained with flat-sheet membranes showed a strong the relationship between pore size and membrane performance in terms of permeate flux and rejection towards polyphenols and sugars. According to these results UF membranes were preferred in the treatment of orange press liquor since they allow to obtain an appropriate combination of permeate flux and lower rejection of polyphenols. At this purpose the effect of operating conditions on the membrane performance was studied by using an UF membrane with a MWCO of 100 kDa, as reported in the following.

3.2 Clarification of orange press liquor: Evaluation of operating conditions

The effect of operating variables such as transmembrane pressure (TMP), temperature (T) and feed flow-rate (Q_f) was evaluated on the performance of hollow fiber UF membranes in terms of permeate flux, membrane fouling and blocking index. Similarly, the effect of these parameters was also investigated in terms of recovery of antioxidant compounds in the permeate stream. In both cases the Response Surface Methodology (RSM) approach was used for the data analysis.

UF experiments were performed by using a laboratory unit (Fig. 3.4) equipped with a hollow fiber polysulphone membrane module supplied by China Blue Star Membrane Technology Co., Ltd (Beijing, China) with an effective membrane area of 0.16 m^2 and a

nominal molecular weight cut-off (MWCO) of 100 kDa. A heat exchanger, placed into the feed tank, was used to keep the feed temperature constant.

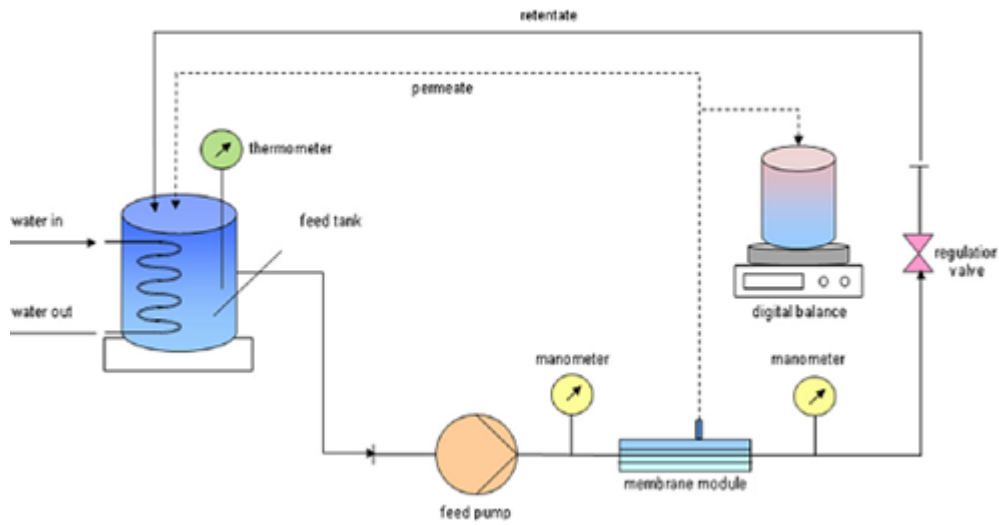


Fig. 3.4. Scheme of UF experimental setup.

This study was performed according to the total recycle configuration in which both permeate and retentate streams were continuously recycled back to the feed tank to ensure a steady state in the volume and composition of the feed. Based on the capability of the experimental set-up and the preliminary single-variable tests, the range of operating conditions was chosen as follows: TMP = 0.2–1.4 bar, $T = 15\text{--}35^\circ\text{C}$ and $Q_f = 85\text{--}245\text{ L/h}$. The levels, code and intervals of variation of the operating variables are given in Table 3.3. Experimental runs were performed according to the Box–Behnken design (Table 3.4) which is composed of 30 runs divided in two blocks, each one with three central points (runs 13, 14, 15 and 28, 29, 30). The mass of collected permeate was measured with an accuracy of $\pm 0.1\text{g}$ every 10 min. Each run was stopped after 180 min of continuous operation.

Table 3.3. Experimental range and levels of the independent variables for Box-Behnken design.

Feed Factors	Code	Variation levels		
		-1	0	1
TMP (bar)	X ₁	0.2	0.8	1.4
Temperature (°C)	X ₂	15	25	35
Feed Flow Rate (L/h)	X ₃	85	165	245

The response variables such as permeate flux, blocking index and fouling index were obtained using equations (1.4), (1.14) and (1.15), respectively. On the other hand, measurement of polyphenols rejection and total antioxidant activity (TAA) were obtained following the procedure showed in section 2.3.4.

The obtained model could explain a 96.31% (expressed R-squared) of the variability in the permeate flux. Analysis of lack-of-fit test showed that the model appears to be adequate for the observed data at the 95% of confidence level with a p-value greater than 0.05 (P= 0.0559, F-ratio 5.46). In addition, a lower values of standard error (0.687447), was obtained. The presence of autocorrelation was evaluated by means of Durbin–Watson (DW) statistic. Since the P-value was greater than 5.0% (P= 0.9699), there is no indication of a serial autocorrelation in the residuals at the 5.0% significance level.

Table 3.4. Experimental design and results of Box-Behnken design.

Run	Block	TMP	Temp	Feed	Permeate	Fouling	Blocking	Polyphenols	TAA
		(bar)	(°C)	Flow rate	flux	Index	index	rejection	(mM trolox)
		X ₁	X ₂	X ₃	Y ₁	Y ₂	Y ₃	Y ₄	Y ₅
1	1	-1	-1	0	8.23	58.91	1.75	10.66	12.48
2	1	1	-1	0	26.41	43.01	1.74	39.79	28.10
3	1	-1	1	0	14.51	54.62	1.37	47.68	25.12
4	1	1	1	0	31.95	75.93	1.38	34.77	23.92
5	1	-1	0	-1	6.81	51.86	2.00	46.64	24.52
6	1	1	0	-1	18.66	67.25	2.00	47.13	24.45
7	1	-1	0	1	10.01	62.92	1.90	40.08	41.84
8	1	1	0	1	21.08	67.00	2.00	54.42	23.50
9	1	0	-1	-1	13.41	64.94	1.47	46.69	19.11
10	1	0	1	-1	18.81	67.18	1.57	50.62	29.41
11	1	0	-1	1	14.43	69.76	1.64	37.34	21.84
12	1	0	1	1	25.49	72.53	1.50	43.49	33.10
13	1	0	0	0	16.56	68.29	1.51	47.48	26.68
14	1	0	0	0	15.55	67.76	1.62	44.07	31.73
15	1	0	0	0	15.25	69.72	1.52	51.51	35.60
16	2	-1	-1	0	8.31	59.33	1.72	9.09	13.75
17	2	1	-1	0	25.33	43.48	1.65	49.18	27.64
18	2	-1	1	0	12.89	54.96	1.5	58.30	23.67
19	2	1	1	0	30.74	76.05	1.37	57.65	23.49
20	2	-1	0	-1	6.77	52.31	2.00	55.60	25.15
21	2	1	0	-1	18.63	67.35	2.00	42.73	24.45
22	2	-1	0	1	8.86	62.96	2.00	42.51	41.91
23	2	1	0	1	21.05	67.49	1.55	49.41	23.46
24	2	0	-1	-1	13.43	65.58	1.51	49.63	19.31
25	2	0	1	-1	18.64	67.40	1.56	51.64	29.41
26	2	0	-1	1	14.37	70.74	1.60	57.47	23.16
27	2	0	1	1	25.52	72.75	1.49	49.98	32.89
28	2	0	0	0	16.6	68.64	1.52	47.12	27.68
29	2	0	0	0	15.52	68.37	1.58	48.83	29.00
30	2	0	0	0	15.32	70.46	1.49	54.28	34.15

Fig. 3.5 shows the linear, quadratic and interaction of each factor plotted in the form of Pareto chart where the effect is significant if its corresponding bar crosses the vertical line at the $P=0.05$ level.

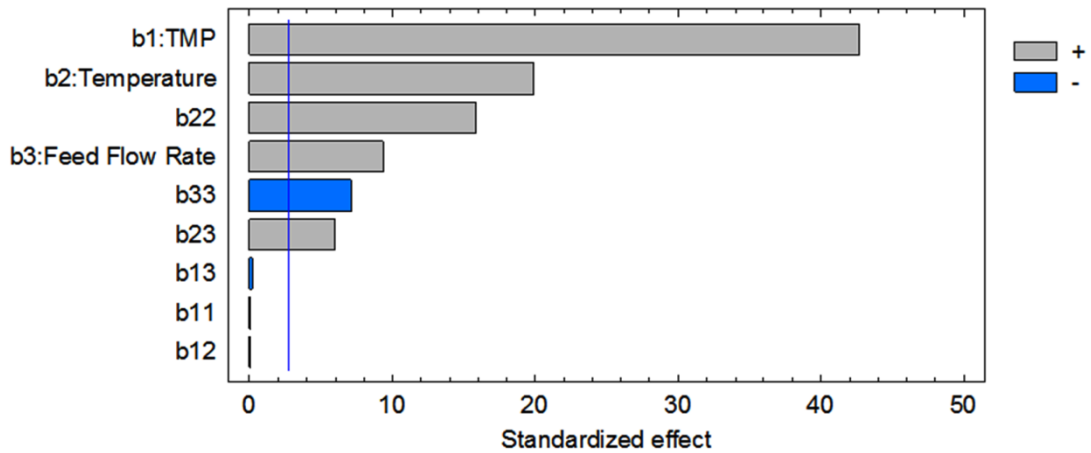


Fig. 3.5. Standardized pareto chart for the permeate flux.

The linear coefficients of TMP (b_1) were found to be the most significant effect to increase the permeate flux, followed by linear coefficient of temperature (b_2), quadratic effect of temperature (b_{22}) and then the linear effect of feed flow-rate (b_3). On the other hand, the quadratic effect of feed flow rate (b_{33}) produces a decrease in the permeate flux with a significant effect ($P \leq 0.05$). The interaction factors as (b_{12}), (b_{13}) and the quadratic effect of TMP (b_{11}) do not produce a significant effect ($P \geq 0.05$) in the permeate flux; therefore, for the next analyses these factors will not be included in the regression model equation of the permeate flux. These results indicate that the interaction of operating variables in the ultrafiltration of orange press liquor has to be considered.

The quadratic regression equation describing the effect of the process variables on the permeate flux in terms of coded levels is reported in the following:

$$Y_1 = 15.79 + 7.34125X_1 + 3.41437X_2 + 1.60313X_3 + 4.01375X_2^2 + 1.45X_2X_3 - 1.7987X_3^2 \quad (3.1)$$

where Y_1 is the predictive permeate flux for the ultrafiltration process. The positive linear coefficients of TMP (b_1), temperature (b_2) and feed flow-rate (b_3) produce an increasing of the permeate flux when these factors are increased. The model developed where used to create the 3D plots. The response surface of the permeate flux is plotted against two operating variables, while the third variable is kept constant (level 0 in Table 3.3).

The TMP has presented a linear effect on the permeate flux for all the values investigated (Fig. 3.6-a and 3.6-c). The curvature in the 3D plot of the permeate flux arises due to the quadratic dependence on temperature and feed flow-rate (Fig. 3.6-b and 3.6-c). In addition, the temperature has a linear effect on the permeate flux after 25°C (level 0). The feed flow-rate produces an increasing of the permeate flux from the level (-1) to the level 0; after this point, an increasing in the feed flow-rate produces a decreasing of the permeate flux (Fig. 3.6-b and 3.6-c).

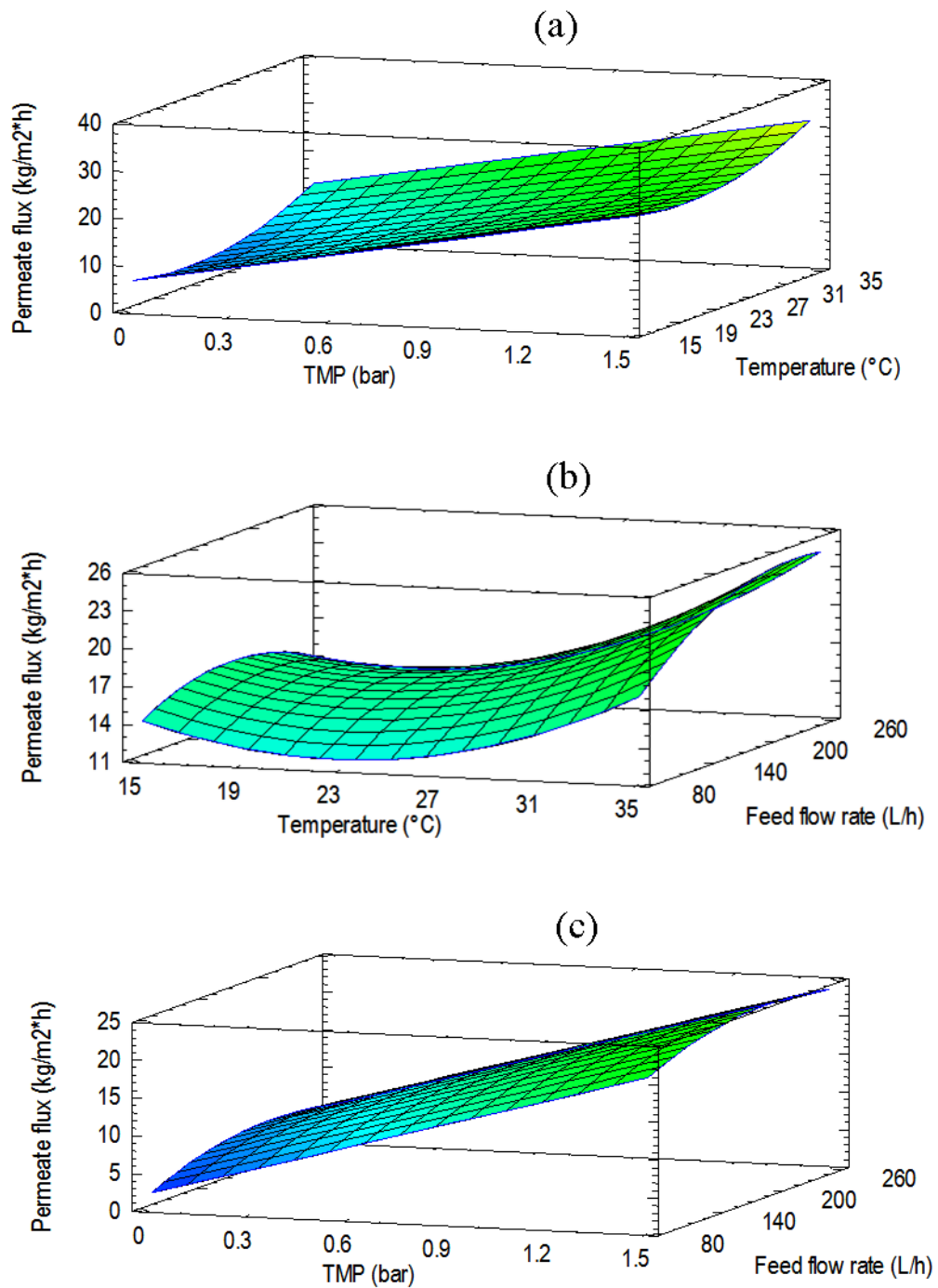


Fig. 3.6. 3D response surface with contour plot of permeate flux.

In Fig. 3.7 the residual (errors) permeate flux was plotted against the predicted flux. The random and also the distribution of the residuals over and below the centreline suggest that the model for the permeate flux is statistically significant.

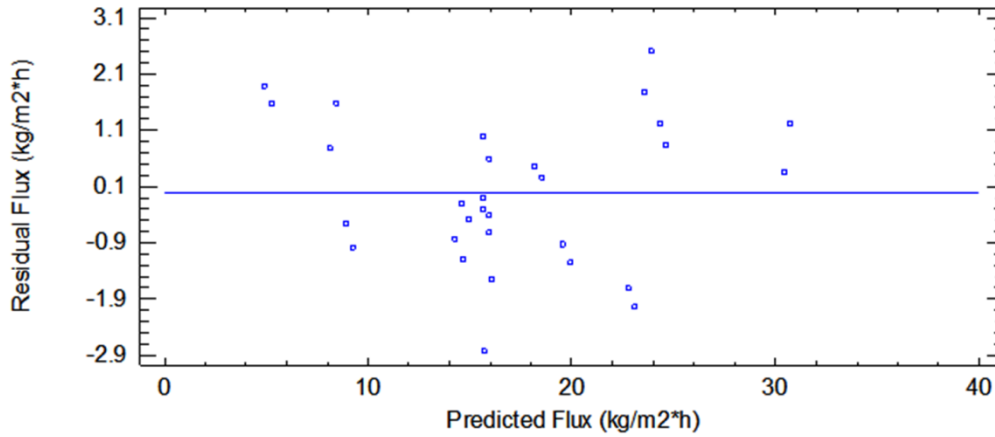


Fig. 3.7. Plot of residuals against predicted response of permeate flux in the UF process.

In the case of fouling index the R-squared statistic obtained indicates that the model as fitted explains 90.47% of its variability. Lack-of-fit test was equal to 0.0175 (F-ratio 10.5). This means that the model as fitted is not completely adequate to represent the experimental data, and a more complex model including other factors should be used. The Standard Error was equal to 1.07706. Since the P-value of the Durbin–Watson statistic test is greater than 5.0% ($P = 0.9700$), there is no indication of serial autocorrelation in the residuals at the 5.0% significance level.

The linear, quadratic and interaction effect depicted in Fig. 3.8 shows that the interaction factor between TMP and temperature (b_{12}) was found to be the most significant effect to increase the fouling index, followed by quadratic effect of TMP (b_{11}) that produces a decreasing in the fouling index.

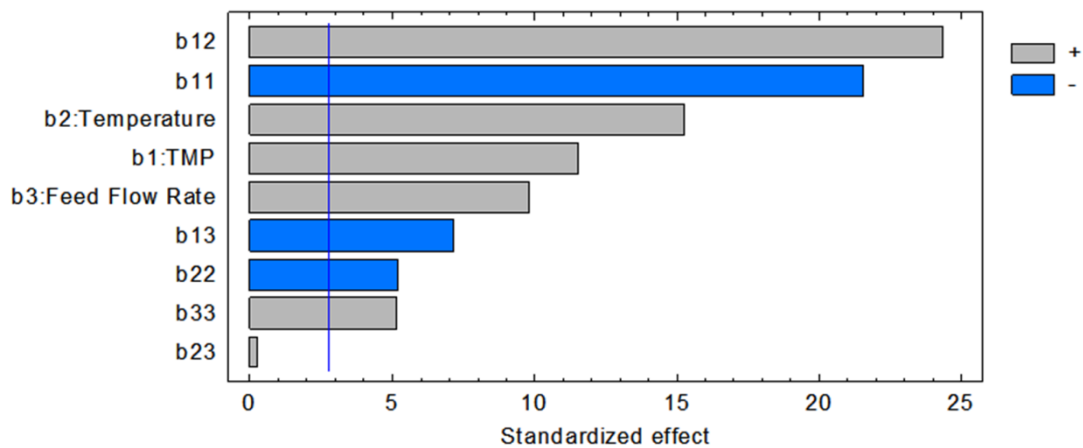


Fig. 3.8. Standardized Pareto chart for fouling index.

The interaction factor between temperature and feed flow rate (b_{23}) is the only factor that does not produce a significant effect ($P \geq 0.05$) in the fouling index. The quadratic regression equation describing the effect of the process variables on the fouling index in terms of coded levels is reported in the following:

$$Y_2 = 68.8733 + 3.10563X_1 + 4.10438X_2 + 2.6425X_3 - 8.52729X_1^2 + 9.2687X_1X_2 - 2.7257X_1X_3 - 2.05979X_2^2 + 2.04646X_3^2 \quad (3.2)$$

where Y_2 is the predictive fouling index for the ultrafiltration process.

Fig. 3.9 shows the response surface of the fouling index plotted against two operating variables while the third variable is kept constant (level 0 in Table 3.3). It is appreciated from the warping of the 3D plot a strong interaction between TMP and temperature (Fig. 3.9-a). The fouling index increased with temperature only at TMP higher than level 0; at lower level the fouling index decreased by increasing the temperature. The fouling index increased by increasing the feed flow-rate (Fig. 3.9-b and 3.9-c).

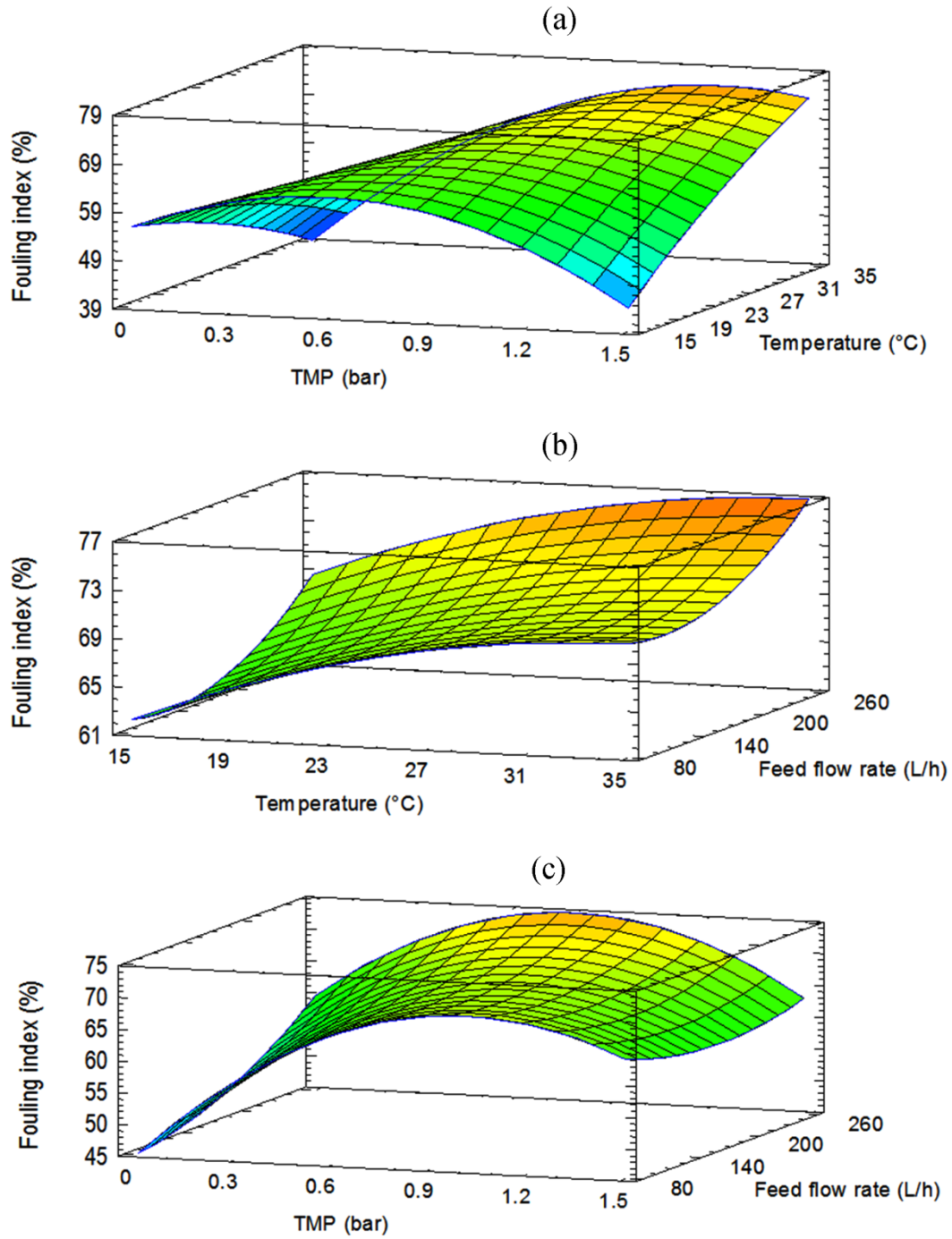


Fig. 3.9. 3D response surface with contour plot of fouling index.

The model obtained for the fouling index appears to be statistically significant as suggested by the random distribution of the residuals over and below the centreline depicted in Fig. 3.10.

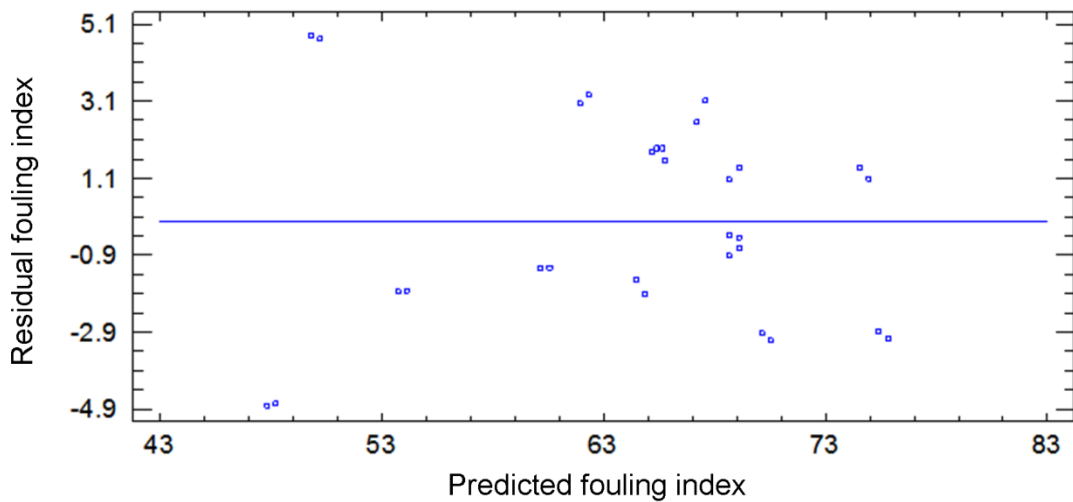


Fig. 3.10. Plot of residuals against predicted response of fouling index.

On the other hand the results obtained for the blocking index have shown a strong relationship between the operating conditions and the type of fouling produced. The model obtained in this case explains 76.36% of the variability in the blocking index. The lack-of-fit analysis showed a lower value in the F-ratio of 1.44 ($p=0.2555$); therefore the model appears to adequate for the prediction of the observed data at the 95.0% confidence level. Serial autocorrelation, evaluated by Durbin–Watson statistic test, was not detected ($P= 0.4672$) and the standard error was equal to 0.106816. In addition, the model for the blocking index is statistically significant as suggested by the random and the distribution of the residuals over and below the centreline (Fig. 3.11).

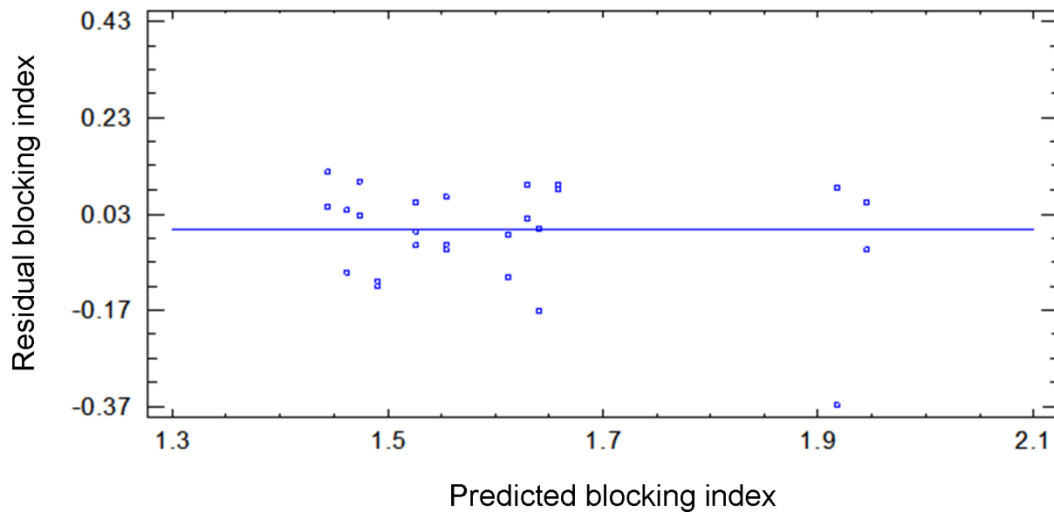


Fig. 3.11. Plot of residuals against predicted response of blocking index.

Pareto chart depicted in Fig. 3.12 shows the linear, quadratic and interaction effect between the studied variables. It is shown that linear effect of TMP (b_1) and feed flow rate (b_3) and the interaction effect for (b_{23}), (b_{13}) and (b_{12}) have not produced a significant effect ($P \geq 0.05$) in the blocking index; consequently, these factors were not included in the regression model. On the other hand, quadratic effect for TMP (b_{11}) was found to be the most significant effect to increase the value of blocking index, followed by the quadratic effect of feed flow rate (b_{33}) and the quadratic effect of temperature (b_{22}).

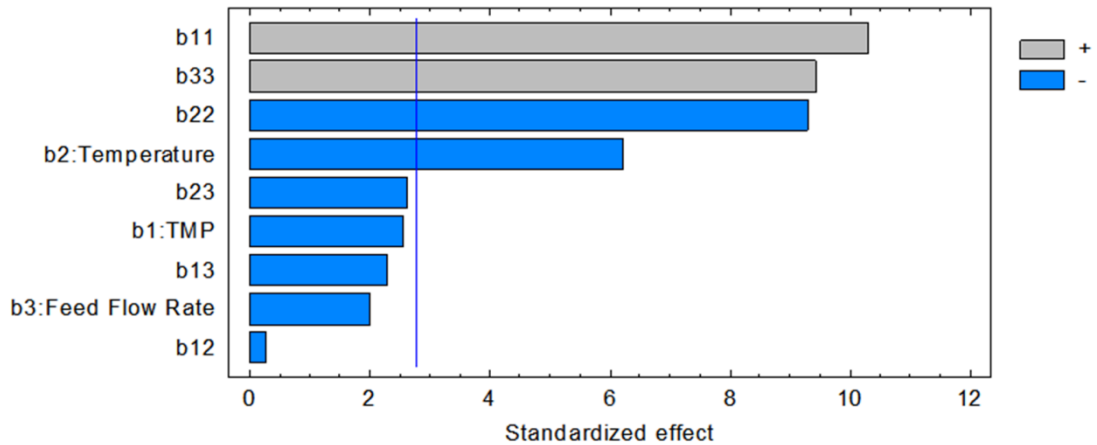


Fig. 3.12. Standardized Pareto chart for blocking index.

The model attained, expressed in terms of quadratic regression, describes the effect of the process variables on the blocking index in terms of coded levels as reported in the following:

$$Y_3 = 1.54 - 0.08375X_2 + 0.204375X_1^2 - 0.18437X_2^2 + 0.186875X_3^2 \quad (3.3)$$

where Y_3 is the predictive blocking index for the ultrafiltration process.

Membrane pore blocking is a complex phenomenon influenced by several factors. Hwang et al., [7] have reported that the type of fouling produced is influenced by three factors: (i) the amount of particles simultaneously arriving at the membrane surface, (ii) the amount of accumulated particles, and (iii) the filtration rate. Fig. 3.13-b and 3.13-c show the effect of the feed flow-rate on the i value. The response surface plots shown a strong interaction between feed flow-rate, temperature and TMP.

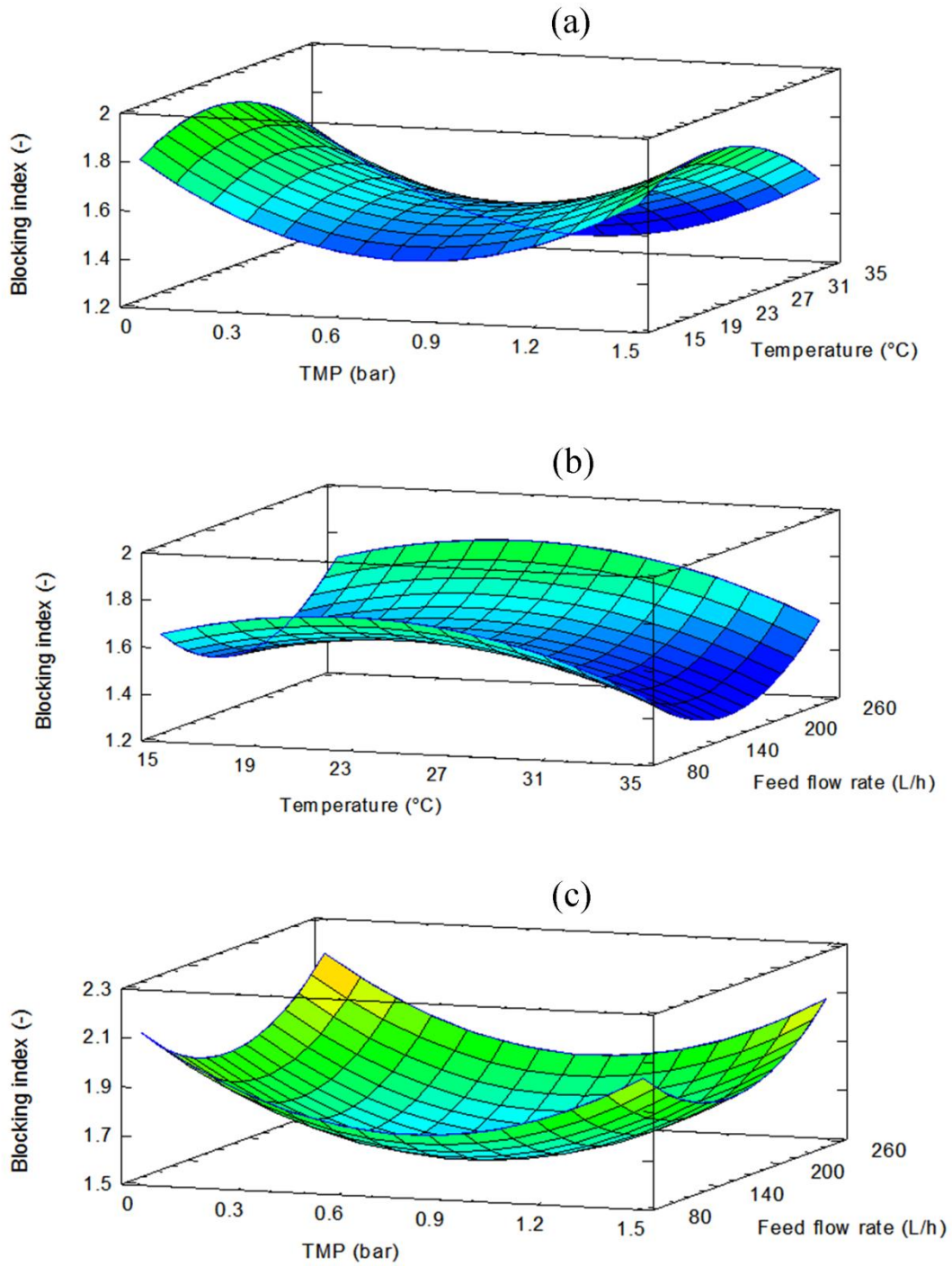
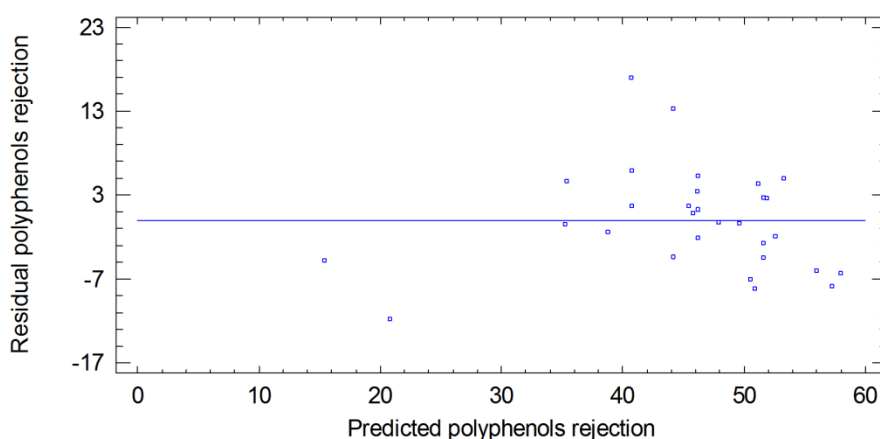


Fig. 3.13. 3D response surface with contour plot of blocking index.

It is appreciated that increases in feed flow-rate from 165 L/h (level 0) until 245 L/h (level 1) produce an increasing on the i value; this means that at level 0 the principal mechanism is a combination of intermediate blocking and standard blocking; however,

when the feed flow-rate is increased the predominant mechanism is the complete pore blocking. When more particles arrive at the membrane surface at the same time, they have less opportunity to migrate to the membrane pores due to the crowding out produced by neighboring particles. Therefore particles have a greater chance to penetrate the pores. It has been also reported that the pore blocking is of more significance under lower pressure [7]. The same effect is shown in Fig. 3.13-a and 3.13-c when at minimum level (-1) of TMP (0.2 bar) the values of the blocking index are closer to $i=2$, where the main mechanism involved is the complete pore blocking ($i=2$). This may be caused by fewer particles simultaneously arriving at the membrane surface.

The effect of operating conditions on the polyphenols rejection and TAA content in the permeate stream was also evaluated. In this case a model explaining 70.37% (expressed in R-squared statistic) of the variability in the polyphenols rejection was obtained. The model appears to be adequate to describe the experimental data with a value of lack-of-fit equal to $p=0.0726$ (F-ratio of 4.69); standard error was equal to 3.73, and serial autocorrelation has not been detected according with the Durbin–Watson statistic ($p=0.5027$; F-ratio 2.62). The residual (errors) of the polyphenols rejection showed a random distribution over and below the centreline (Fig. 3.14).



significant effect on the polyphenols rejection, followed by linear effect of temperature (b_2) and linear effect of TMP (b_1). The factors (b_2), (b_1), (b_{13}) and (b_{33}) appear to produce an increase in the polyphenols rejection while the factors as (b_{12}), (b_{11}) and (b_{22}) produced a decrease in the same item. On the other hand, the factors (b_3) and (b_{23}) did not produce a significant effect ($p \geq 0.05$) in the polyphenols rejection. Therefore the interaction factor (b_{23}) presenting the lowest effect was not included in the regression model equation.

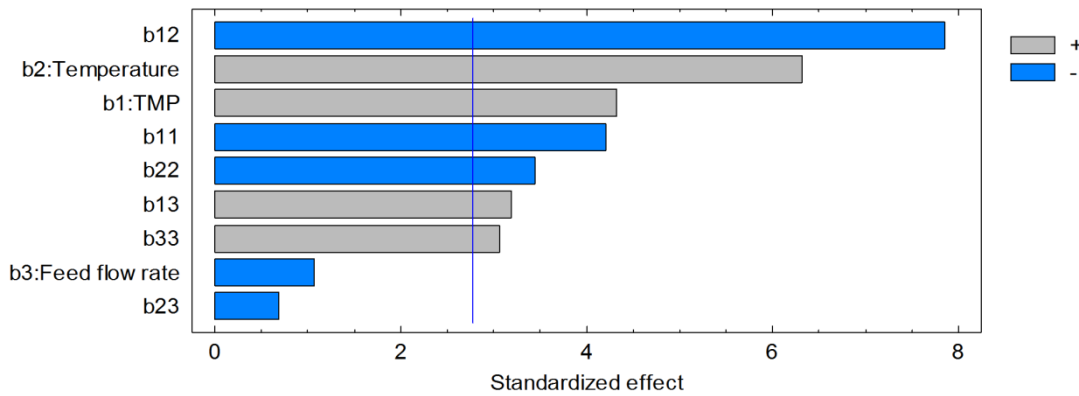


Fig. 3.15. Standardized Pareto chart for total polyphenols rejection.

The quadratic regression describing the effect of each factor on the polyphenols rejection is shown in equation 3.4.

$$Y_4 = -14.03 + 61.02X_1 + 4.33X_2 - 0.30X_3 - 16.02X_1^2 - 1.72X_1X_3 - 0.05X_2^2 + 0.0007X_3^2 \quad (3.4)$$

where Y_4 is the predictive polyphenols rejection for the ultrafiltration process.

The 3D plot depicted in Fig. 3.16, shows the main effect of the studied variables and their interaction on the polyphenols rejection. It is possible to appreciate the significant variation in the polyphenols rejection when the operating conditions were modified in the investigated range. In particular, the polyphenols rejection increased by increasing TMP due to the effect of a solid layer compaction acting as an additional layer, reducing the MWCO of the UF membranes [8].

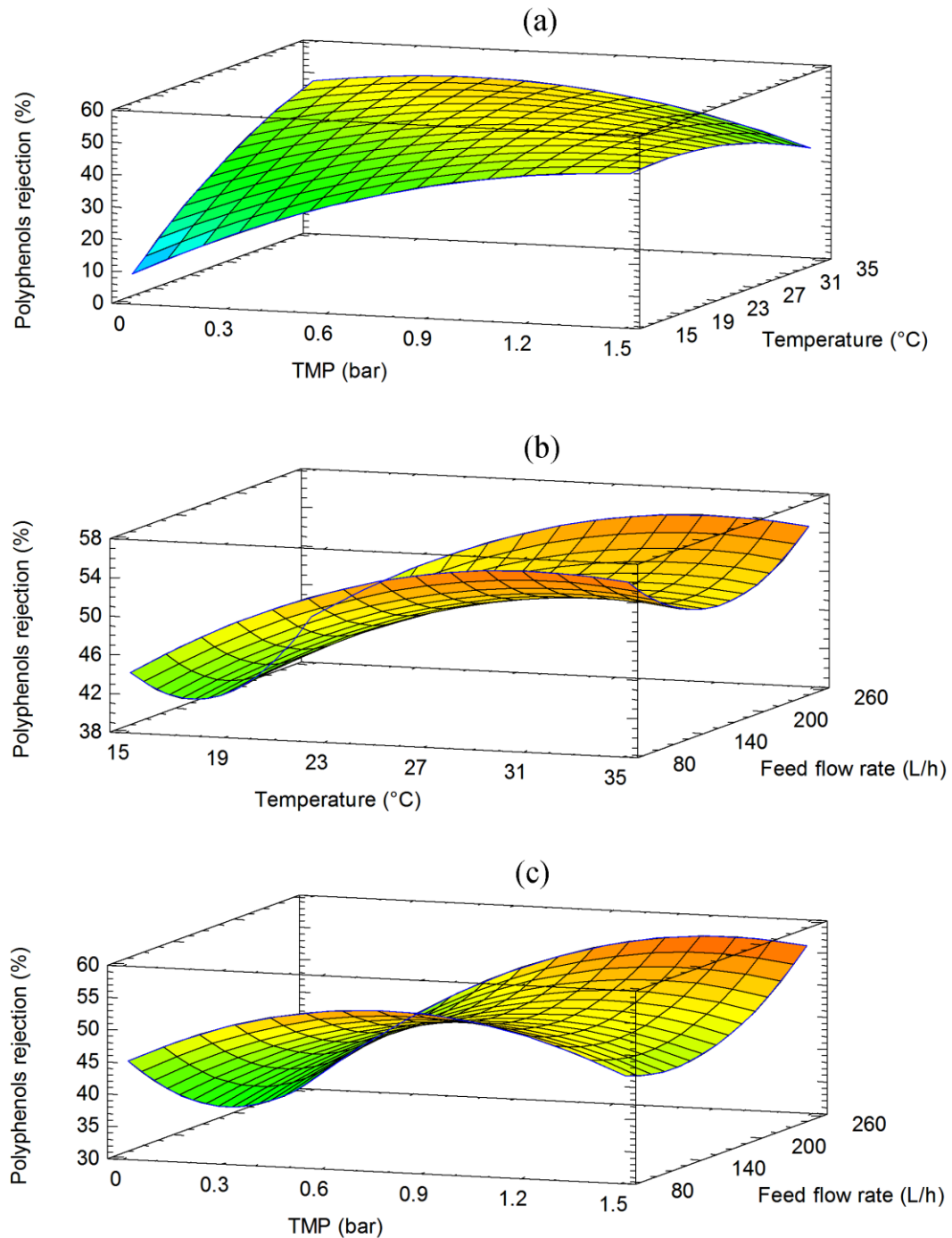


Fig. 3.16. 3D response surface with contour plot for total polyphenols rejection.

This effect was kept until 1.1 bar, where some of the particles (polyphenols) in the solid layer cross through the membrane due to the applied pressure (Fig. 3.16-a and 3.16-c). On the other hand, any change in the temperature will force molecules as proteins to assume a new equilibrium structure. An increase of temperature produced a gradual

destabilization of the main non-covalent interactions, producing exposure of non-polar groups [9]. This destabilization could stimulate the solid layer formation onto the membrane surface, increasing the polyphenols rejection as showed in Fig. 3.16-a and 3.16-b. Meanwhile the Q_f showed a strong interaction with the TMP and T (3.16-b and 3.16-c); the main effect is to reduce the polyphenols rejection due to the reduction of the adjacent boundary layer thickness [10]. This effect was observed up to 165 L/h; after this point an increase in the recirculation flow rate produced an increase in the polyphenols rejection due to more particles arriving at the membrane surface which produce a pore blocking reducing the MWCO [11].

All these modifications can be attributed to concentration polarization and membrane fouling phenomena. During membrane filtration rejected solutes are convectively driven to the membrane surface where they build up producing a concentration polarization boundary layer near the membrane surface. In UF macromolecular solutes and colloidal species usually have insignificant osmotic pressure; in this case the concentration at the membrane surface rises up to a point where a gel precipitation layer is formed on the membrane surface, producing a major resistance to permeate flow. Weis et al. [12] reported that phenolic compounds are the major foulants in the UF process. Therefore, the effect of operating conditions on the molecules rejected (proteins, pectin and polyphenols), responsible of the solid layer formed on the membrane surface, should be strictly considered. According to the obtained, it is possible to conclude that there is a strong relationship between the type of fouling and polyphenols rejection, because changes in the type of fouling produce changes in the polyphenols rejection. Finally, the maximum polyphenols rejection was obtained when the intermediate pore blocking was the governing fouling mechanism.

On the other hand, the antioxidant activity showed by polyphenols is related principally to their concentration, but the operating conditions can affect this capacity. Therefore, the total antioxidant activity (TAA) was evaluated in the permeate stream to determine the effect of operating conditions in the preservation of antioxidant compounds. The regression model built for TAA at different operating conditions could explain the 69.02 % of the variability (expressed in R-squared) with a standard error equal to 3.98. The p-value for lack-of-fit was equal to 0.3935 (F-ratio 1.44). This means that the model as fitted is adequate to explain the variability on the TAA at 95% of confident level. Since

the p-value of the Durbin–Watson statistic test is greater than 0.05 ($p = 0.9986$), there is no indication of serial autocorrelation in the residuals at the 5.0% significance level.

Fig. 3.17 shows the linear, quadratic and interaction coefficients of each operating variable plotted in the form of Pareto chart. It is possible to appreciate that the quadratic effect of T was the most significant followed by (b_2), (b_{13}) and (b_3), whereas the linear effect (b_1), interaction effect (b_{12} , b_{23}) and quadratic effect (b_{11} , b_{33}) did not show a significant effect ($p \geq 0.05$) on the TAA.

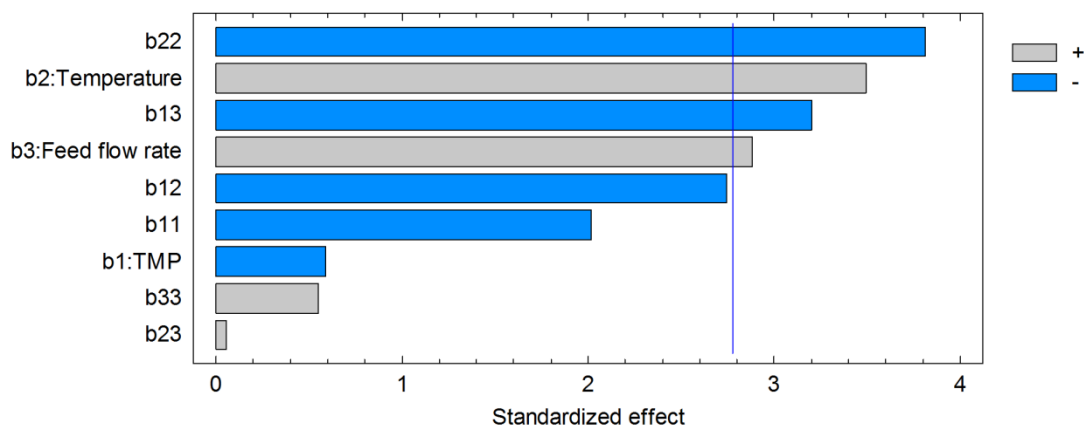


Fig. 3.17. Standardized Pareto chart for TAA in the permeate stream.

The obtained model shown in equation (3.5) describes the linear, quadratic and interaction effect of operating conditions on the TAA in the permeate stream.

$$Y_5 = -44.60 + 43.70X_1 + 3.64X_2 + 0.07X_3 - 8.20X_1^2 - 0.64X_{12} - 0.09X_{13} - 0.06X_2^2 + 0.00009X_{23} + 0.0001X_3^2 \quad (3.5)$$

where Y_5 is the predictive TAA in the permeate stream for the UF process.

Fig. 3.18 shows the 3D response surface for the TAA in the permeate stream. For all Q_f values investigated, an increase in the T (until 28°C) produced an increase in the TAA value of the permeate stream; at temperatures higher than 28°C an increase in the T produced a decrease of the TAA value (Fig. 3.18-b). A similar effect was observed for

the TMP in the range 0.2–0.4 bar; after this point an increase in the TMP produced a decrease in the TAA value (Fig. 3.18-a).

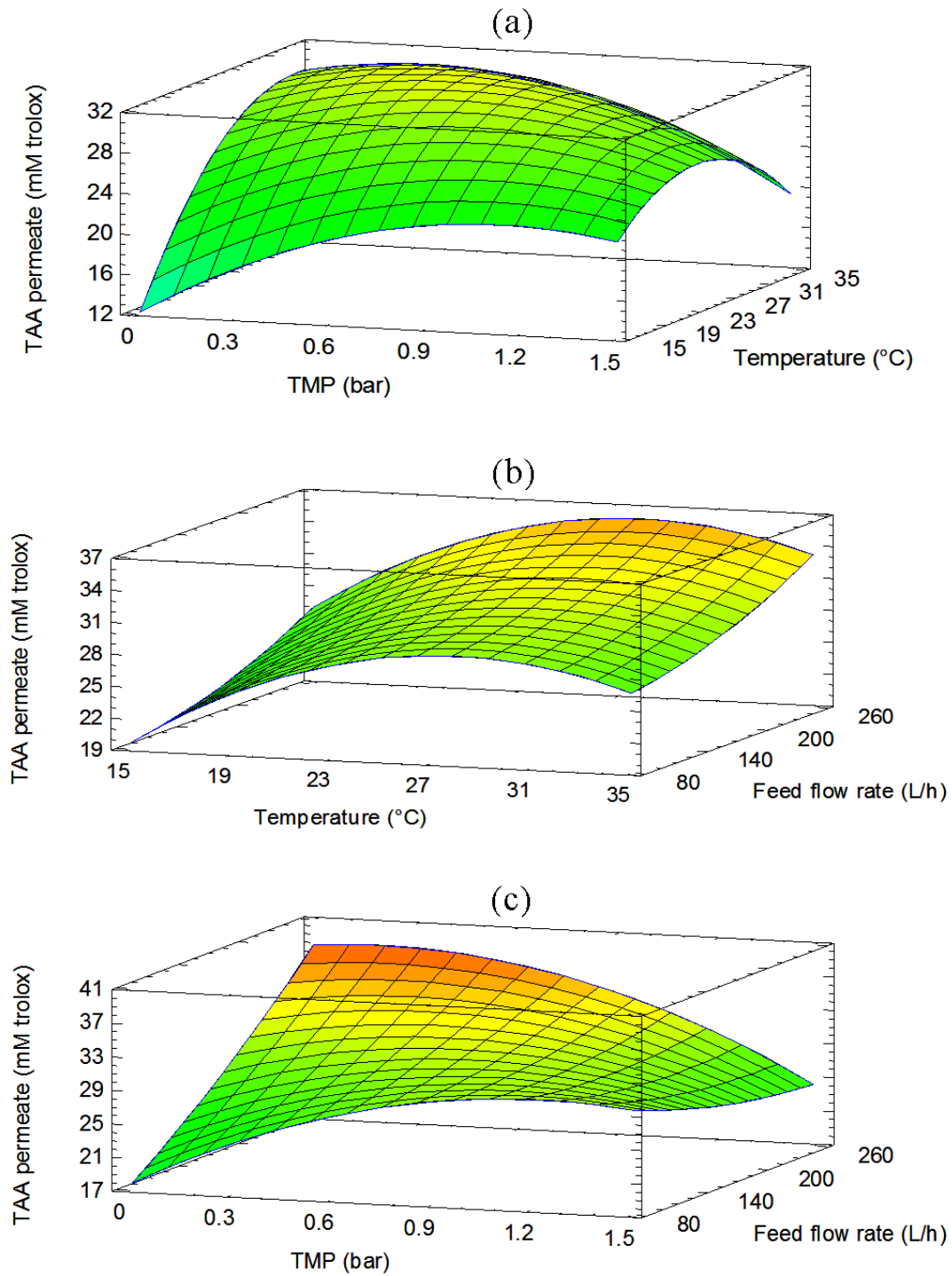


Fig. 3.18. 3D response surface with contour plot for TAA in the permeate stream.

In all the range of TMP values an increase in Q_f enhanced the TAA of the clarified liquor. At the maximum value of Q_f (245 L/h) an increase in TMP produced a decrease in the TAA (Fig. 3.18-c). At the minimum level of Q_f (85 L/h) the increasing in the TAA value took place up to a critical point of TMP where the TAA started to decrease when TMP was increased. The differences in the TAA values at different operating conditions can be correlated with the changes in the polyphenols rejection. The TAA is strictly correlated to the content of polyphenols of the orange press liquor. Proteggente et al. [13] analysed the phenolic composition and the TAA of fresh Sicilian orange juice from pigmented and non-pigmented varieties of orange (*Citrus sinensis* L. Osbeck). They found that concentrations of anthocyanins and hydroxycinnamic acids are highly correlated to the TAA values, while ascorbic acid seems to play a minor role. Their observations were consistent with a previous report in which the antioxidant action of similar varieties was ascribed to the phenolic content [14].

Recent studies have also shown that total phenols determined by Folin–Ciocalteu method can be correlated to the antioxidant activity determined by different methods (ABTS and DPPH assays, for instance) [15]. For this reason, the method described by Singleton et al. [16] has been proposed recently as a standardized method to be used in the routine quality control and measurement of antioxidant capacity of food products and dietary supplements [17]. It has been also reported that thermal treatments, such as conventional and microwave cooking, frying and warm-holding of blanched products produce a modification of polyphenols content and also of antioxidant activity [18,19]. The observed decreasing of TAA after 28°C, could only be attributed to the increasing in polyphenols rejection when the temperature is raised (see also Fig. 3.18-b).

Fig. 3.19 shows the residual plot of TAA in the permeate stream: the dispersion is random over and below the centreline suggesting that the model for the TAA is statistically significant.

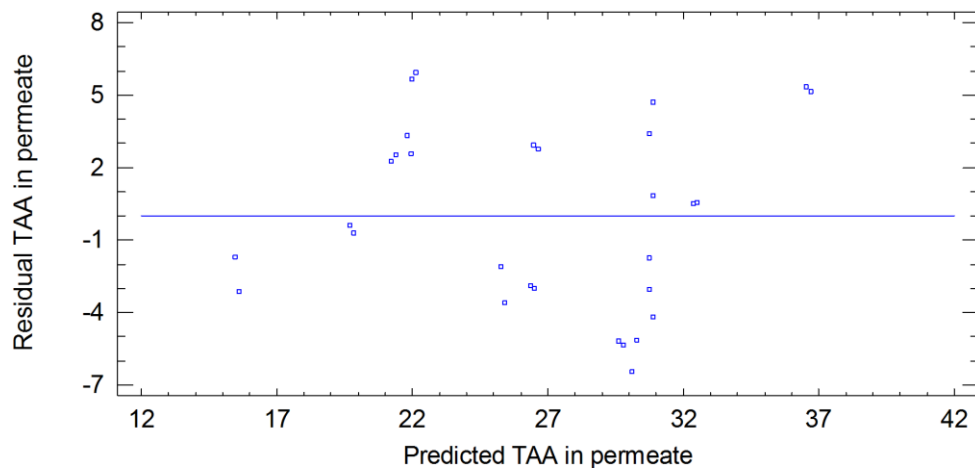


Figure 3.19. Plot of residuals against predicted response of TAA in the permeate stream.

3.2.1 Optimization of multiple responses

The RSM approach permitted to determine the interaction effect between the different factors investigated. In addition, using the desirability function (DF) it was possible to establish the combination of factors suitable to reach the target proposed for the clarification process; this means maximize the permeate flux and minimize the polyphenols rejection as well as the fouling index, simultaneously.

During the experiments performed at several combinations of operating parameters, as depicted in Table 3.4, it was observed that the minimum and maximum limits obtained for the permeate flux were 6.77 and 31.95 kg/m²h, respectively. In the case of fouling index the minimum and maximum limits were 43.01 and 76.05, respectively. Finally, for polyphenol minimum and maximum limits were 9.09% and 58.3%, respectively. These limits were used for the multiple optimization where desirability function (DF) was used to obtain the combination of variables to maximize the permeate flux and minimize the polyphenols rejection as well as the fouling index.

For the maximum overall desirability of 0.52, the coded levels of the operating variables and predicted variables are shown in the Table 3.5.

Table 3.5. Optimization results for the UF of citrus press liquor

Optimized coded level of Variables	X ₁ : TMP	1.4 bar
	X ₂ : Temperature	15°C
	X ₃ : Feed flow-rate	140.4 L/h
Predicted Responses	Permeate Flux (kg/m ² h)	23.51
	Fouling Index (%)	48.27
	Polyphenols rejection (%)	46.04
Overall Desirability		0.52

The results obtained in this section permitted to determine the effect of each factor and the interaction effect of operating conditions on the membrane performance. The results of the optimization showed that a selected combination of operating parameters allow the maximum permeate flux and minimum fouling index, as well as polyphenols rejection.

3.3 Clarification of orange press liquor: UF with tubular PS membrane

Based on the results obtained in the optimization of operating conditions additional experiences of UF by using a membrane with tubular configuration and a higher membrane area, were carried out. The tests were performed by using a pilot laboratory plant (Fig. 3.20) equipped with a tubular PS membrane supplied by China Blue Star Membrane Technology Co., Ltd. (Beijing, China) having a nominal molecular weight cut-off (MWCO) of 100 kDa and an effective membrane area of 1.2 m². Experiments were performed according to the batch concentration mode in which the retentate stream is continuously recycled back to the feed tank.. The operating conditions were selected as follows: TMP= 1.2 bar, T= 21.31±0.23°C and Q_f = 1,140 L/h. The mass of permeate collected, for each experience, was measured with an accuracy of ±0.1 g every 10 min for periods of 345 min. In Table 2.1. physic-chemical characteristics of orange press liquor used as feed in these activities are reported.



Fig. 3.20. Experimental set-up used for the clarification of raw press liquor by UF.

The time course of permeate flux measured in two different experimental runs is reported in Fig. 3.21.

The results showed that there is not a statistically significant difference ($p=0.6715$; $F\text{-ratio}=0.18$) between the means of the two experiences at the 95% confidence level. This means that there is a repetitive behaviour of the membrane in the clarification of orange press liquor. A typical behaviour in the permeate flux, characterized by a drop in the flux values during the process due to the fouling produced on the membrane surface was observed (see section 1.5.3). The initial value of the permeate flux for the first and second run was 5.21 and 5.17 $\text{kg}/\text{m}^2\text{h}$, respectively. The fouling produced during 345 min of processing caused a reduction of permeate flux of 64.49 and 61.31% for the first and second run, respectively, in comparison with the initial value.

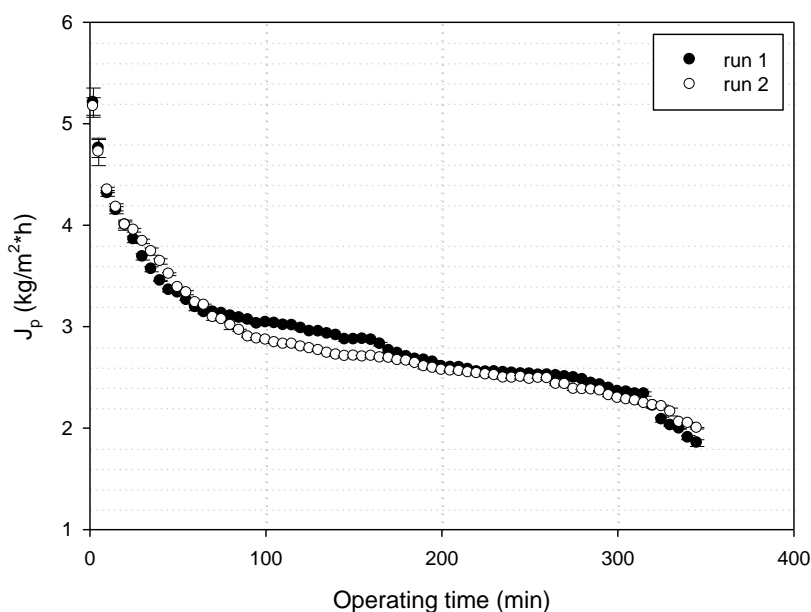


Fig. 3.21. Time course of permeate flux for press liquor with PS ultrafiltration membrane of 100kDa, operating conditions: $T=21.31\pm 0.23^\circ\text{C}$; $\text{TMP} = 1.2$ bar).

A volume reduction factor (VRF) of 9.73 and 8.26 for the first and second run, respectively, was reached.

The results obtained in terms of rejection of hesperidin and sugars content are depicted in Table 3.6. The clarified press liquor, contained 91.49% of hesperidin and 72.83% of sugars of the initial press liquor. Consequently, during UF part of the sugars (27.17%) was retained by the UF membrane. Fig. 3.22 shows the differences between the permeate and concentrate streams after the UF process.

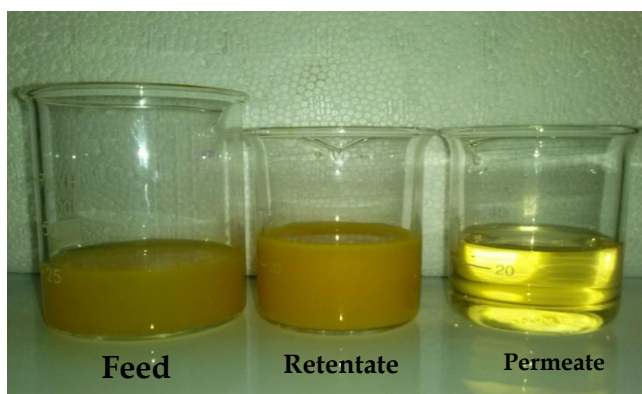


Fig. 3.22. Samples coming from the UF treatment of orange press liquor.

Table 3.6. Results obtained during UF of orange press liquor by using tubular PS membrane.

		ρ (kg/L)	Volume* (L)	VRF** (-)	Hesperidin		Sugars	
					Concentration (mg/L)	Total mass (mg)	Concentration (°brix)	Total mass (g)
First run	Feed	1.0121	22		161.67±6.78	3556.74	4.50	1001.98
	Retentate	1.0214	1.2	9.73	198.88±7.87	238.66	6.00	73.54
	Permeate	1.0070	19.74		164.84±2.47	3253.94	4.00	795.13
Second run	Feed	1.0131	22.14		158.17±14.29	3501.88	4.50	1009.35
	Retentate	1.0195	1.8	8.26	195.83±10.79	352.49	5.75	105.52
	Permeate	1.0073	19.46		154.83±3.96	3012.99	3.75	735.08

*Volume obtained after experimental run of 345 min

**Volume reduction factor reached after experimental run of 345 min

References

- [1] J.E. Lozano. 2003. Separation and Clarification. In: *Encyclopedia of Food Science and Nutrition*, ed. B. Caballero, L. Trugo and P. Finglas, 5187-5196. Elsevier, London, UK.
- [2] R.C.C. Domingues, S.B. Faria Junior, R. Barnardes Silva, V.L. Cardoso, M.H. Miranda Reis. Clarification of passion fruit juice with chitosan: Effects of coagulation process variables and comparison with centrifugation and enzymatic treatments. *Process Biochemistry*, 47 (2012) 467–471.
- [3] Chatterjee S, Chatterjee S, Chatterjee BP, Guha AK. Clarification of fruit juice with chitosan. *Process Biochemistry*, 39 (2004) 2229–32.
- [4] Alvarez S, Riera FA, Alvarez R, Coca J, Cuperus FP, Bouwer ST, et al. A new integrated membrane process for producing clarified apple juice and apple juice aroma concentrate. *Journal of Food Engineering*, 46 (2000) 109–25.
- [5] A. Cassano, B. Jiao and E. Drioli, Production of concentrated kiwifruit juice by integrated membrane processes. *Food Research International*, 37(2) (2004) 139–148.
- [6] S.S. Koseoglu, J.T. Lawhon and E.W. Lusas, Use of membranes in citrus juice processing. *Food Technology*, 44(12) (1990) 90–97.
- [7] K.J. Hwang, C.Y. Liao, K.L. Tung, Analysis of particle fouling during microfiltration by use of blocking models, *Journal of Membrane Science*, 287 (2007) 287–293.
- [8] H. Strathmann, L. Giorno, E. Drioli, An introduction to membrane science and technology, Consiglio Nazionale delle Ricerche, Roma, 2006.
- [9] S. Domodaran, Aminoacids, Peptides and Proteins, in: O. Fennema (Ed.), *Food Chemistry*, Marcel Dekker Inc., New York, 1997, pp. 321–430.
- [10] M. Moresi, I. Sebastiani, Pectin recovery from model solutions using a laboratory-scale ceramic tubular UF membrane module. *Journal of Membrane Science*, 322 (2008) 349–359.
- [11] K.J. Hwang, C.Y. Liao, K.L. Tung, Analysis of particle fouling during microfiltration by use of blocking models. *Journal of Membrane Science*, 287 (2007) 287–293.

- [12] A. Weis, M.R. Bir, M. Nyström, C. Wright, The influence of morphology, hydrophobicity and charge upon the long-term performance of ultrafiltration membranes fouled with spent sulphite liquor. *Desalination*, 175 (2005) 73–85.
- [13] A.R. Proteggente, A. Saija, A. De Pasquale, C.A. Rice-Evans, The compositional characterisation and antioxidant activity of fresh juices from Sicilian sweet orange (*Citrus sinensis* L. Osbeck) varieties. *Free Radical Research*, 37 (2003) 681–687.
- [14] P. Rapisarda, A. Tomaino, R. Lo Cascio, F. Bonina, A. De Pasquale, A. Saija, Antioxidant effectiveness as influenced by phenolic content of fresh orange juices, *Journal of Agricultural and Food Chemistry*, 47 (1999) 4718–4723.
- [15] V. Roginsky, A.E. Lissi, Review of methods to determine chainbreaking antioxidant activity in food. *Food Chemistry*, 92 (2005) 235–254.
- [16] V.L. Singleton, R. Orthofer, R.M. Lamuela-Raventos, Analysis of total phenols and other oxidation substrates and antioxidants by means of Folin–Ciocalteu reagent. *Methods in Enzymology*, 299 (1999) 152–178.
- [17] R.L. Prior, X. Wu, K. Schaich, Standardized methods for the determination of antioxidant capacity and phenolics in foods and dietary supplements. *Journal of Agricultural and Food Chemistry*, 53 (2005) 4290–4302.
- [18] C. Ewald, S. Fjelkner-Modig, K. Johansson, I. Sjöholm, B. Akesson, Effect of processing on major flavonoids in processed onions, green beans, and peas. *Food Chemistry*, 64 (1999) 231–235.
- [19] D. Zhang, Y. Hamazu, Phenolics, ascorbic acid, carotenoids and antioxidant activity of broccoli and their changes during conventional and microwave cooking. *Food Chemistry*, 88 (2004) 503–509.

CHAPTER 4

Fractionation of clarified press liquor

4.1 Introduction

NF membranes are characterized by typical pore sizes in the range 1-3nm which correspond to molecular weight cut-off (MWCO) of 300-500 Da [1]. These membranes in contact with aqueous solutions are also slightly charged due to dissociation of surface functional groups or adsorption of charge solute [2]. NF membranes generally present lower rejection of monovalent ions, higher rejection of divalent ions and higher flux compared to RO membranes [3]. Processes using NF membranes have been found to be extremely efficient for fractionation and concentration of solutes from complex solutions [4]. Consequently, this technology has been widely applied in food and beverage processing such as demineralization of dairy products, concentration of fruit juice and treatment of wastewater in food industry [5-8]. In recent years, a large number of potential applications of NF has been proposed. Mello et al. [9] investigated the concentration of propolis extracts using water and ethanol as solvents by NF; for aqueous solutions, the NF membrane retained around 94% of phenolic compounds and 99% of flavonoids showing high efficiency in the concentration of propolis extracts. In 2009 Diaz-Reinoso et al. [10] investigated the use of integrated membrane processes including UF and NF to obtain fractions enriched in compounds having antioxidant activity from pressed distilled grape pomace. Recently, an UF-NF integrated membrane process has been also proposed by Cissé et al. [11] for the concentration of anthocyanins from roselle extract.

In this work NF membranes were used for the fractionation of the clarified press liquor obtained from the UF process. In particular, the NF process was used as approach to separate phenolic compounds from sugars and low molecular weight compounds. In the first step several flat-sheet membranes were tested, on laboratory scale, in order to identify a suitable membrane with a good performance in terms of permeate flux, and selectivity towards phenolic compounds and sugars. In particular, the investigated

membranes were evaluated for their productivity and rejection towards sugar and phenolic compounds, in selected operating and fluid-dynamic conditions.

Experimental activities aimed at maximize the permeate flux and the rejection towards phenolic compounds and at minimize the rejection towards sugar compounds, simultaneously.

On the base of experimental results obtained in the first step, NF experiment runs were carried out on laboratory scale by using a NF spiral-wound membrane with characteristics similar those of the flat-sheet membrane identified in the first step.

4.2 Nanofiltration with flat-sheet membranes

NF experiments were performed by using a laboratory pilot unit manufactured by Permeare Srl (Milan, Italy). The equipment, depicted in Fig. 4.1, consist of a feed tank with a capacity of 10 L in stainless steel 316 L, a volumetric pump for high pressure operation (up to 75 bar), a cooling devise, a thermometer, a feed flow meter, two pressure cells for flat-sheet membranes having a surface area of 22.7 cm², two manometers to measure the inlet pressure of each cell, a manometer to measure the outlet pressures of both cells and an electric board.



Fig. 4.1. Experimental set-up used for the NF with flat-sheet membranes.

Three flat-sheet membranes (Table 4.1) were selected to evaluate their performance in terms of permeate flux as well as rejection towards hesperidin and sugars (described in section 2.3). Experimental runs were performed according to the batch concentration configuration (BCC) in which the retentate stream was continuously recycled back to the feed tank while the permeate was collected separately. The operating conditions were selected as follows: TMP=17 and 35 bar, $T=34.40\pm 3.75^{\circ}\text{C}$ and $Q_f=500\text{ L/h}$. A total of six experiments (two for each membrane) were carried out. Measurements of permeate flux were performed every 5 min during 200 min of continuous process.

Table 4.1. Characteristics of flat-sheet NF membranes.

Membrane	Manufacturer	Material	Pure water flux (L/m ² h)	Rejection	pH range	Maximum temperature (°C)
NF-PES-10	Microdyn-Nadir	Permanently hydrophilic polyethersulfone	>200	25-40% Na ₂ SO ₄ [*] 5-15% NaCl [*]	0-14	95
NP 030 P	Microdyn-Nadir	Permanently hydrophobic polyethersulfone	>40	80-95% Na ₂ SO ₄ [*]	0-14	95
DSS-NFT-50	Alfa-Laval	Thinfil composite	-	> 98% MgSO ₄ ^{**}	3-10	50

^{*} test conditions: 0.5%, 40 bar, 20°C, stirred cell (700 rpm)

^{**} test conditions: 2000 ppm, 9 bar, 25°C

The hydraulic permeability of selected membranes was measured experimentally (according with the procedure described in section 1.5.2), before each run, in order to determine the resistance of each membrane at the water flux.

Fig. 4.2 shows the permeate flux variation with TMP for each membrane studied using pure water. The results show that J_w increases linearly with TMP over the range of TMP investigated (6.89–35 bar). In general, an increase in the hydraulic permeability is observed by increasing the MWCO, because larger pore sizes lead to higher pure water fluxes. However, it must be noted that water permeability is also affected by the internal structure of the membrane; therefore, other factors in addition to MWCO, such as morphology and hydrophobicity/hydrophilicity, also influence this value [4]. In particular, the NF-PES-10 membrane presented the highest hydraulic permeability equal to $12.79 \text{ L/m}^2 \cdot \text{h} \cdot \text{bar}$, whereas NP-030 and DSS-NFT-50 membranes presented values of 3.36 and $2.59 \text{ L/m}^2 \cdot \text{h} \cdot \text{bar}$, respectively. These differences are an intrinsic characteristics of each membrane related with the polymeric material and structure.

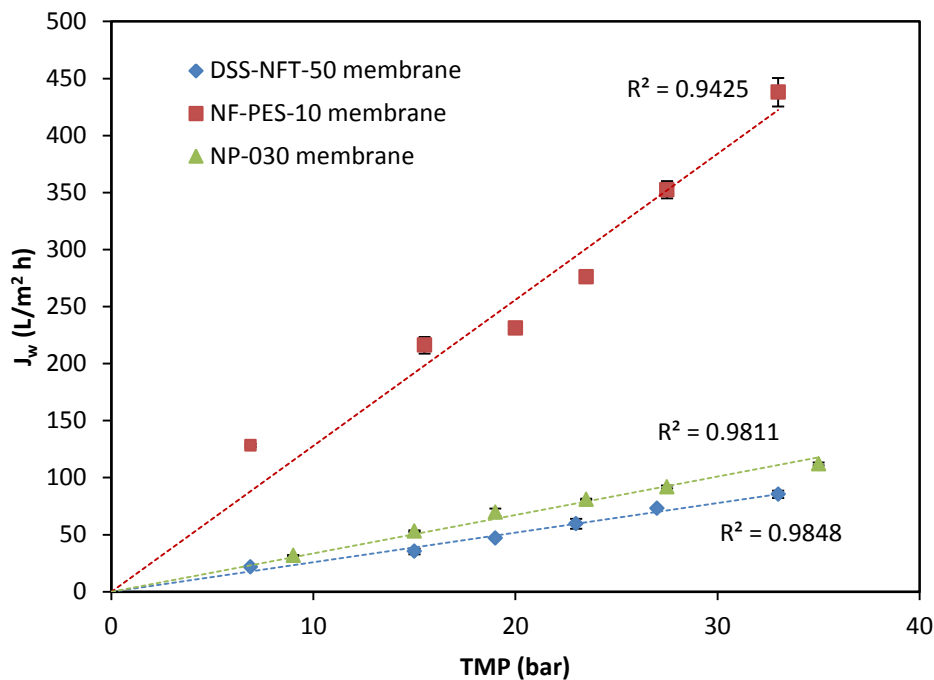


Fig. 4.2. Hydraulic permeability of NF membranes studied. Operating conditions: Temperature= $26.79 \pm 1.72^\circ\text{C}$, $Q_f=500 \text{ L/h}$.

The time course of the permeate flux at 17 bar for all investigated membranes, during the process with clarified press liquor, is depicted in Fig. 4.3. Statistically significant differences ($p=0.000$; $F\text{-ratio}=857.87$) between the average of permeate fluxes for the three membranes investigated were found. According to the obtained results, the NF-PES-10 membrane presented the highest permeate flux in comparison with the other membranes studied.

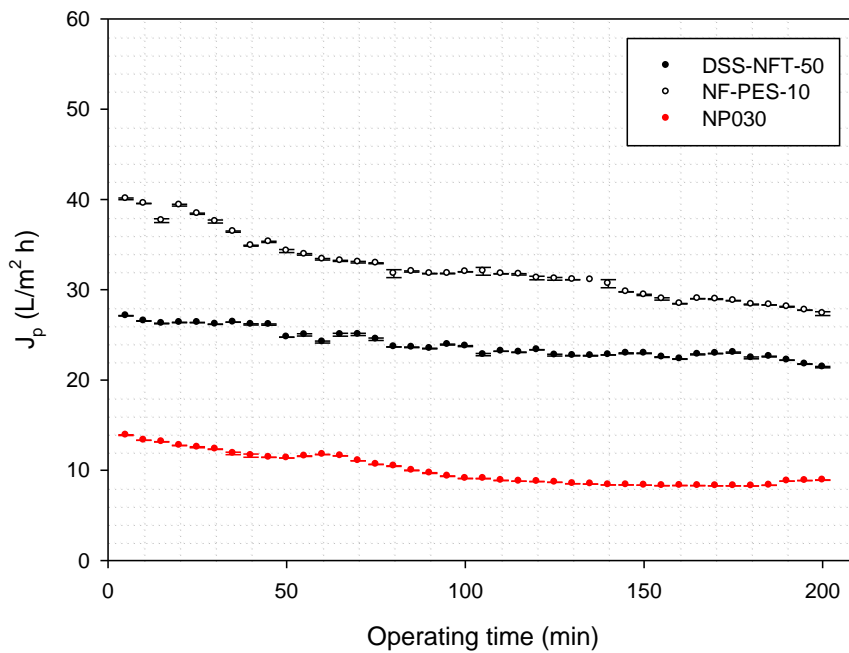


Fig. 4.3. NF of clarified orange press liquor with flat-sheet membranes. Time course of permeate flux. Operating conditions: $TMP=17$ bar; $T=31.25\pm 0.56^\circ C$; $Q_f=500$ L/h.

The differences appreciated between different membranes can be attributed to differences in the type of fouling developed during the process which produced a drop in the permeate flux equal to 21.0%, 31.7% and 35.9% for DSS-NFT-50, NF-PES-10 and NP-030 membranes, respectively.

Fig. 4.4 shows the time course of permeate flux when TMP is increase at 35 bar. Results indicate that there are statistically significant differences ($p=0.000$; $F\text{-ratio}=874.64$) between the means of the three membranes studied. The NP-030 membrane showed the highest drop in the permeate flux (equal to 40.7%), whereas NF-PES-10 and

DSS-NFT-50 membranes presented lower drop of permeate flux values (37.4% and 23.1%, respectively).

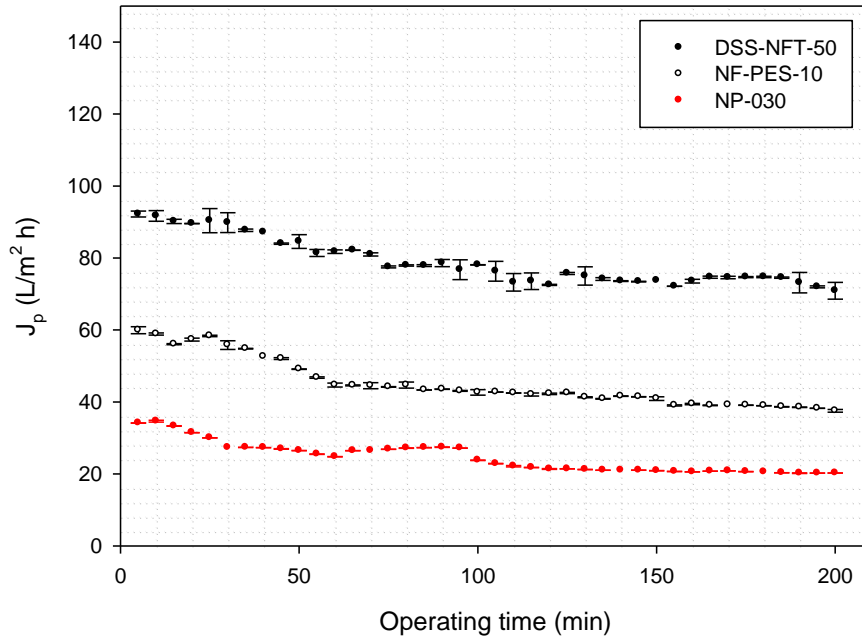


Fig. 4.4. Time course for NF process using flat-sheet membranes. Operating conditions: 35 bar; $T=37.56\pm 0.78^\circ\text{C}$ and $Q_f=500$ L/h.

In Table 4.2 results of analytical determination of hesperidin and sugars (as TSS) in the feed, permeate and retentate streams for each membrane are reported.

Table 4.2. Analytical determination of hesperidin and sugars in samples coming from the treatment of clarified orange press liquor with flat-sheet membranes.

Membrane type	Operating conditions	Sample	Hesperidin (mg/L)	TSS (°Brix)
DSS-NFT-50	17 bar / 31.25±0.56°C	Feed	73.66±0.87	4.0
		Permeate	0	0.75
		Retentate	61.77±1.29	3.75
	35 bar / 37.56±0.78°C	Feed	89.15±2.04	3.0
		Permeate	0	0.5
		Retentate	146.02±5.75	3.5
NF-PES-10	17 bar / 31.25±0.56°C	Feed	59.74±5.53	3.1
		Permeate	9.73±0.37	0.75
		Retentate	79.90±1.64	2.5
	35 bar / 37.56±0.78°C	Feed	110.34±1.94	4.0
		Permeate	4.55±0.82	0.5
		Retentate	122.69±3.35	0.5
NP-030	17 bar / 31.25±0.56°C	Feed	63.79±4.92	3.75
		Permeate	0	0.75
		Retentate	83.17±4.77	2.0
	35 bar / 37.56±0.78°C	Feed	64.27±0.89	4.0
		Permeate	0	0.5
		Retentate	55.16±0.78	2.5

Hesperidin and sugar rejection were determined according to equation (1.1) reported in Chapter 1. Results are shown in Fig. 4.5-a and 4.5-b.

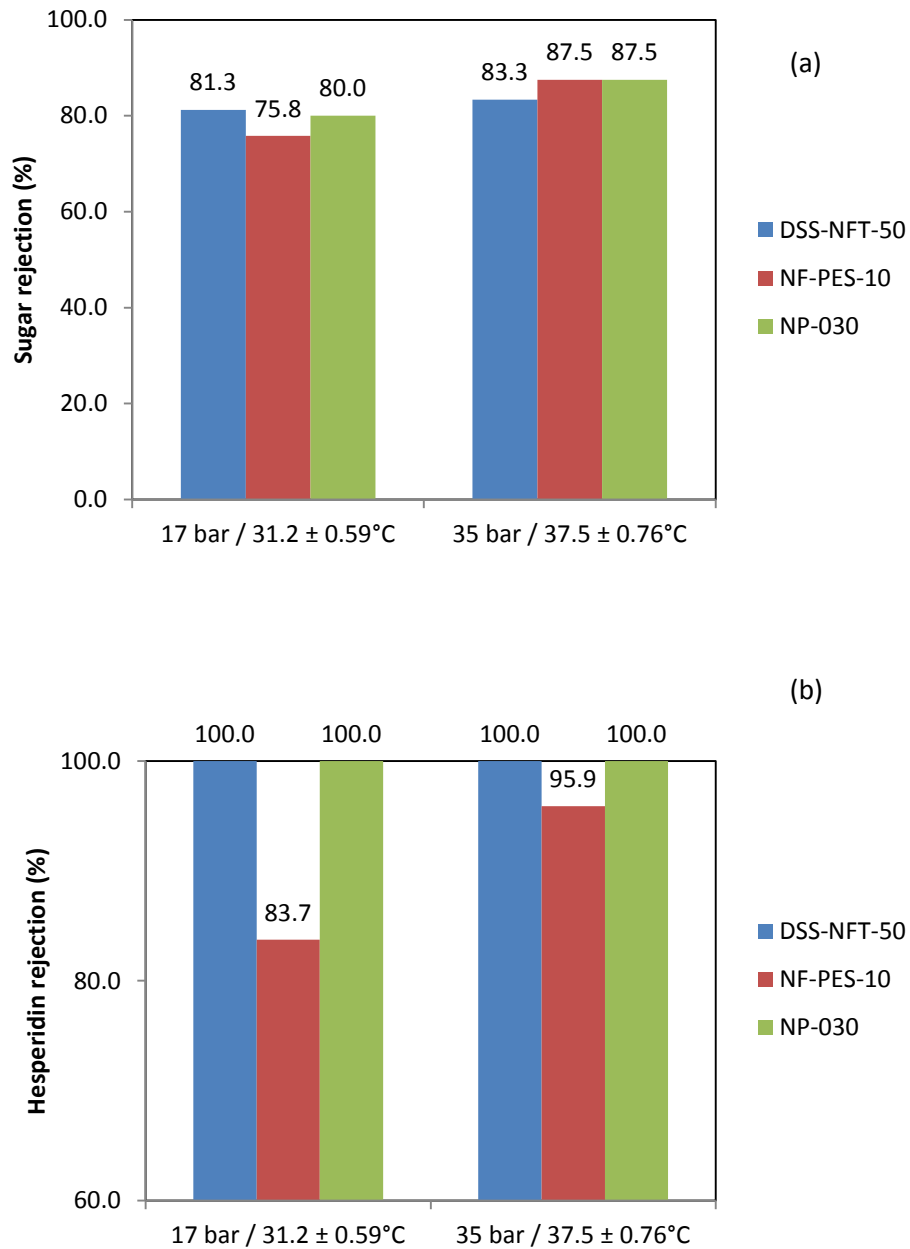


Fig. 4.5. Membrane rejection of (a) sugar and (b) hesperidin for NF flat-sheet membranes.

Results in terms of sugar rejection showed that differences between membranes studied are not significant, with values of rejection closer to 80%. The NF-PES-10 membrane showed the lowest value of hesperidin rejection equal to 95.9%, at 35 bar and 83.7% at 17 bar, whereas DSS-NFT-50 and NP-030 membranes presented a 100% of hesperidin rejection in both investigated pressures (Fig. 4.5-b).

According to the lowest rejection towards sugar compounds observed for the NF-PES-10 membrane and, consequently, to the recovery and separation of sugar compounds in the permeate fraction, this membrane was selected to carry out experiments with a spiral-wound configuration having a higher membrane surface area.

4.3 Nanofiltration with a spiral-wound membrane module

On the base of the results obtained with flat-sheet membranes, the NF-PES-10 membrane, showing a lower value of sugar rejection at 17 bar and a rejection towards hesperidin higher than 80%, was selected to carry out experimental runs with a spiral-wound membrane module. The characteristics of the membrane in spiral-wound configuration are depicted in Table 4.3.

Table 4.3. Properties of 2.5 x 40 in. spiral-wound NF-PES-10 membrane.

Material	Polyethersulfone
NMWCO (Da)	1,000
Maximum operating pressure (bar)	40
Maximum operating temperature (°C)	50
NaCl retention (%)	5-15
Na ₂ SO ₄ retention (%)	25-40
pH range	2-11
Membrane charge at neutral pH	Negative
Membrane surface area (m ²)	1.6

NF experiments were performed by using a laboratory bench plant supplied by Matrix Desalination Inc. (Florida, USA) (Fig. 4.6). The equipment consists of a feed tank with a capacity of 20 L, a stainless steel housing suitable for containing a 2.5x40 in. spiral-wound membrane module, a high pressure pump, two pressure gauges for the control of the inlet and outlet pressures, a pressure control valve and a coiling coil, fed with tap water, used to control the feed temperature.



Fig. 4.6. Experimental set-up used for the NF of clarified orange press liquor with a spiral-wound membrane module.

Experimental runs were performed according to the batch concentration configuration (BCC) in which the retentate stream was continuously recycled back to the feed tank. Operating conditions were selected as follows: TMP=17 bar, $T=20.73\pm 1.40^{\circ}\text{C}$. The permeate flux was measured every 5 min during 90 min of continuous process up to a VRF of 5.28.

The time course of permeate flux for the selected NF membrane is shown in Fig. 4.7. The initial permeate flux was of about $15 \text{ L/m}^2\text{h}$ and values reached at the steady-state were of about $5 \text{ L/m}^2\text{h}$. Conidi., et al. [4] found initial permeate flux and steady-state values of $10.4 \text{ L/m}^2\text{h}$ and $3.4 \text{ L/m}^2\text{h}$, respectively, when the press liquor was treated by using the same NF membrane at a TMP of 6 bar and an operating temperature of 20°C .

The typical flux decay, equal to 61.60%, observed in Fig. 4.7 can be attributed to concentration polarization and fouling phenomena. Membrane fouling is a relevant parameter to consider because it reduces productivity as well as the membrane life [12]. Fouling is a complex phenomenon depending on specific membrane–solution interactions and caused by the deposition of small colloidal particles on the inner walls of the membrane pores (standard blocking), the blocking of the membrane pore openings (complete blocking) and the build-up of particles in the form of a cake layer [13]. Susanto et al. [14] investigated the adsorption of polyphenols from green tea on the surface and inside PES membranes. According to this work the adsorptive fouling of polyphenols on PES membranes is influenced by the pore size, polar interactions (van

der Waals, electron donor–acceptor interaction) and multiple hydrogen bonds towards the additive polyvinylpyrrolidone (PVP) in PES. An increase of both adsorbed amount and affinity for polyphenol binding to PES with increasing PVP content has been also reported by Cartalade and Vernhet [15]. In addition, mixtures of polyphenols with other components, such as polysaccharides, could form aggregates having a strong contribution to adsorptive fouling of PES membranes [16].

The results obtained for the NF-PES-10 membrane in terms of rejection were of 62.02% for the hesperidin and 50% for the sugar compounds (Table 4.4).

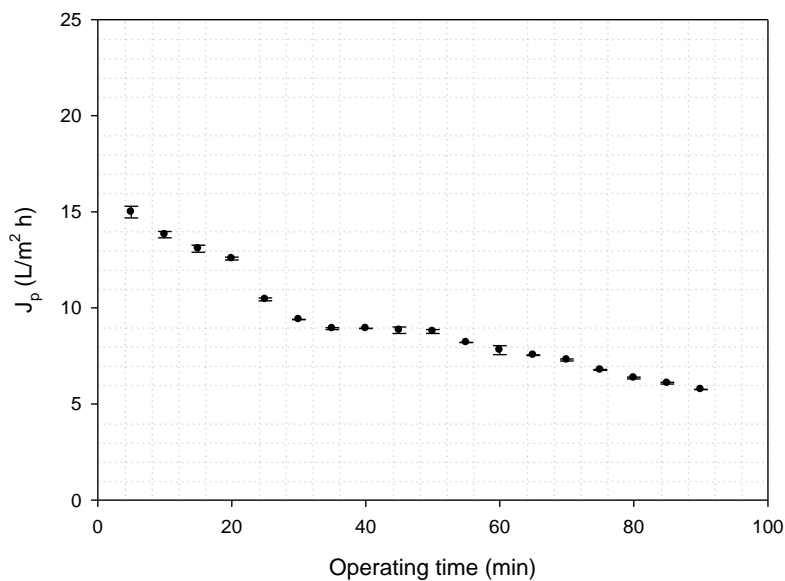


Fig. 4.7. Time course of NF process with NF-PES-10 spiral wound membrane. Operating conditions: TMP=17 bar, $T=20.73\pm 1.40^\circ\text{C}$.

In comparison with the results reported by Conidi, et al. [4] the results of sugar rejection were higher, probably due to the differences in the VRF reached, that in our case was higher. The increase in the feed concentration produces an increasing of fouling phenomena which produces an increasing of sugar rejection.

According to the mass balance of the process, the obtained retentate stream contained 70.59% of the initial mass of hesperidin, accordingly sugar compounds were reduced of 59.74% in comparison with the initial feed (Table 4.4). The retentate stream obtained in the NF process was used as feed in the final concentration step performed by OD.

Table 4.4. Results of hesperidin and sugars rejection obtained with the NF-PES-10 membrane. Operating conditions: TMP=17 bar, T=20.73±1.40°C.

	Volume (L)	ρ (kg/L)	Hesperidin			Sugars		
			Concentration (mg/L)	Weight of Hesperidin (mg)	Rejection (%)	Concentration °brix	Mass of Sugars (mg)	Rejection %
Initial (feed)	33.92	1.008	135.48±0.83	4595.48		4	1367.65	
Permeate	27.50	1.003	51.46±0.40	1415.15	62.02	2	551.65	50.00
Retentate	5.94	1.030	544.89±1.40	3236.65		9	550.64	

References

- [1] J. Rautenbach, A. Gröschl. Separation potential of nanofiltration membranes. *Desalination*, 77 (1990) 73–84.
- [2] J.H. Tay, J. Liu, D.D. Sun. Effect of solution physic–chemistry on the charge property of nanofiltration membranes. *Water Research*, 36 (2002) 585–598
- [3] C.K. Diawara. Nanofiltration process efficiency in water desalination. *Separation and Purification Review*, 37 (2008) 303–325.
- [4] C. Conidi, A. Cassano, E. Drioli, Recovery of phenolic compounds from orange press liquor by nanofiltration. *Food and Bioproducts Processing*, 90 (2012) 867–874
- [5] L.D. Barrantes, C.V. Morr. Partial deacidification and demineralization of cottage cheese whey by nanofiltration. *Journal of Food Science*, 62 (1997) 338–341.
- [6] L. Braeken, B. Van Der Bruggen, C. Vandecasteele. Regeneration of brewery waste water using nanofiltration. *Water Research*, 38 (2004) 3075–3082.
- [7] R. Ferrarini, A. Versari, S. Galassi. A preliminary comparison between nanofiltration and reverse osmosis membrane for grape juice treatment. *Journal of Food Engineering*, 50 (2001) 113–116.
- [8] G. Rice, S. Kentish, V. Vivekanand, A. Barber, A. O’Connor, G. Stevens. Membrane-based dairy separation: a comparison of nanofiltration and electrodialysis. *Developments in Chemical Engineering and Mineral Processing*, 13 (2005) 43–54.
- [9] B.C.B.S. Mello, J.C.C. Petrus, M.D. Hubinger. Concentration of flavonoids and phenolic compounds in aqueous and ethanolic propolis extracts through nanofiltration. *Journal of Food Engineering*, 96 (2010) 533–539.
- [10] B. Diaz-Reinoso, A. Moure, H. Domínguez, J.C. Parajó. Ultra-and nanofiltration of aqueous extracts from distilled fermented grape pomace. *Journal of Food Engineering*, 91 (2009) 587–593.
- [11] M. Cissé, F. Vaillant, D. Pallet, M. Dornier. Selecting ultrafiltration and nanofiltration membranes to concentrate anthocyanins from roselle extract (*Hibiscus sabdariffa* L.). *Food Research International*, 44 (2011) 2607–2614.
- [12] S.L. Nilsson. Protein fouling of UF membrane: causes and consequences. *Journal of Membrane Science*, 52 (1990) 121–142.

- [13] H.A. Mousa, S.A. Al-Hitmi. Treatability of wastewater and membrane fouling. *Desalination*, 217 (2007) 65–73.
- [14] H. Susanto, Y. Feng, M. Ulbricht. Fouling behavior during ultrafiltration of aqueous solutions of polyphenolic compounds during ultrafiltration. *Journal of Food Engineering*, 91 (2009) 333–340.
- [15] D. Cartalade, A. Vernhet.. Polar interactions in flavan-3-ol adsorption on solid surfaces. *Journal of Agricultural and Food Chemistry*, 54 (2006) 3086–3094.
- [16] M. Ulbricht, W. Ansorge, I. Danielzik, M. König, O. Schuster. Fouling in microfiltration of wine: the influence of the membrane polymer on adsorption of polyphenols and polysaccharides. *Separation and Purification Technology*, 68 (2009) 335–342.

CHAPTER 5

Concentration of NF retentate by osmotic distillation

5.1 Introduction

The concentration of fruit juices is a consolidated process in the food industry, because it ensures a longer storage life and an easier transportation of the product. Generally, this process is performed by thermal evaporation methods. Chen and Song [1] developed a fresh-preserving concentrated pomegranate juice producing method adopting a low temperature vacuum process for the concentration of the filtered juice. Pang et al. [2] patented a method in which the clarified juice was concentrated by thermal evaporation and then submitted to pasteurization before the aseptic packaging. Although evaporation processes are widely used for juice concentration it is known that thermal treatments produce a colour degradation and a reduction of most thermally sensitive compounds, with a consequent remarkable quality decline of the final product [3].

New tendencies associated with product quality improvement and energy saving have guided the development of minimal processing techniques. In this context membrane processes appear as suitable techniques since they are low-cost and athermal separation techniques, which involve no phase change when compared with traditional evaporation processes.

Membrane concentration processes, such as reverse osmosis (RO), membrane distillation (MD) and osmotic distillation (OD), present some attractive options to overcome limitations associated with vacuum evaporation. In particular, OD is a novel athermal membrane-separation process based on the use of a macroporous hydrophobic membrane separating two aqueous solutions having different solute concentration: a dilute solution on one side and a hypertonic salt solution (concentrated brine stripper) on the opposite side. The driving force of the process is given by a water vapour pressure gradient across the membrane generated by the difference in water activity

between the two sides of the membrane. The hydrophobic nature of the membrane prevents penetration of the pores by aqueous solutions, creating air gaps within the membrane. The water vapour pressure gradient across the membrane determines a transfer of vapour across the pores from the high-vapour pressure phase to the low one [4,5]. This migration of water vapour results in the concentration of the feed and dilution of the osmotic agent solution (Fig. 5.1)

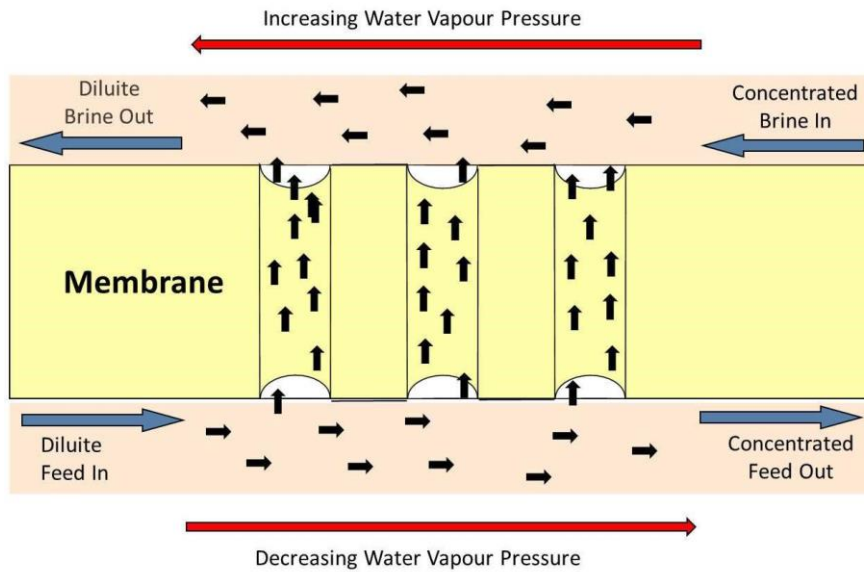


Fig. 5.1. Schematic representation of water vapour flux through an OD membrane.

The water transport through the membrane can be summarized in three steps: 1) evaporation of water at the dilute vapour-liquid interface; 2) diffusional or convective vapour transport through the membrane pore; 3) condensation of water vapour at the membrane/brine interface.

Since the OD process is operated at room temperature and atmospheric pressure, products can be concentrated without mechanical and thermal damage. Therefore OD is an attractive process for the concentration of solutions containing thermo-sensitive compounds such as fruit juices and pharmaceuticals. Several applications of OD in the concentration of fruit juices have been investigated by different authors [6-11]. In these works the potential of OD for a better preservation of the quality of the raw material has been clearly confirmed.

In this work the OD process was used to concentrate the retentate stream obtained in the previous NF process, described in Chapter 4. This step was devoted to the concentration of polyphenols through the removal of water in the NF retentate fraction.

Experimental activities related to the concentration of the NF retentate by OD are reported in the following.

The membrane performance, in terms of productivity (evaporation flux) was analysed and discussed.

OD experiment was performed by using as feed solution the NF retentate whose characteristics, in terms of hesperidin and sugar content, are depicted in Table 4.2. Experimental run was performed by using a laboratory plant supplied by Itest Srl. (Corato, Bari, Italy).

The schematic diagram of the OD experimental set-up is depicted in Fig. 5.2. The equipment consists of two independent compartments, one for the feed solution (the NF retentate), the other for the stripping solution.

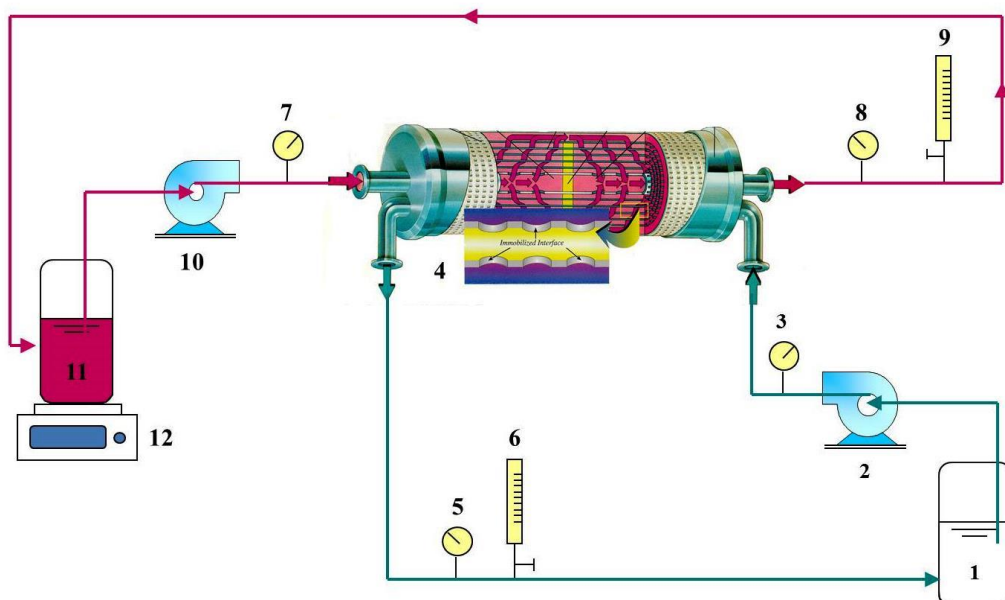


Fig. 5.2. Schematic diagram of OD experimental set-up.

The unit featured a Liqui-Cell Extra-Flow 2.5 x 8-in. membrane contactor (Membrana, Charlotte, USA) containing microporous polypropylene hollow fibers (having external and internal diameters of 300 μm and 220 μm , respectively) with an average pore diameter of 0.2 μm and a total membrane surface area of 1.4 m^2 . Characteristics of OD membrane module are reported in Table 5.1. The feed solution was pumped through the shell side of the membrane module; a calcium chloride dihydrate solution of 60% w/w was pumped through the fiber lumens (tube side). Feed and stripping solution were recirculated through the contactor in a counter-current mode with an average flow-rate of 1.5 L/min. TMP in both compartments were kept constants at 0.105 bar, whereas the temperature was maintained almost constant in both compartments at $24.59 \pm 1.15^\circ\text{C}$ and $24.89 \pm 1.12^\circ\text{C}$ in the shell side and tube side, respectively.

Table 5.1. Characteristics of Liqui-Cell Extra-Flow membrane contactor.

Characteristics		
Fiber	Fiber type	Celgard [®] Microporous Polypropylene Hollow fiber
	External diameter	0.30 mm
	Internal diameter	0.22 mm
	Length	160 mm
	Pore diameter	30 nm
	Porosity	~ 40%
Cartridge Operating Limits	Maximum transmembrane	4.13 bar
	Temperature range	40°C
Cartridge Characteristics	Cartridge Dimensions (DxL)	80x280 mm
	Effective Surface Area	1.4 m^2
	Effective Area/Volume	29.3 cm^2/cm^3
	Fiber Potting Material	Polyethylene

The volume ratio between feed solution and stripper was 1:2, in order to prevent a significant dilution of the brine solution with a consequent decreasing of the driving force during the process. Evaporation fluxes (J_w) were determined gravimetrically measuring the weight of the water extracted from the NF retentate by means of a digital

balance placed under the feed tank. After each trial, the pilot plant was cleaned first by rinsing the tube side and shell side with de-ionized water. Then, the shell side was cleaned with a KOH solution at 2% w/w for 1 h at 40°C. After a short rinsing with de-ionized water a citric acid solution at 2% w/w was circulated for 1 h at 40°C. A final rinsing with de-ionized water was carried out.

5.2 Experimental results

Fig. 5.3-a shows the time course of the evaporation flux and TSS content during the concentration of NF retentate by OD. The initial evaporation flux equal to 0.59 kg/m²h, decreased gradually up to reach a final value of 0.39 kg/m²h when the TSS content of the press liquor was at 30.4°Brix. The flux decline can be attributed to the decrease in brine concentration (Fig. 5.3-b). Alves et al. [12] reported that the dilution of the brine solution leads the decrease in vapour pressure of the osmotic agent and, consequently, to the reduction of the driving force for water transport through the membrane. In addition, the increase of feed concentration is related with an increasing of the feed viscosity that can raise the resistance to mass transfer in the liquid phase and, consequently, to determine a polarization effect leading to a lower driving force [13,14].

Similar results were obtained in the OD concentration of different clarified juices (kiwifruit, citrus, carrot, passion fruit, cactus pear, etc.) on laboratory and semi-industrial scale [6,7,15-17].

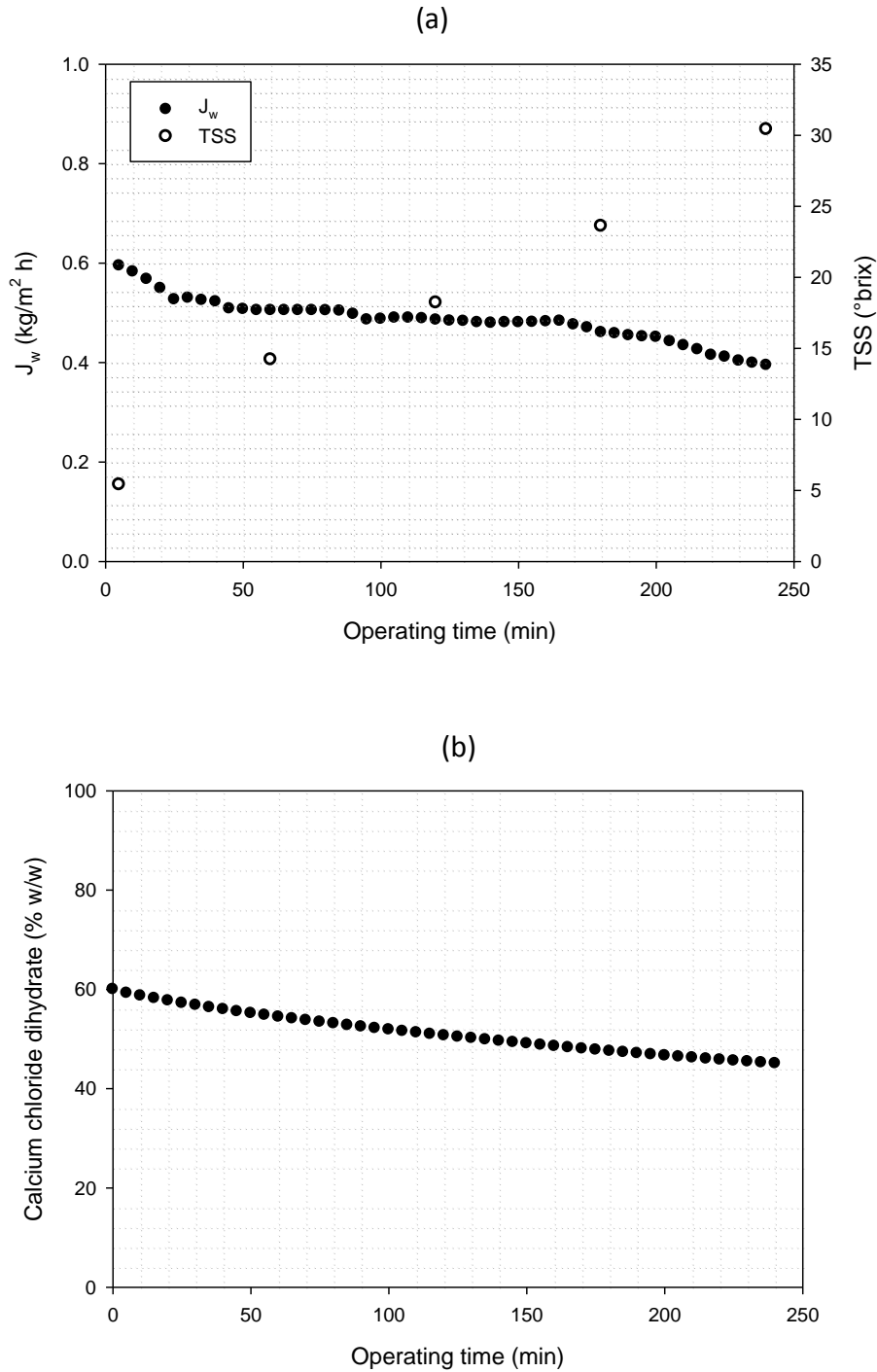


Fig. 5.3. Treatment of NF retentate by OD. Time course of (a) evaporation flux and TSS content; (b) calcium chloride dihydrate concentration.

The evolution of the hesperidin concentration during the OD process is shown in Fig. 5.4. In the final OD sample with a TSS content of 30.5 °Brix the concentration of hesperidin was 1020 mg/L. Traditional concentration methodologies such as

heating/evaporation processes (microwave heating, rotary vacuum evaporator and evaporation at atmospheric pressure) have been associated with changes in the colour parameters (L, a and b) [18] as well as degradation of sugars which accelerate anthocyanin breakdown and enhance non-enzymatic browning during thermal processing [19]; in this case, the increase of the colour intensity can be attributed to an increasing in the concentration of polyphenols (Fig. 5.5), since the concentration was carried out at temperatures (25°C) that do not represent a risk for the development of the above phenomena.

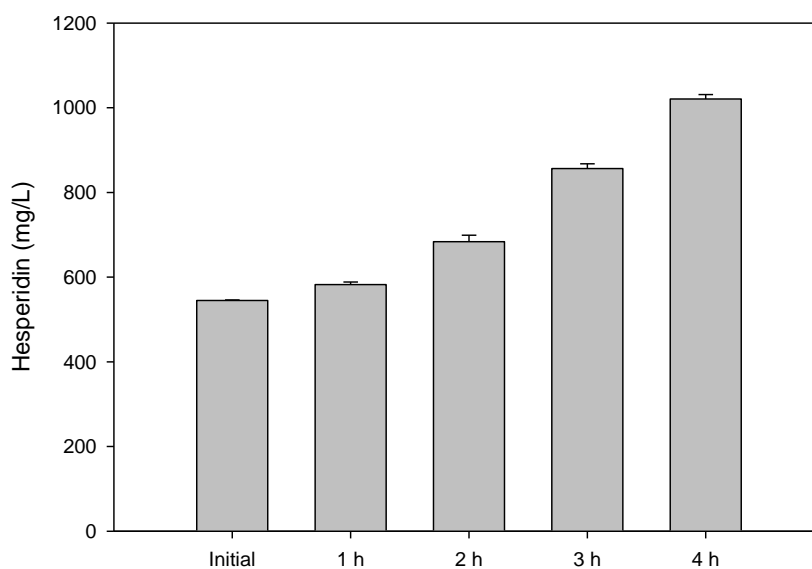


Fig. 5.4. Evolution in concentration of hesperidin during OD.

On the base of experimental results a conceptual process design was proposed to obtain concentrated fractions enriched in phenolic compounds from orange press liquor. According to the proposed process, depicted in Fig. 5.6, the raw press liquor is clarified by UF in order to obtain a clarified liquor depleted in suspended solid and macromolecules. The clarified liquor is then submitted to a NF step in order to separate sugars compounds from phenolics.

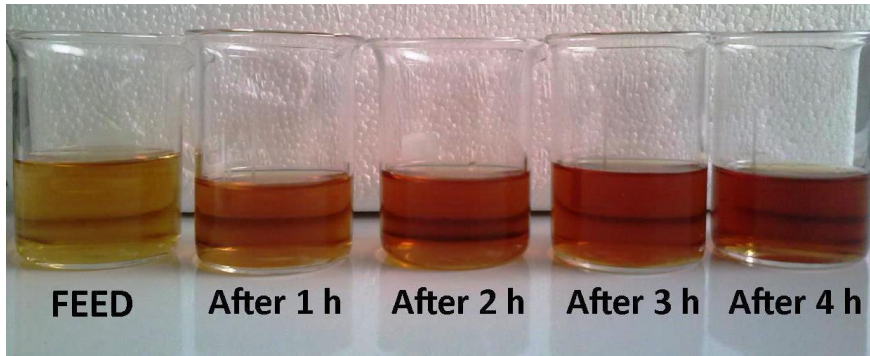


Fig. 5.5. Samples collected at different times during the concentration of the NF retentate by OD.

The NF permeate, enriched in sugar compounds, can be of interest for food applications. The NF retentate fraction can be submitted to a final concentration step by OD: the final product, with high antioxidant activity due to the concentration of phenolic compounds is of potential interest for nutraceutical or food applications.

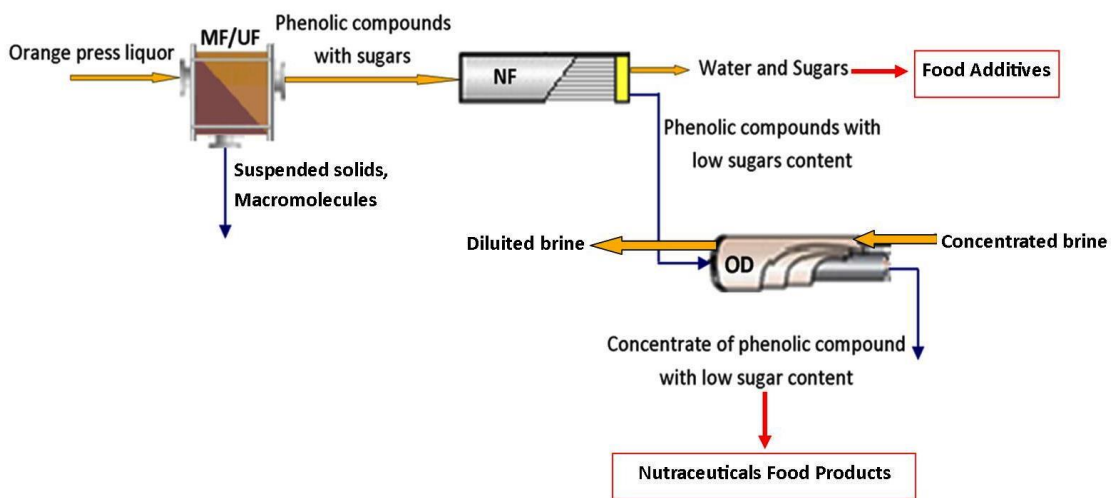


Fig. 5.6. Conceptual process design for the treatment of citrus press liquor based on an integrated membrane process.

The proposed process leads to significant advantages in terms of reduction of environmental impact, recovery of high-added value component, reduction of depolluting costs, saving of water and energy requirements.

References

- [1] M. Chen, J. Song. 1994. Fresh-preserving concentrated pomegranate juice producing method. Patent CN 1080492(A).
- [2] F. Pang, H. Wang, G. Lu. 2008. Concentrated pomegranate clear juice manufacturing technique. Patent CN 101283823(A).
- [3] B. Jiao, A. Cassano, E. Drioli. Recent advances on membrane processes for the concentration of fruit juices: a review. *Journal of Food Engineering*, 63 (2004) 303–324.
- [4] P.A. Hogan, R.P. Canning, P.A. Peterson, R.A. Johnson, A.S. Michaels. A new option: osmotic distillation. *Chemical Engineering Progress*, 94 (1998) 49–61.
- [5] N. Nagaraj, B.S. Patil, P.M. Biradar.. Osmotic membrane distillation – A brief review. *International Journal of Food Engineering*, 2 (2006), article 5.
- [6] A. Cassano, E. Drioli. Concentration of clarified kiwifruit juice by osmotic distillation. *Journal of Food Engineering*, 79 (2007) 1397–1404.
- [7] A. Cassano, C. Conidi, R. Timpone, M. D’Avella, E. Drioli. A membrane-based process for the clarification and the concentration of the cactus pear juice. *Journal of Food Engineering*, 80 (2007) 914–921.
- [8] C. Hongvaleerat, L.M.C. Cabral, M. Dornier, M. Reynes, S. Ningsanond. Concentration of pineapple juice by osmotic evaporation. *Journal of Food Engineering*, 88 (2008) 548–552.
- [9] R.B. Rodrigues, H.C. Menezes, L.M.C. Cabral, M. Dornier, G.M. Rios, M. Reynes. Evaluation of reverse osmosis and osmotic evaporation to concentrate camu–camu juice (*Myrciaria dubia*). *Journal of Food Engineering*, 63 (2004) 97–102.
- [10] P.E. Shaw, M. Lebrun, M. Dornier, M.N. Ducamp, M. Courel, M. Reynes. Evaluation of concentrated orange and passionfruit juices prepared by osmotic distillation. *LWT-Food Science and Technology*, 34 (2001) 60–65.
- [11] A. Kozák, A. Rektor, G. Vatai. Integrated large-scale membrane process for producing concentrated fruit juices. *Desalination*, 200 (2006) 540–542.
- [12] V.D. Alves, B. Koroknai, K. Bélafi-Bakó, I.M. Coelho. Using membrane contactors for fruit juice concentration. *Desalination*, 162 (2004) 263–270.
- [13] A. Altan, M. Maskan. Rheological behavior of pomegranate (*Punica granatum L.*) juice and concentrate. *Journal of Texture Studies*, 36 (2005) 68–77.

- [14] M.A. Magerramov, A.I. Abdulagatov, N.D. Azizov, I.M. Abdulagatov. Effect of temperature, concentration, and pressure on the viscosity of pomegranate and pear juice. *Journal of Food Engineering*, 80 (2007) 476–489.
- [15] A. Cassano, E. Drioli, G. Galaverna, R. Marchelli, G. Di Silvestro, P. Cagnasso. Clarification and concentration of citrus and carrot juices by integrated membrane processes. *Journal of Food Engineering*, 57 (2003) 153–163.
- [16] F. Vaillant, E. Jeanton, M. Dornier, G.M. O'Brien, M. Reynes, M. Decloux. Concentration of passion fruit juice on an industrial pilot scale using osmotic evaporation. *Journal of Food Engineering*, 47 (2001) 195–202.
- [17] F. Vaillant, M. Cisse, M. Chaverri, A. Perez, M. Dornier, F. Viquez, C. Dhuique-Mayer. Clarification and concentration of melon juice using membrane process. *Innovative Food Science and Emerging Technology*, 6 (2005) 213–220.
- [18] M. Maskan. Production of pomegranate (*Punica granatum* L.) juice concentrate by various heating methods: colour degradation and kinetics. *Journal of Food Engineering*, 72 (2006) 218–224.
- [19] H.J. Suh, D.O. Noh, C.S. Kang, J.M. Kim, S.W. Lee. Thermal kinetics of color degradation of mulberry fruit extract. *Nahrung*, 47 (2003) 132–135.

CONCLUSIONS

This PhD dissertation aimed at evaluating the potential of an integrated membrane system in the recovery of high-added value compounds, as polyphenols, from the orange press liquor, a by-product of the citrus industry. The strategy was focused on the use of three different membrane operations such as UF, NF and OD in order to obtain a final product enriched in phenolic compounds with a reduction in the sugar content.

Different MF and UF membranes were analysed for their potential in the clarification of the raw press liquor. The study of membrane characteristics and operating conditions on laboratory scale permitted to select a suitable membrane and the combination of operating parameters to maximize the permeate flux and minimize the rejection of polyphenols. Experiments on larger scale were carried out, on the base of previous results, by using a tubular PS membrane producing a clarified press liquor containing 91% and 72.83% of hesperidin and sugars present in the raw liquor, respectively.

The clarified liquor was submitted to a fractionation step performed by using a NF process. Studies performed with three flat-sheet NF membranes allowed to identify suitable membrane to concentrate phenolic compounds reducing the sugar content simultaneously. Experimental activities performed with this membrane in spiral-wound configuration permitted to obtain a retentate stream containing 70.43% of the hesperidin contained in the clarified liquor with a sugar reduction equal to 59.74%.

The NF retentate was submitted to a final concentration step by in which a concentrated solution with a content of hesperidin 6.39 times higher than the initial one was produced.

On the base of experimental results a conceptual process design for the treatment of orange press liquor was formulated. The proposed process offers new perspectives for the valorisation of by-products coming from the citrus industry.

According to their composition in phenolic and sugar compounds, different fractions produced in the proposed integrated membrane system appear of interest to develop

new formulations for nutraceutical and food applications. Significant advantages can be achieved in terms of reduction of environmental impact, recovery of high-added value compounds, saving of water and energy consumption.

The present PhD dissertation can be considered a starting point for further investigations devoted to improve the purification of phenolic compounds from citrus by-products (i.e. evaluating the fractionation of clarified press liquor with NF membranes in a sequential design) and to evaluate the bioactive properties (including antiallergic, antidiabetic, antiinflammatory, antiviral, antiproliferative, and anticarcinogenic activities) of the produced fractions.

ANNEX

Publications.

International Journals:

René Ruby-Figueroa, Alfredo Cassano, Enrico Drioli. Ultrafiltration of orange press liquor. Optimization of operating conditions for the recovery of antioxidant compounds by response surface methodology, *Separation and Purification Technology* 98 (2012) 255-261

Beatriz Cancino-Madariaga, Rene Ruby, Carolina Luisa Astudillo, Jorge Saavedra, Mariane Lutz, Analysis of the membrane fouling mechanisms involved in clarified grape juice ultrafiltration using statistical tools. *Industrial and Engineering Chemistry Research*, 51 (2012) 4017–4024

René Ruby-Figueroa, Alfredo Cassano, Enrico Drioli, Ultrafiltration of orange press liquor: Optimization for permeate flux and fouling index by response surface methodology. *Separation and Purification Technology*, 80 (2011) 1-10.

Beatriz Cancino-Madariaga, Carlos Felipe Hurtado, Rene Ruby. Effect of pressure and pH in ammonium retention for nanofiltration and reverse osmosis membranes to be used in recirculation aquaculture Systems (RAS). *Aquacultural Engineering*, 45 (2011) 103-108

Mariane Lutz, Katterin Jorquera, Beatriz Cancino, Rene Ruby, Carolina Henriquez. Phenolics and antioxidant capacity of Table grape (*Vitis vinifera* L.) Cultivars Grown in Chile. *Journal of Food Science*, 76 (7) (2011) C1088-C1093

Book chapters:

Frank Lipnizki, René Ruby-Figueroa. 2013. Membrane operations in the brewing and sugar production. In *Integrated Membrane Operations in the Food Production*, ed. A. Cassano and E. Drioli, published by Verlag Walter de Gruyter & Co., Berlin

Alfredo Cassano, René Ruby-Figueroa, Enrico Drioli. Membrane Separation. In *Food Processing*, ed. Theodoros Varzakas. Taylor and Francis Group (Boca Raton, Florida)

Conferences

Oral Presentation:

R. Mazzei, E. Piacentini, E. Drioli, R.A. Ruby-Figueroa, L. Giorno. Olive mil waste water processed by intensified biocatalytic membrane reactor as source of phytotherapics. VIII Congreso Ibero-Americano en Ciencia y Tecnologia de Membranas, Salta, Argentina, 24-27 aprile 2012

Poster presentation:

R.A. Ruby-Figueroa, A. Cassano, E. Drioli. Effect of operating conditions on permeate flux and total resistance during the ultrafiltration of orange press liquor. ITM seminar day, Rende (CS), 14 luglio 2011.

R.A. Ruby-Figueroa, Alfredo Cassano, Enrico Drioli. Analysis of performance of MF and UF membranes in the clarification of citrus wastewaters by Multivariate Analysis. 2nd Training Workshop on “Functionalized membranes for wastewater treatment – nanoparticles and surface modifications”, Cetraro (CS), 15-17 maggio 2013.